

Curriculum vitae

Povilas Kavaliauskas

EDUCATION

PhD (December 2025)

Molecular Microbiology & Immunology

University of Maryland, Baltimore School of Medicine, USA

MSc (2016–2018)

Microbiology & Biotechnology

Vilnius University, Lithuania

BSc (2012–2016)

Molecular Biology

Vilnius University, Lithuania

RESEARCH & INDUSTRY EXPERIENCE

University of Maryland, School of Medicine (Baltimore, USA)

PhD Student – Dr. V. Bruno Lab | 2020–2025

- Translational research on host-pathogen interactions, and immune evasion by using multi-omics, in vitro and in vivo techniques.
- Collaborated with various partners on functional validation.

Kaunas University of Technology (Kaunas, Lithuania)

Visiting Scientist – Dr. V. Mickevičius Group | 2020–Present

- Synthesized and characterized novel antibacterial, antifungal, antiviral compounds.
- Co-led SAR optimization efforts for antimicrobial candidates.

UAB Biossyd (Kaunas, Lithuania)

Scientific Product Development Advisor | 2022–Present

- Advising preclinical strategy and compound selection for therapeutic R&D pipeline.
- Bridging academic findings to product development.

Weill Cornell Medicine, Cornell University (New York, USA)

Research Associate – Dr. T. Walsh Lab | 2016–2020

- Developed in vivo models for antimicrobial evaluation.
- Conduct and led animal studies of candidate therapies (lung, systemic, ocular).

Lithuanian University of Health Sciences (Kaunas, Lithuania)

Consulting Scientist (Animal Models) | 2017–2019

- Designed large animal models of infection for translational drug testing.

Institute of Infectious Diseases & Pathogenic Microbiology (Prienai, Lithuania)

Co-Founder, Head of Pathogenic Microbiology Department | 2017–Present

- Oversaw research initiatives on intracellular pathogens and diagnostics.
- Supervised development of in vitro/in vivo testing platforms.
- Design antiviral candidates (SARS-CoV-2) and screening platforms (EU funded).

J. Bardzilauskienė Clinical Microbiology Lab (Vilnius, Lithuania)

Medical Microbiologist/Mycologist | 2014–2016

- Processed clinical samples, performed mycological and general diagnostics, and AST by CLSI and EUCAST guidelines.

Department of Microbiology, LSMU (Kaunas, Lithuania)

Volunteer → Research Assistant – Dr. R. Planciūnienė Lab | 2008–2012

- Supported culture and molecular biology work on clinical pathogens (isolation, AST, genotyping).

Abstract

Title of dissertation: Multi-Omics–Based Discovery of Host Receptors Driving the Pathogenesis of Emerging Fungal Pathogens.

Povilas Kavaliauskas, Doctor of Philosophy, 2025.

Dissertation directed by: Vincent M. Bruno, PhD

Professor Institute for Genome Sciences & Department of Microbiology and Immunology University of Maryland School of Medicine

Emerging fungal pathogens such as *Candida auris*, *Lomentospora prolificans*, and *Scedosporium* spp. present urgent clinical challenges due to their intrinsic antifungal resistance and ability to cause invasive disease in immunocompromised patients. The molecular basis of their interactions with host epithelial cells remains poorly defined. This dissertation develops a multi-omics discovery strategy that integrates affinity pulldown assays, quantitative proteomics, phosphoproteomics, and transcriptomics to identify host receptors mediating fungal adhesion. Three receptors—integrin $\beta 4$ (ITG $\beta 4$), epidermal growth factor receptor (EGFR), and hepatocyte growth factor receptor (c-MET)—were prioritized. Functional assays demonstrated that ITG $\beta 4$ is a conserved adhesion receptor for multiple fungal species, with chitin identified as a candidate ligand. In parallel, phosphoproteomic profiling revealed that *L. prolificans* dynamically modulates host signaling through EGFR and c-MET phosphorylation. These findings define ITG $\beta 4$, EGFR, and c-MET as clinically relevant host receptors, providing novel insight into epithelial pathogenesis and establishing potential targets for host-directed antifungal interventions.

Multi-Omics–Based Discovery of Host Receptors Driving the Pathogenesis of Emerging
Fungal Pathogens

by Povilas Kavaliauskas

Dissertation submitted to the Faculty of the Graduate School of the
University of Maryland, Baltimore in partial fulfillment
of the requirements for the degree of
Doctor of Philosophy

2025

Dedication

I dedicate this thesis to the memory of Dr. Rita Planciūnienė, my first mentor in medical microbiology and a dear friend. Her guidance, encouragement, and example shaped the foundation of my scientific path. Although she is no longer with us, her influence and inspiration remain deeply present in my work.

Acknowledgments

I would like to express my sincere gratitude to my dissertation advisor, Dr. Vincent Bruno, for his guidance, support, and mentorship throughout this work. His insight and commitment to scientific rigor have been invaluable in shaping this dissertation and my development as a scientist. I am also deeply grateful to Dr. Thomas J. Walsh for his continuous guidance and advice, which have greatly influenced my scientific growth.

I thank my dissertation committee—Dr. Robert Ernst, Dr. David Rasko, Dr. Eileen Barry, and Dr. Vidmantas Petraitis—for their constructive feedback and important perspectives that strengthened this work. I am also grateful to many colleagues across multiple laboratories, including Dr. Riley Risteen, Karen Graf, and Marcia Cortes (UMB), as well as Ruta Petraitiene, MD (CDI), Dr. Ramunė Grigalevičiūtė (Lithuanian University of Health Sciences), and Ruta Prakapaite (Biozentrum, Basel) for their contributions and advice. I appreciate the support of Dr. Michail Lionakis and his laboratory (NIH) and Dr. Ashraf Ibrahim (UCLA) for their collaboration in *in vivo* studies.

I gratefully acknowledge the Henry Schueler 41 & 9 Foundation for supporting my doctoral fellowship and making this research possible. Finally, I thank my family for their constant support and encouragement, and my friends, colleagues, and mentors for their role in my personal and scientific journey.

Table of Contents

<i>Curriculum vitae</i>	1
<i>Abstract</i>	3
<i>Dedication</i>	iii
<i>Acknowledgments</i>	iv
<i>Table of Contents</i>	v
<i>List of Tables</i>	viii
<i>List of Figures</i>	ix
<i>List of Abbreviations</i>	xii
Chapter 1: Introduction	1
Emerging fungal pathogens.....	1
Clinical presentation of <i>Candida auris</i> infections.....	4
Clinical forms of infections caused by <i>Scedosporium</i> and <i>Lomentospora</i> species.....	6
Treatment of infections caused by <i>Candida auris</i>	8
Strategies to treat infections caused by <i>Scedosporium</i> and <i>Lomentospora</i> species.....	13
Molecular pathogenesis of emerging fungal pathogens	14
Pathogenesis of <i>Candida auris</i> : Adhesion and colonization of skin and indwelling catheters .	15
Host immune response to <i>Candida auris</i>	18
Pathogenesis of <i>Scedosporium</i> and <i>Lomentospora</i> : Early fungal interaction with lung epithelial cells.....	21
Host immune response to <i>Scedosporium</i> and <i>Lomentospora</i>	25
Study design and rationale.....	28
Chapter 2: Integrin $\beta 4$ Functions as the Keratinocyte Receptor Mediating <i>Candida auris</i> Adhesion to Host	29
Introduction	29
Materials and methods.....	32
Cell lines and culture conditions	32
Fungal strains and culture conditions	32
Preparation of biotinylated HaCaT protein lysates.....	33
Expression of human INTG $\beta 4$ -GFP in HEK293.....	34
Whole-cell affinity purification using <i>C. auris</i> and biotinylated HaCaT proteins	34
Streptavidin purification and proteomic analysis	35
<i>Candida auris</i> thermal inactivation	35
Protease K digestion of <i>C. auris</i> surface proteins	36

Pulldown using purified chitin	36
Validation of target protein binding to fungal isolates by immunoblot.....	37
Tissue culture infection - Preparation of inoculum and infection of the cells.....	38
siRNA mediated INTG β 4 silencing in human and mouse keratinocytes.....	38
INTG β 4 blockage using antibodies.....	39
Cytokine ELISA.....	40
Results and discussion.....	41
Whole-Cell Affinity Pulldown Identifies Integrin β 4 as a Host Protein Binding <i>Candida auris</i>	41
Integrin β 4 Facilitates <i>Candida auris</i> Binding to Keratinocytes.....	47
Integrin β 4 Is Not Required for the Innate Immune Response of HaCaT Keratinocytes to <i>Candida auris</i>	53
Integrin β 4 binding to <i>Candida auris</i> is not dependent on Als4112 but is mediated through ITG β 4 interaction with chitin.....	55
Conclusions.....	62
Chapter 3. Multi-omics–Guided Identification of EGFR and c-MET as Host Receptors Mediating Lomentospora prolificans Adhesion to Human Lung Epithelial Cells.....	66
Introduction.....	66
Materials and methods.....	68
Ethics statement.....	68
Fungal strains and culture conditions.....	69
Cell lines and culture conditions.....	69
<i>L. prolificans</i> induced damage to HSAEC1-Kt cells.....	69
<i>Galleria mellonella</i> infection model.....	70
Actin filamentation staining.....	71
RNA sequencing (RNA-seq).....	71
Proteomic and phosphoproteomic analysis.....	72
Preparation of biotinylated HSAEC1-KT protein lysates.....	73
Whole-cell affinity purification using <i>L. prolificans</i> and biotinylated HSAEC1-KT proteins .	74
Streptavidin Enrichment and Proteomic Analysis.....	74
Tissue culture infection experiments.....	75
Immunoblotting.....	76
siRNA mediated c-MET and EGFR silencing in HSAEC1-Kt cells and adhesion assay.....	76
Pharmacological manipulation of EGFR and cMET in HSAEC1-Kt cells and adhesion assay	77
Cytokine analysis by ELISA.....	78
Murine model of pulmonary lomentosporiasis.....	78

Results and discussion.....	79
<i>Lomentospora prolificans</i> exhibits pathogenicity in <i>Galleria mellonella</i> and neutropenic murine models	79
Interaction of <i>L. prolificans</i> with human airway epithelial cells.....	83
Multi-omic analysis of <i>L. prolificans</i> infected HSAEC1-KT cells	87
EGFR and c-MET growth factor receptors mediate host interaction with <i>Lomentospora prolificans</i>	92
EGFR and c-MET are phosphorylated in HSAEC1-KT cells following <i>Lomentospora prolificans</i> infection	97
EGFR and c-MET govern <i>L. prolificans</i> adhesion and immune responses in HSAEC1-KT human airway epithelial cells	100
The effect of EGFR and c-MET inhibition on survival in a neutropenic murine model of pulmonary lomentosporiasis.....	106
Conclusions	108
Chapter 4. Integrin β4 is a receptor for emerging fungal pathogens.....	111
Introduction	111
Materials and methods.....	111
Fungal strains and culture conditions	112
Cell lines and culture conditions	112
Whole-cell affinity purification using <i>L. prolificans</i> and biotinylated HSAEC1-KT and A549 proteins	113
Immunoblotting	113
Results and discussion.....	114
Integrin β 4 from airway epithelial cells can bind to <i>L. prolificans</i>	114
Integrin β 4 promotes <i>L. prolificans</i> adherence to airway epithelial cells.....	117
Integrin β 4 promotes adherence of <i>S. apiospermum</i> and <i>S. boydii</i> to airway epithelial cells..	119
Conclusions	121
Chapter 5. Future directions.....	125
ITG β 4 in <i>C. auris</i> colonization and persistence	125
EGFR and c-MET in <i>L. prolificans</i> pathogenesis	126
<i>In Vivo</i> validation through conditional knockout systems.....	127
Appendix.....	129
References:	136

List of Tables

Table 1.1: The fungal strains used for this study 44

Table 3.1: List of primary antibodies used for immunoblotting detection 88

List of Figures

Figure 1.1. Examples of echinocandin antifungal drugs used as a first-line treatment option for <i>C. auris</i> infections.	19
Figure 1.2. Examples of azole antifungal drugs used to treat infections caused by <i>Candida</i> species.	21
Figure 1.3. Examples of newly approved antifungal drugs used to treat infections caused by <i>Candida</i> species.	22
Figure 1.4. <i>Candida auris</i> adhesins Als4112 and Scf1 are important for colonization of skin through interaction with host extracellular matrix proteins.	26
Figure 1.5. Host response to <i>C. auris</i> skin colonization and infection. NK – natural killer cells, Th17 – Th17 type lymphocytes.	29
Figure 1.6. Representative photomicrographs of <i>Scedosporium apiospermum</i> , <i>Scedosporium boydii</i> , and <i>Lomentospora prolificans</i> hyphi and conidia morphology.....	33
Figure 1.7. Representation of <i>Scedosporium</i> and <i>Lomentospora</i> strategies to adhere to human airway epithelial cells via interaction with host extracellular matrix proteins (ECM) and other surface exposed proteins.	35
Figure 1.8. The host immune response to <i>Scedosporium</i> and <i>Lomenstorspora</i> pulmonary infections.	37
Figure 2.1. Schematic representation of the whole-cell affinity pulldown technique used to identify keratinocyte-derived host surface proteins that directly bind <i>Candida auris</i> . .	53
Figure 2.2. <i>Candida auris</i> isolates representing distinct genetic clades are capable of binding host ITG β 4 derived from HaCaT cells.	55
Figure 2.3. Integrin β 4 can associate with diverse pathogenic yeast species.....	56
Figure 2.4. Recombinant ITG β 4–GFP fusion protein, but not GFP alone, was able to bind <i>Candida auris</i>	57
Figure 2.5. siRNA-mediated suppression of ITG β 4 in human HaCaT and mouse XB-2 keratinocytes significantly reduced <i>Candida auris</i> binding.	59
Figure 2.6. Antibody-mediated blockade of ITG β 4 reduced <i>Candida auris</i> binding to keratinocytes.	61
Figure 2.7. ITG β 4 is required for antibody-mediated suppression of <i>Candida auris</i> adhesion to HaCaT human keratinocytes.....	62
Figure 2.8. Overexpression of ITG β 4 in HEK293 cells results in increased <i>Candida auris</i> binding.	63
Figure 2.9. ITG β 4 is not involved in the innate immune response of HaCaT keratinocytes to <i>Candida auris</i>	66

Figure 2.10. <i>C. auris</i> adhesin Als4112 is not involved in interaction with ITGβ4.	68
Figure 2.11. Heat inactivation, but not protease K digestion of <i>C. auris</i> suppressed ITGβ4 binding.....	69
Figure 2.12. Purified chitin can bind ITGβ4 but not EGFR in pulldown assay.....	70
Figure 2.13. Chitin synthesis inhibition reduces ITGβ4 binding to <i>Candida albicans</i> SC5314 under FBS-free conditions.	72
Figure 2.14. ITGβ4 overexpression enhances HEK293 cell adhesion to chitin and chitosan surfaces.	73
Figure 3.1. Virulence of <i>Lomentospora prolificans</i> isolates in the <i>Galleria mellonella</i> infection model.	93
Figure 3.2. <i>Lomentospora prolificans</i> DI16-483 induces lethality in a neutropenic murine pulmonary model.	95
Figure 3.3. The HSAEC1-Kt infection with <i>L. prolificans</i> does not induces significant cell death over 72 hours period of infection.	97
Figure 3.4. Invasion of HSAEC1-KT human small airway epithelial cells by <i>Lomentospora prolificans</i> requires actin cytoskeleton rearrangement and it is partly blocked by cytochalasin D.	99
Figure 3.5. The changes of gene expression in HSAEC1-Kt cells following infection with <i>L. prolificans</i> DI16-483 at 3 (A), 6 (B), and 16 (C) hours post infection (p.i.).....	101
Figure 3.6. The changes in proteome and phospho-proteome profiles of HSAEC1-Kt cells following infection with <i>Lomentospora prolificans</i> DI16-483	102
Figure 3.7. Integrated pathway analysis (IPA) predicts activation of growth factor receptor signaling in HSAEC1-KT cells following <i>Lomentospora prolificans</i> (L.p) infection, with comparative profiling against the closely related species <i>Scedosporium apiospermum</i> (S.a) and <i>Scedosporium boydii</i> (S.b).....	104
Figure 3.8. Schematic representation of the whole-cell affinity pulldown technique used to identify human small airway epithelium-derived host surface proteins that bind <i>L. prolificans</i>	106
Figure 3.9. Proteomic LC-MS pulldown experiments identified multiple host cell surface proteins that directly interact with <i>Lomentospora prolificans</i> conidia.	107
Figure 3.10. EGFR directly binds <i>Lomentospora prolificans</i> conidia and germlings in affinity pulldown assays.	108
Figure 3.11. c-MET directly binds <i>Lomentospora prolificans</i> conidia and germlings in affinity pulldown assays.	109
Figure 3.12. Proteomic-based analysis of EGFR Tyr1197 phosphorylation dynamics in HSAEC1-Kt cells during <i>Lomentospora prolificans</i> infection.....	110

Figure 3.13. Proteomics-based profiling of c-MET phosphorylation during <i>Lomentospora prolificans</i> infection of HSAEC1-Kt cells.	111
Figure 3.14. EGFR Tyr 1197 phosphorylation is induced by <i>Lomentospora prolificans</i> infection of HSAEC1-KT cells.	113
Figure 3.15. EGFR silencing by siRNA in HSAEC1-KT human airway epithelial cells reduces the adhesion of <i>Lomentospora prolificans</i>	114
Figure 3.16. c-MET silencing by siRNA in HSAEC1-KT human airway epithelial cells reduces the adhesion of <i>Lomentospora prolificans</i>	116
Figure 3.17. Pharmacological inhibition of EGFR and c-MET with FDA approved inhibitors reduces <i>Lomentospora prolificans</i> adhesion to HSAEC1-KT human airway epithelial cells.	117
Figure 3.18. EGFR silencing alters cytokine responses in HSAEC1-KT cells infected with <i>Lomentospora prolificans</i>	118
Figure 3.20. Effect of EGFR and c-MET inhibition on survival in a neutropenic murine model of pulmonary <i>Lomentospora prolificans</i> infection.	120
Figure 4.1. <i>L. prolificans</i> can bind integrin $\beta 4$ across all tested isolates in Protease K and heat inactivation non-depended manner.	126
Figure 4.2. <i>L. prolificans</i> binds integrin $\beta 4$ derived from A549 cell lysates but not no fungi empty tube controls.	126
Figure 4.3. Binding of recombinant integrin $\beta 4$ –GFP fusion protein to <i>Lomentospora prolificans</i> clinical isolates.	127
Figure 4.4. Integrin $\beta 4$ mediates <i>Lomentospora prolificans</i> adherence to airway epithelial cells.	128
Figure 4.8. Integrin $\beta 4$ mediates adherence of <i>Scedosporium boydii</i> and <i>Scedosporium apiospermum</i> to airway epithelial cells.	130
Figure 4.6. Pulldown of endogenous integrins $\beta 4$ and $\alpha 6$ from HSAEC1-KT cells with <i>Lomentospora prolificans</i> isolate DI16-489.	132
Figure 4.7. Integrin $\beta 4$ binding to <i>Lomentospora prolificans</i> is not inhibited by laminin.	133

List of Abbreviations

ABC	ATP-binding cassette
CFU	Colony forming units
CNS	Central Nervous System
CSI-4	Chitin Synthesis Inhibitor 4
DMEM	Dulbecco's Modified Eagle Medium
ECM	Extracellular matrix
EGFR	Epidermal Growth Factor Receptor
ELISA	Enzyme-linked immunosorbent assay
FPPL	Fungal Priority Pathogens List
GPI	Glycosylphosphatidylinositol
hTERT	Human telomerase reverse transcriptase
ITG β 4	Integrin β 4
LC-MS	Liquid chromatography–coupled tandem mass spectrometry
MIC	Minimal Inhibitory Concentration
MOI	Multiplicity of infection
PRM	Peptidorhamnomannans
PVDF	Polyvinylidene difluoride
SAGM	Small Airway Epithelial Cell Growth Medium
TLR's	Toll like receptor
WHO	World Health Organization

Chapter 1: Introduction

Emerging fungal pathogens

Global fungal disease results in a substantial and underappreciated public health burden [1-3]. Recent estimations indicate ~6.5 million incident invasive fungal infections annually and ~3.8 million associated deaths, of which ~2.5 million are directly attributable to fungal disease [1, 4]. The World Health Organization (WHO) introduced the Fungal Priority Pathogens List (FPPL) in 2022 to highlight fungal species associated with the greatest global health burden and resistance threat. The FPPL stratifies pathogens into critical, high, and medium priority groups, underscoring the urgent need to expand therapeutic options, address the limitations of the current antifungal armamentarium, and advance fundamental understanding of fungal biology and pathogenesis [1, 2, 4].

Invasive fungal infections are most frequently caused by a relatively limited group of pathogens, predominantly *Aspergillus fumigatus*, *Candida albicans*, and species in the order *Mucorales*. The global annual incidence of invasive candidiasis (including candidemia) exceeds 1.5 million cases, with approximately 995,000 deaths each year [1, 4, 5]. Invasive candidiasis, confirmed by histology or imaging, carries a high mortality burden where mortality rates frequently range between 30–60%, with some ICU-based population studies reporting mortality approaching 40–60% despite standard antifungal therapy. *C. albicans* remains the most commonly identified species in invasive disease, although non-*albicans Candida* species are becoming increasingly prominent [1]. Among them, *C. auris* has emerged globally as an urgent threat, known for its ability to

cause healthcare-associated outbreaks, its persistence in the hospital environment, and its frequent multidrug resistance. Unlike *C. albicans*, *C. auris* isolates display high antifungal resistance and a robust ability to form biofilms and remains poorly understood in terms of pathogenesis and host interactions [6].

Among filamentous molds, *Aspergillus fumigatus* is the most common agent of invasive fungal infections, particularly in immunocompromised hosts such as hematopoietic stem cell and solid organ transplant recipients, and those with hematologic malignancies [7]. Invasive pulmonary aspergillosis is associated with poor clinical prognosis where several meta-analyses in patients with severe influenza estimated incidence at approximately 10–11% of hospitalized individuals, with mortality rates exceeding 50%. Mortality rates associated with invasive pulmonary aspergillosis are particularly high in profoundly neutropenic patients and are further elevated in cases caused by azole-resistant *A. fumigatus* strains [2].

Mucormycoses, fungal infections cause by filamentous molds belonging to the order *Mucorales* (including species form the genera *Rhizopus*, *Mucor*, and *Lichtheimia*), have emerged with increasing frequency, especially in patients with diabetes mellitus, hematologic malignancies, or those receiving corticosteroids [8, 9]. These devastating fungal infections are characterized by rapid progression, multi-organ dissemination, and extensive tissue destruction, often necessitating aggressive antifungal therapy combined with extensive surgical debridement, which may result in significant disfigurement [9, 10]. In disseminated mucormycosis, or mucormycosis with rhino-cerebral involvement, the outcome is usually very poor. Even with correct, timely and aggressive antifungal therapy, the mortality rates are usually greater than 50% [9].

Beyond these well-recognized pathogens, an increasing number of less common fungi have been identified as significant opportunistic agents of invasive disease resulting in substantial mortality. Species within the genera *Scedosporium* and *Lomentospora*, as well as *Fusarium* and other rare molds, are now associated with life-threatening infections in severely immunocompromised patients or immunocompetent patients with near drowning experience or traumas [5, 11, 12]. These organisms are notable for their intrinsic resistance to multiple antifungal classes, leaving few, if any, consistently effective therapeutic options. Infections caused by *Scedosporium* and *Lomentospora* typically present as pulmonary disease with subsequent dissemination to multiple organs, most notably the central nervous system in the case of *L. prolificans*, although the underlying pathogenic mechanisms remain poorly understood [13, 14]. In contrast, *Fusarium* species frequently cause soft tissue, bone, and ocular infections, and are commonly associated with fungemia and widespread multi-organ involvement [15, 16].

Historically, pathogens such as *C. albicans*, *A. fumigatus*, and *Rhizopus oryzae* (Mucorales) have been studied extensively in terms of molecular pathogenesis, drug development, pharmacology and genetics [5, 9, 16]. However, there are still significant gaps of knowledge surrounding the more recently recognized and emerging fungal pathogens, such as *L. prolificans*, *Scedosporium spp.*, and *C. auris*. In this chapter I will discuss the current knowledge on these rare fungal pathogens, including epidemiology, treatment and host-pathogen interactions [11, 12, 14-16].

Clinical presentation of *Candida auris* infections

C. auris causes nosocomial infections across settings with sustained colonization pressure such as use of disinfectants, intensive device use, and broad-spectrum antimicrobial exposure. High-risk populations include patients in intensive care units and residents of nursing facilities, where transmission is linked to shared equipment and environmental persistence, especially in linens, sinks, and floor mops [17]. Besides elderly and critically sick patients, neonates constitute a distinct vulnerable group. Neonatal *C. auris* cases are primarily associated with prematurity, low birth weight, invasive devices, and prior antimicrobial, with outbreaks demonstrating rapid transmission and clinically significant invasive disease [18]. In critically ill adults, colonization at multiple body sites predicts subsequent candidemia and marks a continuum from carriage to invasive infection [6].

Bloodstream infection is the predominant invasive presentation and is frequently associated with colonization of intravascular devices, such as indwelling vascular catheters which continuously seed *C. auris* directly to the bloodstream resulting in persistent candidemia [6, 19]. In addition to candidemia, *C. auris* also presents as catheter-associated infections, surgical-site and wound infections, and device-adjacent soft-tissue disease in patients with prolonged hospitalization and multiple invasive procedures. These syndromes often require systemic antifungal therapy combined with local surgical debridement or device removal for durable control [6, 20]. Consistent with this, the urinary tract is an increasingly common site of *C. auris* detection in hospitalized patients, particularly among catheterized patients [20, 21]. Large datasets and prevalence studies have demonstrated that *C. auris* can be frequently recovered from urine, but

Careful clinical judgment is required to distinguish colonization from true infection before initiating therapy [21, 22]. Respiratory tract and pleural involvement have been described typically in ventilated patients with multiple comorbidities, though definitive attribution is challenging because isolation from non-sterile sites may represent colonization rather than infection. Therefore, the clinical decision often requires additional guidance by histological confirmation of invasion [20, 22].

C. auris infection outcomes and overall survival vary significantly by host factors, timeliness of diagnosis, antimicrobial susceptibility, effectiveness of source control, and the virulence of the *C. auris* isolate causing invasive and disseminated infection with multi-organ involvement [23, 24]. Candidemia infections caused by *C. auris* are associated with a greater mortality and longer hospital stays compared to similar infections caused by other *Candida* species, while ICU-directed analyses suggest that severity of illness and device burden are dominant determinants of prognosis [24]. Interestingly, echinocandin exposure with emergent resistance, azole non-susceptibility, and diagnostic delays remain central therapeutic challenges that worsen survival and result in poor treatment prognosis among affected patients [25].

The overall clinical spectrum of *C. auris* is defined by catheter-associated candidemia with complications involving wounds, urinary tract, and possible skin-derived translocation. Careful clinical judgment is crucial to distinguish invasive infection from colonization-derived detection.

Clinical forms of infections caused by *Scedosporium* and *Lomentospora* species

Scedosporium spp. and *Lomentospora prolificans* cause opportunistic, invasive fungal infections across a spectrum of patients, with the highest risk observed in patients with hematologic malignancies, profound or prolonged neutropenia, hematopoietic stem cell or solid-organ transplantation, and those receiving intensive immunosuppressants [16, 26]. Interestingly, among patients with cystic fibrosis and structural lung disease, these molds can colonize and cause local infections without substantial tissue invasion and systemic spread [26, 27].

Among the *Scedosporium spp.*, the most common species that causes infection include *S. apiospermum*, *S. boydii*, *S. aurantiacum*, and less commonly, *S. dehoogii*. *Lomentospora prolificans* (formerly *Scedosporium prolificans*). These species are phylogenetically distinct and have recently been placed in its own genus [28, 29]. While morphologically phenotypically similar and closely related, these classifications are clinically meaningful because species differ in epidemiology and antifungal susceptibility [11, 27].

By species, *S. apiospermum* and *S. boydii* classically cause eumycetoma (skin and soft-tissue infection) and a wide range of localized or invasive infections such as pulmonary, sinus, osteoarticular, ocular, and endocarditis. Interestingly, these fungi have well documented tropism for the central nervous system (CNS), and fungal lesions are often expected to be observed in scedosporiosis disease following near-drowning and during end stage airway colonization in cystic fibrosis patients. Clinically, scedosporiosis often presents as allergic bronchopulmonary disease in chronically colonized cystic fibrosis patients, lung mycetoma formation, and post-transplant invasive disease.

Endocarditis and urinary tract infections are described but less frequent [11]. *S. aurantiacum* is increasingly shown to colonize the airways of cystic fibrosis patients prior to administration of mucus-producing medications and in severe infections (pulmonary, soft-tissue, and disseminated), including fatal cases after near-drowning. *S. aurantiacum* isolates often exhibit high MICs across multiple classes of currently available antifungals, making these infections extremely challenging to manage in the clinical setting [30, 31].

In contrast, *L. prolificans* is distinguished by rapid angioinvasion, frequent hematogenous dissemination, and even more limited susceptibility to current antifungals, in comparison to *Scedosporium* species. Disseminated infections of *L. prolificans* in neutropenic or transplant populations carry high mortality, whereas focal osteoarticular or ocular disease may occur after trauma or surgery in otherwise immunocompetent individuals. These infections are characterized with poor treatment response and often relapse [14, 31-33]. In otherwise immunocompetent individuals, *L. prolificans* is more likely to cause localized infections, often after trauma or surgery. Osteoarticular disease has been described following fractures or joint injuries in children and adults, sometimes progressing to chronic osteomyelitis and septic arthritis that respond poorly to antifungal therapy alone. Several reports describe the necessity of repeated surgical debridement combined with prolonged antifungal therapy, often using voriconazole in combination with terbinafine or antifungal-loaded bone cement, to achieve even partial responses [34, 35]. Ocular diseases, including keratitis, endophthalmitis, and panophthalmitis, have also been documented, usually in the setting of immunosuppression or direct ocular trauma. These infections are particularly devastating and frequently require enucleation, although

rare cases of prolonged survival on investigational antifungals such as olorofim have been reported [36].

Infections caused by *Scedosporium* and *Lomentospora* species represent some of the most challenging scenarios in clinical mycology [14-17]. While species of the *S. apiospermum* complex are more often linked to localized pulmonary or soft tissue disease with the potential for dissemination in immunocompromised hosts, *L. prolificans* is characterized by rapid angioinvasion, early hematogenous spread, and near pan-resistance to antifungal drugs, leading to exceedingly poor outcomes in disseminated disease due to rapid progression and multi-organ involvement.

Treatment of infections caused by *Candida auris*

Successful treatment of *Candida auris* depends upon early species-level identification at the clinical laboratories, susceptibility testing, rapid initiation of an active antifungal agent, and rigorous source control, such as removal of infected intravascular devices. Treatment delays at any step are consistently linked to increased mortality in candidemia patients and further outbreaks in the hospital setting [37]. Echinocandins, β -1,3-D-glucan synthase inhibitors, are recommended as initial therapy for most invasive presentations owing to their favorable activity against bloodstream isolates and biofilm-forming populations (**Figure 1.1**). Data from endemic centers similarly support echinocandin-first strategies for the treatment of *C. auris* candidemia [38].

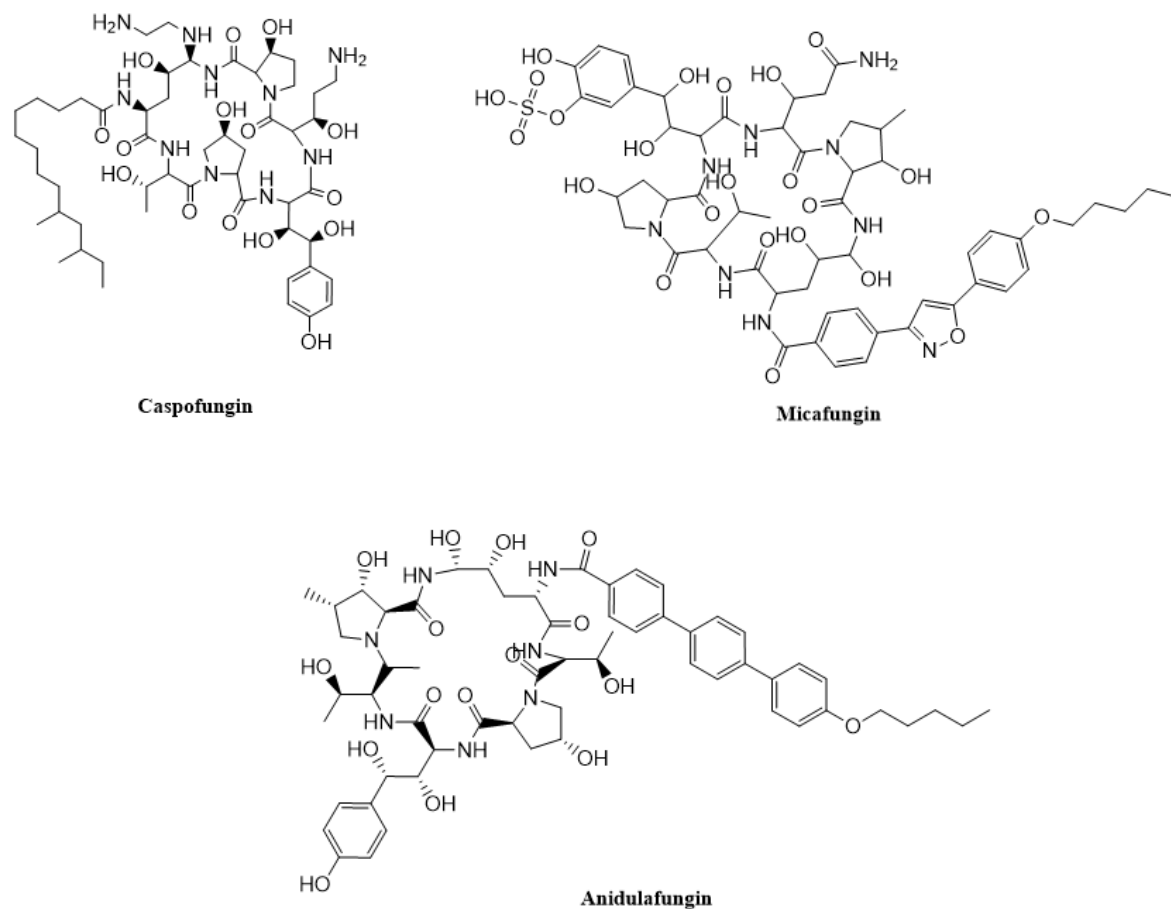


Figure 1.1. Examples of echinocandin antifungal drugs used as a first-line treatment option for *C. auris* infections.

Despite the first line use of echinocandins, resistance during therapy is an increasing concern. Echinocandin resistance in *C. auris* and other *Candida* species, is mediated primarily by mutation in the *FKS1* gene, which encodes β -1,3-D-glucan synthase. Genomic analyses of serially collected isolates demonstrated stepwise accumulation of *FKS1* mutations under drug pressure, with corresponding MIC elevations and clinical failures in persistent infections [39-42]. Azoles, such as fluconazole, voriconazole, and isavuconazole are also widely used to treat infections caused by *Candida* species, although azole-resistance is a very common problem among

C. auris isolates (**Figure 1.2**) [43]. Azole resistance is commonly driven in part by Y132F and K143R mutations in the *ERG11* gene, which encodes lanosterol 14 α -demethylase, a cytochrome P450 enzyme essential for ergosterol biosynthesis [47]. These amino acid substitutions remodel the azole-binding pocket of the enzyme, thereby lowering drug affinity and diminishing the inhibitory effect of azole antifungals [44-46]. In addition to target-site alterations, resistance is frequently compounded by upregulation of efflux transporters. These pumps fall into two major families: ATP-binding cassette (ABC) transporters, such as *CDR1* and *CDR2*, which use ATP hydrolysis to actively export azoles, and major facilitator superfamily (MFS) transporters, most notably *MDR1*, which rely on proton gradients for drug efflux. Overexpression of ABC transporters is strongly linked to broad-spectrum azole resistance, whereas *MDR1* upregulation confers resistance primarily to fluconazole [47-49]. Together, *ERG11* mutations and efflux pump activity synergize to compromise the efficacy of azoles, limiting the use of oral step-down antifungal regimens and complicating long-term management of resistant infections. [44, 50].

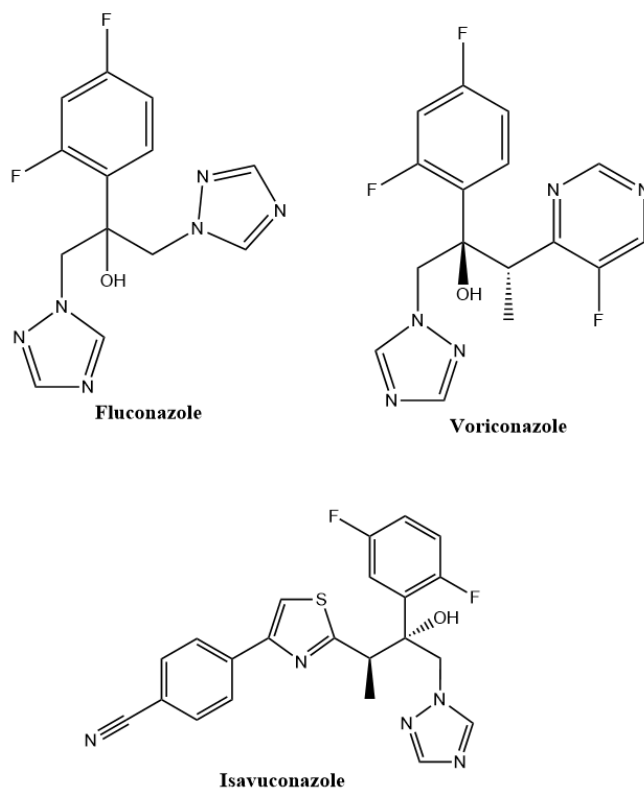


Figure 1.2. Examples of azole antifungal drugs used to treat infections caused by *Candida* species.

In clinical cases of *C. auris* infections where echinocandin MICs are elevated but not completely resistant, some treatment centers consider pharmacokinetic optimization (higher pharmacological exposure) to maintain steady exposure of drugs in accordance of PK/PD data [51]. Liposomal amphotericin B serves as an alternative when echinocandins cannot be used or are ineffective, however, variable polyene MICs and toxicity considerations necessitate careful clinical monitoring [52].

Among novel and newly approved antifungals, ibrexafungerp, fosmanogepix, and rezafungin show promise in managing *C. auris* and other drug-resistant *Candida* species infections (**Figure 1.3**).

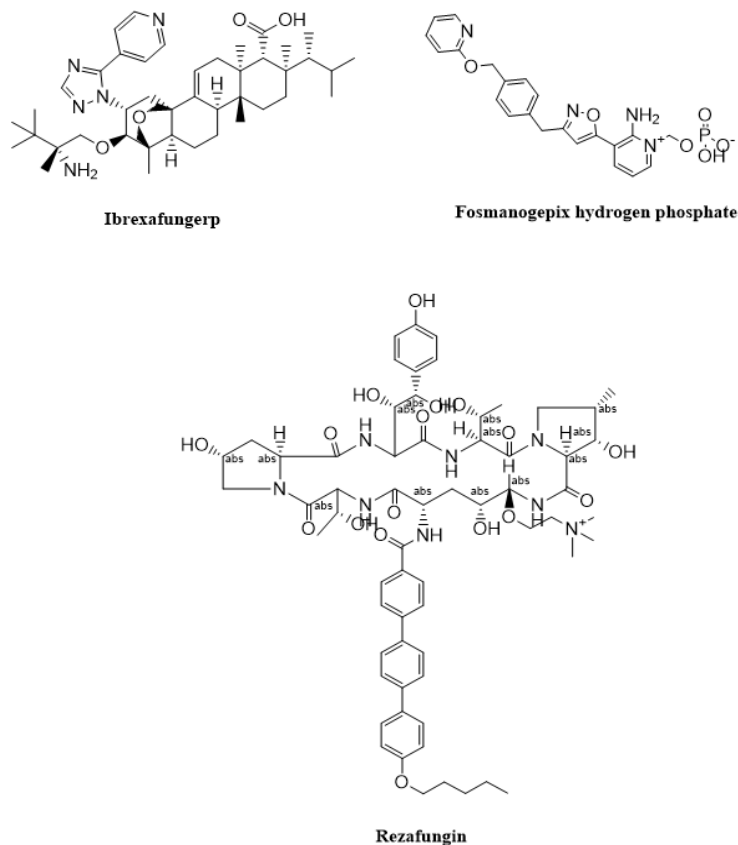


Figure 1.3. Examples of newly approved antifungal drugs used to treat infections caused by *Candida* species.

Ibrexafungerp, a first-in-class oral triterpenoid glucan synthase inhibitor, exhibits broad *in vitro* activity against *C. auris*, including many azole- and echinocandin-resistant isolates [53-54]. Delayed-start murine models and early clinical experiences show reduced fungal burdens and clinical responses in invasive candidiasis due to *C. auris*, making ibrexafungerp a potential step down or salvage therapy option when susceptibility and clinical context align (**Figure 1.3**) [53-55]. Fosmanogepix, a first-in-class antifungal prodrug, inhibits Gwt1p, a conserved inositol acyltransferase encoded by the *GWT1* gene. Gwt1p is an essential endoplasmic reticulum membrane protein that catalyzes the acylation of inositol in glycosylphosphatidylinositol (GPI) anchor

precursors, a critical early step in GPI anchor biosynthesis required for the proper localization and function of many cell wall mannoproteins. Inhibition of Gwt1p disrupts cell wall integrity and impairs fungal growth. Fosmanogepix has demonstrated potent in vitro activity and provided significant survival benefits in murine disseminated *Candida auris* infection models. (**Figure 1.3**) [56, 57]. Rezafungin, a long-acting echinocandin with a prolonged half-life with once weekly dosing, retains activity against most *C. auris* isolates, including some with reduced susceptibility to other echinocandins and shows favorable efficacy in murine *C. auris* models (**Figure 1.3**) [58].

Strategies to treat infections caused by *Scedosporium* and *Lomentospora* species

Infections caused by *Scedosporium* and *Lomentospora* require an approach that integrates rapid species level identification using microscopical phenotypic assays or MALDI-TOFF, antifungal susceptibility testing, aggressive source control, and reversal of immunosuppression or neutropenia. Treatment outcomes and therapeutic responses are linked to the particular causative agent and the antifungal resistance profiles of isolates. For example, isolates from the *S. apiospermum* complex are comparatively more susceptible to certain triazoles, whereas *L. prolificans* exhibits broad non-susceptibility to amphotericin B, azoles, and echinocandins, with high case-fatality in disseminated disease [29].

For scedosporiosis, voriconazole is the first line of therapy. Clinical and experimental models demonstrate activity of voriconazole alone and in combinations with other antifungals against *S. apiospermum*, with reports of cure in localized and invasive disease when accompanied by source control and therapeutic drug monitoring

[59, 60]. Surprisingly, amphotericin B guided therapy is generally inferior, and echinocandins have limited utility as monotherapy [29].

Lomentosporiosis presents a distinct therapeutic problem. *In vitro* and clinical datasets show uniformly high MICs to most approved antifungal agents and mortality in disseminated infection is markedly elevated despite treatment [31, 61]. Voriconazole monotherapy often fails, although combination therapies such as voriconazole plus systemic terbinafine improve survival and response rates compared [14]. New and investigational antifungal agents expand options for *L. prolificans* salvage therapy. Olorofim (formerly F901318), an orotomide that inhibits dihydroorotate dehydrogenase, shows potent *in vitro* activity against *Scedosporium* spp. and *L. prolificans* and has been used compassionately, including disseminated lomentosporiosis [36, 62]. Fosmanogepix (formerly APX001) demonstrates low MICs against *Scedosporium* and *Lomentospora* and activity in disseminated murine models [63].

The lack of available treatment options for infection causes by *Scedosporium* and *Lomentospora* highlights the need for development of novel antifungal compounds, new combinational therapies, and host-directed therapeutics.

Molecular pathogenesis of emerging fungal pathogens

Understanding the molecular mechanisms that drive pathogenesis is essential to reducing the morbidity and mortality caused by emerging fungal pathogens because it connects genotype, regulated virulence machinery, and host–pathogen interactions to clinical phenotypes and therapeutic commodities. Understanding both host and pathogen determinants that enable tissue invasion, immune evasion, biofilm formation, and

environmental persistence provides tools to develop pathogen and host-directed therapeutics [7, 64]. In *C. auris*, thermotolerance, osmotolerance, robust biofilm architecture, cell-wall remodeling, and drug-resistance mechanisms couple with skin and device colonization to drive disease progression, although a detailed understanding of the molecular mechanisms is lacking [65, 66]. In *Scedosporium* spp. and *L. prolificans*, intrinsic multidrug resistance, epithelial attachment, tissue invasion, and angioinvasive spread, particularly in neutropenic hosts could be exploited for therapeutic modulation [28]. By mapping these circuits with genetics and multi-omics, and validating them in translational models, detailed understanding of molecular pathogenesis provides the rationale to discover novel antifungal targets, optimize combination regimens, and develop adjunctive host-directed therapies that improve outcomes emerging fungal pathogens, such as *C. auris* and *Scedosporium* and *Lomentospora*.

Pathogenesis of *Candida auris*: Adhesion and colonization of skin and indwelling catheters

Candida auris has the unique ability to colonize the skin, indwelling vascular catheters and persist in the hospital environment, which underpins its rapid spread [67]. Unlike *C. albicans*, which preferentially colonizes mucosal sites, *C. auris* efficiently establishes itself on keratinized epithelial surfaces. Experimental models have demonstrated that *C. auris* isolates can survive long-term on murine and porcine skin, and resist desiccation and chemical disinfection. These properties are likely to contribute to the observed transmission of *C. auris* in healthcare settings [66]. This persistence is driven by a combination of fungal surface proteins, metabolic flexibility, and biofilm formation.

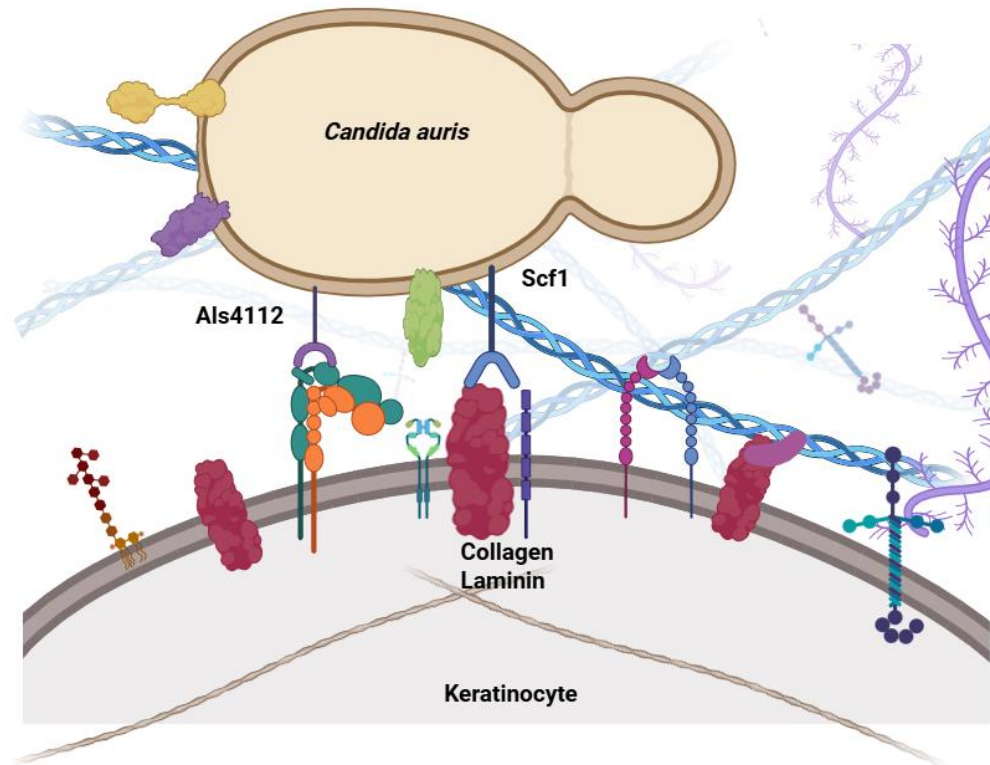


Figure 1.4. *Candida auris* adhesins Als4112 and Scf1 are important for colonization of skin through interaction with host extracellular matrix proteins.

Recently, *C. auris* specific adhesins have been identified, including Als4112 and Scf1, which are critical for binding to skin epithelium, promoting colonization, and contributing to virulence [68, 69]. *C. auris* Scf1 mediates broad adhesion to abiotic and biological substrates via exposed cationic residues rather than the hydrophobic interactions typical of canonical fungal adhesins (**Figure 1.4**). Loss of *SCF1* impairs biofilm formation, epidermal colonization, catheter colonization, and virulence in systemic models, indicating a central role in both persistence and invasive potential [68,69]. On the other hand, Als4112, an ALS-family adhesin upregulated in skin-like niches, promotes attachment to keratinocytes and binds extracellular-matrix ligands, with preferential interactions reported for basement-membrane components such as laminin. Deletion of *ALS4112* reduces epidermal burden in epicutaneous mouse models and

attenuates dissemination, underscoring its contribution to colonization fitness and pathogenesis (**Figure 1.4**) [69].

Als4112 and Scf1 remain the only adhesion molecules of *C. auris* that have been experimentally discovered and characterized to date. However, based on observations in other fungal pathogens, it is highly likely that *C. auris* harbors a broad repertoire of cell-surface proteins and engages multiple host receptors to facilitate adhesion, persistence, and possibly invasion. In *C. albicans*, for example, adherence and invasion are mediated by several adhesins and invasins, including members of the Als family and Hwp1. These fungal effectors interact with host receptors such as epidermal growth factor receptor (EGFR) and hepatocyte growth factor receptor (*c*-MET), forming multi-receptor complexes that trigger phosphorylation cascades, cytoskeletal rearrangements, and actin-dependent endocytosis of fungal cells [70, 71].

At present, there is no direct evidence that *C. auris* undergoes intracellular invasion of epithelial cells. Most available data indicate that the pathogenic lifestyle is dominated by skin colonization, biofilm formation, and environmental persistence on abiotic surfaces [69]. Nonetheless, by analogy to *C. albicans* and invasive molds, it is plausible that *C. auris* could exploit growth factor receptors or extracellular matrix (ECM) proteins such as laminin, fibronectin, or vitronectin [72-74]. Such interactions might enhance its ability to adhere, persist, or even penetrate host barriers through yet uncharacterized mechanisms.

While Als4112 and Scf1 represent the first described components of the *C. auris* adhesin repertoire, the broader network of adhesin–ligand and receptor-mediated interactions remain unexplored. Defining whether this pathogen can engage receptor

tyrosine kinases like EGFR and *c*-MET, or other ECM-associated host factors, will be crucial to delineating its molecular strategies of colonization and identifying novel therapeutic or preventive targets.

Host immune response to *Candida auris*

Candida auris elicits a distinctive host immune response that differs in several respects from the better-characterized immune response to *C. albicans*. At the level of innate immunity, studies using *in vitro* and animal models have shown that *C. auris* is able to persist on the skin and survive in superficial niches such as the stratum corneum, where its recognition by pattern-recognition receptors appears to be blunted (**Figure 1.5**) [75, 76].

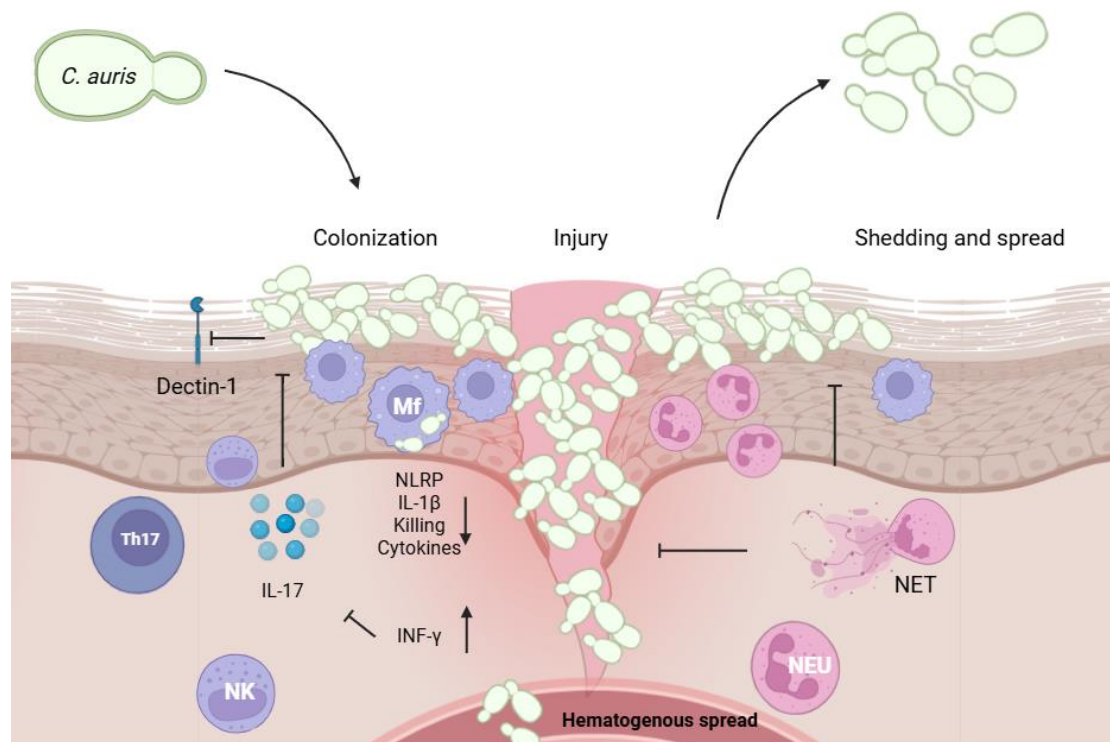


Figure 1.5. Host response to *C. auris* skin colonization and infection. NK – natural killer cells, Th17 – Th17 type lymphocytes.

In barrier tissues, such as the skin and mucosa, activation of the Dectin-1/TLR2/TLR4 axis by *C. auris* cell wall components is muted when compared to the *C. albicans* cell wall components. This suppression is in part due to differences in the architecture of the outer mannan layer and glycosylation which effectively reduce *C. auris* engagement by phagocytes [77]. This dampened sensing due to the structural modifications correlates with poor neutrophil recruitment and killing relative to *C. albicans*, which has a cell wall that is much more immunogenic [78]. Murine and swine skin models demonstrate that control of colonization depends on IL-17 receptor signaling by epithelial and innate lymphoid compartments, consistent with the centrality of the type-17 axis in antifungal defense at epithelial surfaces (**Figure 1.5**) [77-79]. *C. auris* dampens IL-17 signaling, thus establishing a niche for long term persistence and spread. Work in these animal models has established that *C. auris* persists in the skin structures, sheds to the environment, and seeds healthcare-associated transmission. These features reinforce the importance of early innate immune response at the skin interface (**Figure 1.5**) [78, 79].

Interestingly neutrophil responses constitute a major point of divergence from *C. albicans*. In human *ex vivo* assays, zebrafish or murine models, neutrophils mount robust oxidative bursts, phagocytosis, and NETosis (neutrophil degranulation) against *C. albicans* but respond weakly to *C. auris* where NET release is minimal, and phagocytic uptake and killing are markedly reduced [78]. These data identify neutrophil evasion as a hallmark of *C. auris* pathogenesis and likely contribute to its ability to maintain high burdens on skin and to disseminate in vulnerable hosts (**Figure 1.5**) [80].

Mononuclear phagocytes internalize *C. auris* but frequently fail to sterilize. In macrophages, *C. auris* survives and can damage host cells while avoiding strong NLRP3 inflammasome activation and IL-1 β release [81]. Comparative transcriptional and metabolic analyses indicate that *C. auris* deploys distinct metabolic programs after phagocytosis that blunt canonical inflammasome outputs [81]. By contrast, *C. albicans* readily triggers inflammasome signaling in macrophages and dendritic cells, with implications for downstream T-cell priming and protective cytokine production (**Figure 1.5**) [82, 83].

Cutaneous infection models further support the idea that *C. auris* actively dampens host immune responses. Intradermal *C. auris* infection recruits neutrophils, inflammatory monocytes, macrophages, dendritic cells, NK cells, and T cells, however, a predominance of IFN- γ can suppress IL-17–mediated protection and exacerbate dermal injury [84]. Conversely, strains or genetic backgrounds that favor filamentation or aggregation elicit stronger IL-17 responses, greater neutrophil engagement, and lower fungal burdens, suggesting that morphotype and surface architecture tune the balance between pathogenic IFN- γ –dominant inflammation and protective type-17 immunity [85]. In classic *C. albicans* skin and mucosal models, coordinated Th1/Th17 responses are typically protective without the same IFN- γ –driven antagonism of IL-17 signaling (**Figure 1.5**) [79, 86].

Adaptive immunity to *C. auris*, like *C. albicans*, mimics the barrier emphasis on the IL-17 axis [86,87]. Th17 cells and the effector cytokines IL-17A/F and IL-22 are essential to restrain epithelial burdens and promote chemokine-guided neutrophil killing. Vaccinology studies have identified conserved fungal cell wall proteins as potential

immunotherapeutic targets. The *C. albicans* Als3p-based vaccine, NDV-3A, elicits cross-reactive antibodies and CD4⁺ T-cell responses that extend protection to *Candida auris*. In preclinical models, NDV-3A reduced *C. auris* biofilm formation, enhanced macrophage-mediated killing, and conferred significant protection against lethal disseminated infection in mice. At the same time, the detrimental potential of IFN- γ -skewed responses in *C. auris* skin disease underscores simple boosting may be insufficient and the quality and polarity of the response are critical for protection (**Figure 1.5**) [87].

Collectively, these findings demonstrate that *C. auris* possesses unique traits that attenuate host immune recognition through cell-wall remodeling and active modulation of host responses, thereby enabling sustained persistence on mammalian skin and abiotic surfaces. This immune evasion, together with biofilm formation and environmental hardiness, facilitates efficient colonization of both hosts and healthcare environments, promoting ongoing transmission of this emerging pathogen.

Pathogenesis of *Scedosporium* and *Lomentospora*: Early fungal interaction with lung epithelial cells

The molecular mechanisms underlying the pathogenesis of the emerging molds *Scedosporium* and *Lomentospora* remain poorly understood, yet these fungi are increasingly recognized as clinically significant opportunistic pathogens. Their remarkable environmental persistence, particularly in soil, polluted water, and hospital settings, facilitates continuous exposure and infection risk [13]. A key virulence trait is the production of multiple types of melanin, which protects against oxidative stress, antifungal agents, and host immune defenses, thereby enhancing survival during infection

[88]. In addition, the their conidia enables efficient aerosolization and deep penetration into the distal airways, where they can establish infection in pulmonary tissue and, in some cases, disseminate to the central nervous system (**Figure 1.6**).

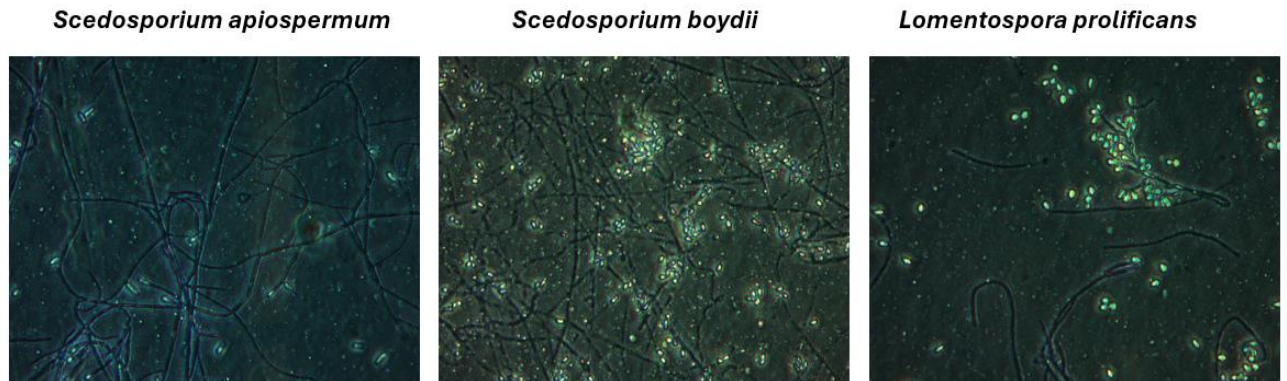


Figure 1.6. Representative photomicrographs of *Scedosporium apiospermum*, *Scedosporium boydii*, and *Lomentospora prolificans* hyphi and conidia morphology. The fungal elements were visualised by lactophenol cotton blue staining.

When inhaled, *Scedosporium* and *Lomentospora* conidia reach the small airways, where they come into close contact with airway epithelial cells and initiate adhesion. This adhesion represents a crucial step in the establishment of infection, as it enables the fungi to resist clearance mechanisms within the respiratory tract. In the absence of effective adhesion, conidia would be rapidly eliminated through continuous mucociliary clearance and airflow during respiration, thereby preventing colonization and subsequent tissue invasion [89].

Adhesion of *Scedosporium* and *Lomentospora* to lung epithelium is multi-factorial and begins with rapid, avid binding of conidia to pneumocytes, followed by germination and intercellular hyphal penetration (**Figure 1.7**) [89, 90]. Studies using A549 cells, type II pneumocytes derived cancerous cell, have shown that *S. aurantiacum*

conidia attach to A549 cells within 4 hours, with scanning electron microscopy showing germ tubes breaching epithelial junctions and no appreciable conidial internalization. This is in contrast to some *Aspergillus* and Mucorales models that undergo epithelial uptake via growth factor receptor dependent pathways (**Figure 1.7**) [90]. Cell-wall peptidorhamnomannans (PRM) function as bona fide adhesins with yet unknown host ligand. Blocking PRM–host interactions with purified PRM or anti-PRM antibodies inhibits adherence of *Scedosporium* conidia to epithelial monolayers and identifies a 25-kDa epithelial binding partner PRM that is conserved across the *Scedosporium* and *Lomentospora* complex, supporting a shared adherence mechanism [91]. *S. apiospermum* also deploys fibronectin-binding surface molecules that allows conidia bind both immobilized and soluble human fibronectin, and competitive or antibody blockade decreases attachment to lung epithelial cells, consistent with an ECM-bridging route (**Figure 1.7**) [92]. It not known whether this fungal-host ECM interaction results in downstream signaling or if the interaction, beyond the adhesion, is biologically relevant and further driving the infection.

S. apiospermum expresses a fucose-specific lectin (SapL1) that binds human bronchial epithelial cells in a fucose-dependent manner, implicating glycan recognition as an adhesion strategy [93]. Ultrastructural phenotypic work across *Scedosporium* and *Lomentospora* species shows robust conidial attachment and early germination on lung cell monolayers, with epithelial injury ensuing as hyphae extend along and between cells (**Figure 1.7**) [93].

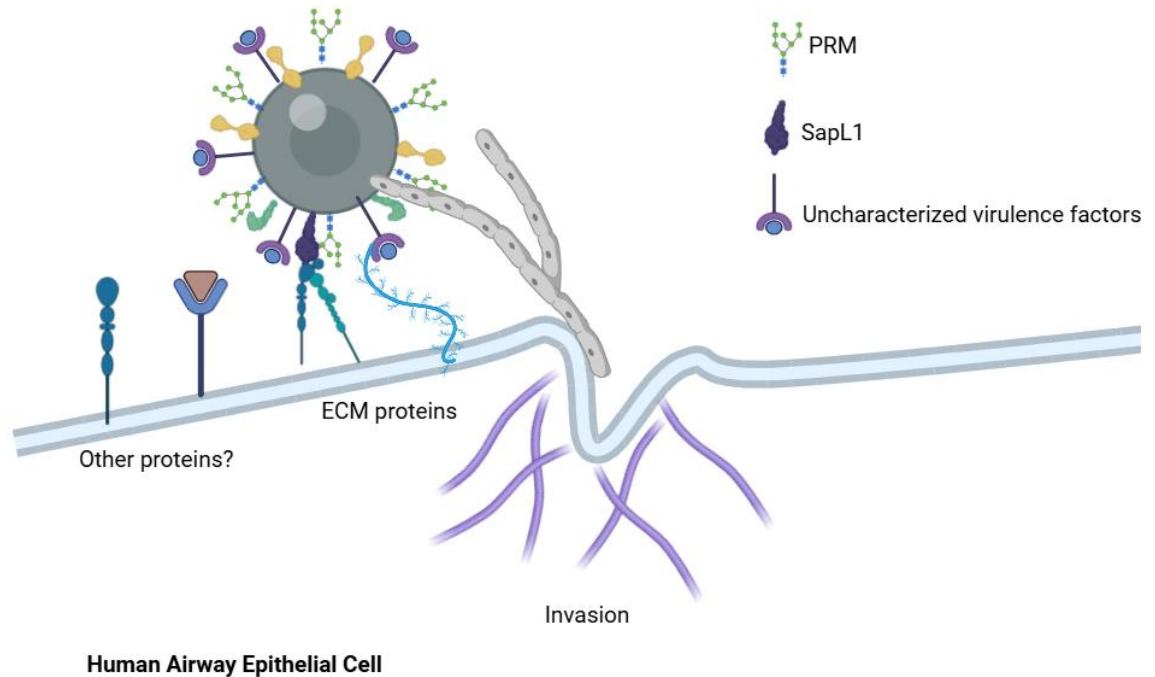


Figure 1.7. Representation of *Scedosporium* and *Lomentospora* strategies to adhere to human airway epithelial cells via interaction with host extracellular matrix proteins (ECM) and other surface exposed proteins. PRM – peptidorhamnomannans, SapL - fucose-specific lectin.

Adhesion of *Scedosporium* and *Lomentospora* to the lung epithelium is rapid and predominantly extracellular, driven by peptidorhamnomannan–host interactions, extracellular-matrix bridging (for example via fibronectin), and glycan–lectin recognition, which together promote conidial germination, intercellular hyphal extension, and early epithelial injury (**Figure 1.7**) [92]. It also remains unclear whether the interaction between *Scedosporium* or *Lomentospora* surface molecules and host ECM components initiates downstream signaling cascades within airway epithelial cells, and if so, what the biological relevance of these processes might be beyond adhesion itself. In well-studied fungi such as *A. fumigatus*, engagement of ECM proteins like fibronectin, laminin, or vitronectin not only promotes adhesion but also activates host signaling pathways that influence epithelial integrity, cytokine secretion, and recruitment of

immune effector cells [92, 94, 95]. These interactions can modulate host immune recognition, contribute to epithelial damage, and enhance tissue invasion. By contrast, whether *Scedosporium* and *Lomentospora* exploit similar mechanisms remains to be determined, highlighting a critical gap in understanding how these molds orchestrate infection and persistence within the host lung environment.

It remains plausible that these emerging fungal pathogens also engage additional epithelial receptors that are highly expressed at the cell surface and may deploy alternative invasion mechanisms under distinct microenvironmental conditions. Notably, much of the current knowledge is based on studies using the transformed A549 alveolar epithelial line, accordingly it is uncertain whether identical adhesion and invasion strategies operate in primary, non-transformed airway epithelia or *in vivo*, underscoring the need for validation in physiologic human models and relevant animal systems [96].

Host immune response to *Scedosporium* and *Lomentospora*

Conidial peptidorhamnomannans and related rhamnomannan-rich glycoconjugates are major characterized pathogen-associated molecular patterns (REF??). Murine macrophages sense conidia via MyD88, TLR4, and CD14, with PRM/rhamnomannan fractions driving MAPK activation, I κ B α degradation, and secretion of TNF, IL-6, and CXCL10; removal of PRM abrogates cytokine induction [97]. Glycosphingolipids—especially glucosylceramides (GlcCer) are also immunoactive, enhancing pro-inflammatory responses and fungicidal activity in macrophages and, *in vivo*, skewing toward Th1/Th17-type cytokines [98]. Melanization further shapes early host sensing and survival where genetic disruption of the PIG1-

regulated DHN-melanin pathway in *S. apiospermum* compromises resistance to host-derived stresses, consistent with melanin's ROS-scavenging and immune-evasive roles (Figure 1.8) [99].

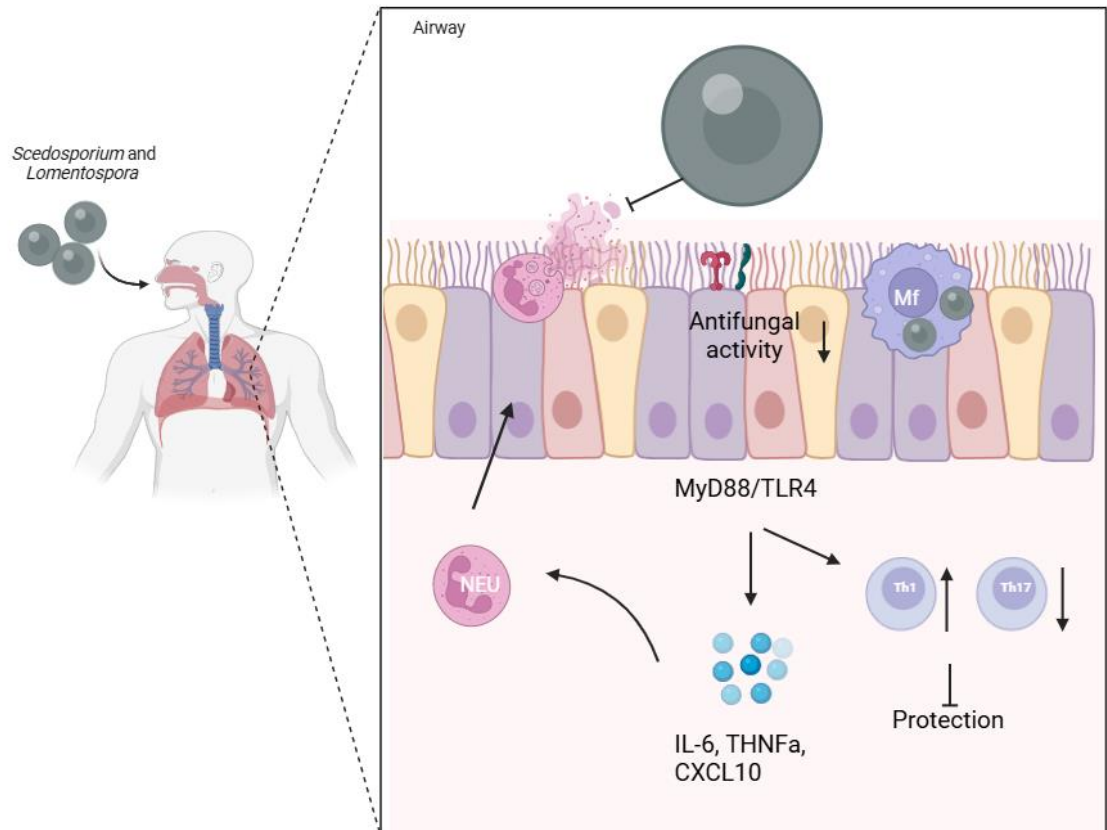


Figure 1.8. The host immune response to *Scedosporium* and *Lomentospora* pulmonary infections. NEU – neutrophils, Th1 – Th1 type lymphocytes, Th17 – Th17 type lymphocytes, Mf – macrophages.

Neutrophils and mononuclear phagocytes are central effectors but their efficacy is variable. In classic *in vitro* assays, *Scedosporium* and *Lomentospora* conidia and hyphae are phagocytosed and elicit oxidative burst, yet antifungal killing is usually defective, particularly against *L. prolificans* [100]. Exogenous IFN- γ and GM-CSF can synergistically boost neutrophil superoxide generation and antifungal activity, suggesting

cytokine-dependent rescue of otherwise suboptimal effector function. Macrophage interactions are likewise complex, where *L. prolificans* PRM can promote macrophage activation and early TNF- α production but has also been shown to drive macrophage death and immunomodulation, indicating that cell-wall ligands can both modulate phagocytes depending on context and dose. In lung and systemic models, this imbalance likely contributes to tissue damage, angiogenesis, and hematogenous spread typical of severe scedosporiosis and lomentosporiosis (**Figure 1.8**) [100].

Adaptive immunity to these molds is less extensively studied than for *Aspergillus* or *Candida* but several similarities have been characterised. PRM can actively skew the adaptive response toward non-protective profiles as seen in murine invasive scedosporiosis, where PRM immunization reduced pro-inflammatory cytokines, increased IgG1, and expanded regulatory T cells without augmenting Th17, worsening survival after challenge. Also, fungal glycosphingolipids provide a counterpoint that *L. prolificans* GlcCer elicits Th1/Th17-leaning cytokines and recruits inflammatory cells *in vivo*, suggesting that selected lipid antigens may be harnessed to drive protective cellular responses [98, 101, 102].

Collectively, available data point to a protective role for Th1/Th17-polarized responses at mucosal and deep-tissue sites, with antibody alone unlikely to suffice given the organisms' melanin-mediated stress resistance, biofilm formation, and angiogenesis [101, 102].

Study design and rationale

Infections caused by emerging fungal pathogens such as *Scedosporium* species, *L. prolificans* and *Candida auris* are increasingly recognized as major threats to human health. *C. auris* has become a global concern due to its capacity for rapid spread in healthcare settings, persistence on surfaces, and frequent multidrug resistance, which complicates outbreak control and treatment. *L. prolificans*, on the other hand, is notorious for causing disseminated infections in immunocompromised patients, including transplant recipients and those with hematologic malignancies, where treatment options are extremely limited and outcomes are often fatal. Despite their rising clinical impact, virtually nothing is known about the molecular mechanisms that govern how these pathogens interact with the host during infection.

The goal of this thesis work was to define novel host–pathogen interactions that facilitate *L. prolificans* and *C. auris* persistence and disease progression, with a particular emphasis on the pulmonary environment where infections often initiate. To achieve this, we employed a broad discovery pipeline which combined omics-based approaches with functional validation strategies to identify host surface proteins that act as receptors for these fungi. Once candidate host targets were shown to physically interact with fungal cells, their downstream roles in promoting adhesion, immune evasion, or tissue invasion were systematically evaluated. This work provides an essential foundation for understanding the biology of these underexplored pathogens and for guiding the development of novel host-directed or pathogen-targeted therapeutic strategies.

Chapter 2: Integrin β 4 Functions as the Keratinocyte Receptor Mediating *Candida auris* Adhesion to Host

Introduction

Candida auris (*C. auris*) is a multidrug-resistant yeast that has emerged globally as a healthcare-associated pathogen capable of sustained nosocomial transmission, environmental persistence, and difficult eradication using standard healthcare-associated cleaning and disinfection strategies [3, 103]. Clinically, *C. auris* presents along a spectrum from asymptomatic skin colonization to invasive disease. While candidemia is the most common presentation, *C. auris* can also cause wound infections, otitis, and genitourinary infections in patients with substantial healthcare exposure, innate and acquired immunopathology and various surgically implanted medical devices [104]. Due to profound antifungal resistance, infections caused by *C. auris* often result in high treatment costs for healthcare and elevated mortality rates [105].

Genomically, *C. auris* comprises at least five well-supported phylogeographic clades (I–V) with distinct antifungal resistance profiles and clinical/ecological tendencies [43]. Epidemiological molecular surveillance data demonstrated that Clade II (East Asian) is disproportionately recovered from ear infections, whereas Clades I, III, and IV are more often implicated in invasive outbreaks [43, 106]. Comparative pathogenesis studies using vertebrate and invertebrate animal models clearly demonstrate clade-dependent heterogeneity in virulence. When tested in a murine neutropenic model of bloodstream infection, *C. auris* isolates spanning four different clades produced a variable spectrum of survival and tissue burden in a manner that suggested disease severity reflects both clade biology and host context [107, 108].

C. auris establishes initial contact with the host predominantly through the skin, where it exhibits robust colonization of keratinized epithelium leading to subsequent colonization of deeper dermal layers [79, 109]. Surface colonization factor 1 (SCF1), a GPI-anchored adhesin, is crucial for *C. auris* adhesion to skin surfaces and biofilm formation on implanted medical devices [68]. Another *C. auris* adhesin, Als4112, is important for *C. auris* adhesion to keratinocytes through its interaction with host extracellular matrix proteins such as laminins and collagen V [69]. Despite these findings, the host receptors for *C. auris* and their function during colonization, dissemination, and systemic infection processes remain incompletely understood.

Single-cell RNAseq analysis of *C. auris* infected murine skin demonstrated recruitment of neutrophils, inflammatory monocytes, macrophages, dendritic cells, NK cells, and T lymphocytes that are known for expression of various pattern recognition receptors, such as TLR's, C-lectins, NLR's, RIG and others [110]. Interestingly, *C. auris* undermines skin immunity during reinfection by skewing T-cell responses toward IFN- γ -secreting Th1 cells via IL-12 derived from inflammatory macrophages and monocyte-derived dendritic cells which, in turn, results in the loss of protective IL-17-mediated responses [84, 110]. Furthermore, the structurally altered outer mannan layer of the *C. auris* cell wall modulates host immune polarization toward these nonprotective Th1 responses [84]. The *C. auris*-induced production of IFN- γ exacerbates dermal damage and paradoxically facilitates persistent *C. auris* skin infection.

Despite recent advances in understanding *C. auris* infection biology, very little is known about the specific host surface receptors on keratinocytes or within the dermis that engage *C. auris* adhesins. Importantly, known *C. auris* adhesins such as SCF1 and

Als4112 do not account for all of the ability of *C. auris* to adhere to host cells as deletion mutants of these adhesins still have some ability to adhere, although both mutant are severely attenuated compared to the wild-type isolates of *C. auris* [68]. Thus, there are likely additional, as yet uncharacterized, fungal ligands that contribute to colonization and virulence. The existence of yet uncharacterized adhesins not only broadens our understanding of *C. auris* pathogenesis, but also opens new opportunities for therapeutic intervention. In the same manner, host-derived receptors capable of mediating adhesion and persistence on skin are almost certainly more diverse than currently described in literature, although yet none have been conclusively identified. Defining these host–pathogen molecular interactions is critical, as their elucidation could provide novel targets for host-directed therapies or prophylactic strategies aimed at disrupting the earliest steps of *C. auris* colonization and subsequent infection.

In this chapter, I present an omics-guided strategy to identify and characterize a previously unrecognized role for integrin $\beta 4$ (ITG $\beta 4$) in mediating *Candida auris* adhesion to keratinocytes. Functional validation demonstrated that silencing of ITG $\beta 4$ expression, or its blockade using monoclonal antibodies, significantly reduced *C. auris* burden on both human and murine keratinocytes. Furthermore, biochemical assays revealed that chitin can associate with ITG $\beta 4$, supporting its potential role as a fungal ligand expressed by *C. auris* and implicating the ITG $\beta 4$ –chitin axis as a key mechanism of host–pathogen interaction during *C. auris* colonization.

Materials and methods

Cell lines and culture conditions

The Human keratinocyte cell line (HaCaT cells) was kindly provided by Dr. J. Pedra (University of Maryland, Baltimore School of Medicine) and cultured in Dulbecco's Modified Eagle Medium (DMEM; Gibco, 11965092) supplemented with 10% heat-inactivated fetal bovine serum (FBS; SigmaAldrich, F4135) and 1% Penicillin–Streptomycin (Pen-Strep; Gibco, 15140122). Mouse XB-2 keratinocytes (ATCC, CL-177) were maintained on mitomycin C-treated murine 3T3-J2 fibroblast feeder layers in DMEM supplemented with 20% heat-inactivated FBS and 1% Pen-Strep. HEK293 cells (provided by Dr. D. Gaykalova, University of Maryland, Baltimore School of Medicine) were cultured in poly-D-lysine–coated tissue culture flasks in DMEM supplemented with 10% heat-inactivated FBS and 1% Pen-Strep.

Fungal strains and culture conditions

Candida auris isolates from the AR Isolate Bank (CDC) were kindly provided by Dr. Mary Ann Jabra-Rizk (University of Maryland School of Dentistry). The wild-type strain (WT), Als4112 deletion mutant (Δ ALS4112), the complemented strain (Δ ALS4112:ALS4112), , previously described by [69], were also provided by Dr. Mary Ann Jabra-Rizk and maintained as frozen glycerol stocks at -80°C . (**Table 1.1**) Unless otherwise specified, fungal strains were sub-cultured from frozen stocks onto potato dextrose agar (PDA, BD Difco, 213400) plates and incubated overnight at 37°C . Two or three well-isolated colonies were subsequently transferred to yeast extract–peptone–dextrose (YPD) broth and grown overnight at 37°C with agitation at 150 rpm.

Table 1.1. The fungal strains used for this study.

Isolate	Strain number
<i>Candida albicans</i>	SC5314
<i>Candida auris</i>	AR-0381
<i>Candida auris</i>	AR-0382
<i>Candida auris</i>	AR-0383
<i>Candida auris</i>	AR-0384
<i>Candida auris</i>	AR-0385
<i>Candida auris</i>	AR-0386
<i>Candida auris</i>	AR-0387
<i>Candida auris</i>	AR-0388
<i>Candida auris</i>	AR-0389
<i>Candida auris</i>	Δ ALS4112
<i>Candida auris</i>	Δ ALS4112:ALS4112
<i>Candida glabrata</i>	b62
<i>Candida tropicalis</i>	PT
<i>Cryptococcus neoformans</i>	H99

Preparation of biotinylated HaCaT protein lysates

HaCaT cells were seeded into 100-mm tissue culture plates at a density of 5×10^6 cells/plate and grown to near confluency. Confluent monolayers were placed on ice for 10 min and washed three times with 10 mL of ice-cold DPBS. Cell-impermeable Sulfo-NHS-SS-biotin (BroadPharm, 325143) was dissolved in DMSO and diluted in PBS (pH 8.0) to a final concentration of 0.5 mg/mL. The biotinylation reagent was applied to the cells and incubated on ice for 1 h with gentle rocking. Following incubation, the reagent was aspirated, and unreacted Sulfo-NHS-SS-biotin was quenched with quenching buffer (1 \times PBS, pH 8.0, 100 mM glycine) for 10 min on ice. Labeled cells were subsequently washed three times with ice-cold DPBS containing 1 mM PMSF. Cells were then lysed in 2 mL of lysis buffer (5.6% n-octyl- β -D-glucopyranoside, 1 \times DPBS, 1 mM PMSF, 1 \times

protease inhibitor cocktail set), scraped, and collected. Lysates were sonicated briefly and clarified by centrifugation at $10,000 \times g$ for 10 min at 4°C . Protein concentration was determined using either the Pierce BCA Protein Assay Kit (Pierce, 23225) or the Qubit Protein Quantification Kit (Invitrogen, Q33211). Protein lysates were aliquoted into microcentrifuge tubes and stored at -80°C until further use.

Expression of human INTG β 4-GFP in HEK293

HEK293 cells were seeded into poly-D-lysine-coated 100-mm culture plates at a density of 3.8×10^5 cells/mL. Following overnight incubation, cells were transfected with $12 \mu\text{g}$ of pINTGB4-GFP (Addgene #205092) using TransIT-LT1 (MirusBio, MIR 2304) transfection reagent. After 24 h, INTG β 4-GFP expression was verified by fluorescence microscopy. For protein extraction, cells were placed on ice for 10 min, and 1 mL of lysis buffer (5.6% n-octyl- β -D-glucopyranoside, $1\times$ DPBS, 1 mM PMSF, $1\times$ protease inhibitor cocktail) was added before scraping. Lysates were sonicated and clarified by centrifugation at $20,000 \times g$ for 10 min at 4°C , and the supernatant was collected. Protein concentration was quantified using either the Pierce BCA Protein Assay Kit or the Qubit Protein Quantification Kit. Lysates were aliquoted into microcentrifuge tubes and stored at -80°C until further use.

Whole-cell affinity purification using *C. auris* and biotinylated HaCaT proteins

C. auris AR-0382 and AR-0387 were grown in YPD medium as described above. Overnight cultures were centrifuged at $10,000 \times g$ for 10 min at 4°C , the supernatant was aspirated, and *C. auris* pellets were washed three times with ice-cold $1\times$ DPBS

supplemented with 1 mM PMSF. Cells were counted using a hemocytometer, and approximately 8×10^8 *C. auris* cells were incubated with 5 mg of surface-biotinylated HaCaT proteins at 4 °C with gentle rotation overnight. Following incubation, cells were pelleted by centrifugation at $10,000 \times g$ for 5 min, and the supernatant was collected and designated as flow-through (FT). Pelleted cells were then washed three times with 600 μ L of ice-cold wash buffer (1 \times DPBS, 1 mM PMSF, 1 \times protease inhibitor cocktail). Bound host proteins were subsequently eluted by adding 200 μ L of lysis buffer (6 M urea, 5.6% n-octyl- β -D-glucopyranoside, 1 \times DPBS, 1 mM PMSF, 1 \times protease inhibitor cocktail) and incubating at room temperature for 10 min. Samples were sonicated briefly, centrifuged at $20,000 \times g$ for 3 min, and the resulting supernatant, designated as eluted proteins (EP), was collected and stored at -80 °C until further analysis.

Streptavidin purification and proteomic analysis

For proteomic LC–MS analysis and protein identification, proteins obtained from whole-cell affinity purification were dialyzed against 1 \times DPBS. Biotinylated proteins were subsequently enriched using streptavidin-conjugated magnetic beads (Pierce, 88816). Bead-bound proteins were then submitted to the Proteomics and Metabolomics Core Facility at Weill Cornell Medicine (Cornell University) for human protein identification by LC–MS/MS.

***Candida auris* thermal inactivation**

To prepare heat-inactivated *C. auris*, cultures were grown overnight in YPD broth as described above. Cells were harvested by centrifugation, washed three times with 1 \times

DPBS containing 1 mM PMSF, and resuspended in 1 mL of the same buffer. Thermal inactivation was performed by incubating the cell suspension in a heat block at 95 °C for 1 h. Complete inactivation was confirmed by plating 10 μ L of the heated suspension on PDA plates and verifying the absence of growth. The heat-killed cells were subsequently washed three times with 1 \times DPBS supplemented with 1 mM PMSF, counted using a hemocytometer, and approximately 8×10^8 cells were used for whole-cell affinity pulldown experiments.

Protease K digestion of *C. auris* surface proteins

C. auris was harvested from overnight YPD broth, washed 3 times using 1 \times DPBS. The washed cells were then suspended to digestion buffer (1X PBS, 1 mM calcium chloride) and Protease K (SigmaAldrich, P6556) was added to a concentration of 150 μ g/mL. The surface proteins of *C. auris* were digested at 37 °C with shaking at 150 rpm for 3 hours. After protease K digestion, cells were centrifuged at 10,000 \times g for 10 min, supernatant was discarded, and the protease K inactivated by incubating cells with 1 mM PMSF for 10 mins. The digested cells were then washed 1 \times DPBS supplemented with 1 mM PMSF. Viability was confirmed by plating on PDA and the Protease K digested *C. auris* was counted using a hemocytometer, and approximately 8×10^8 cells were used for whole-cell affinity pulldown experiments.

Pulldown using purified chitin

Commercially available chitin (Santa Cruz Biotechnology, sc-280638) was placed into 2 mL microcentrifuge tubes, washed three times with 1 \times DPBS containing 1 mM

PMSF, and resuspended in 100 μ L of the same buffer. The prepared chitin suspension was then used for pulldown assays with 5 mg of protein lysate, as described above.

Validation of target protein binding to fungal isolates by immunoblot

Fungal isolates were grown and harvested as described above. Pellets were washed three times with ice-cold 1 \times DPBS supplemented with 1 mM PMSF. Cells were counted using a hemocytometer, and approximately 8×10^8 cells were used for pulldown experiments using non-biotinylated HaCaT proteins, recombinant INTGB4-GFP or GFP produced in HEK293 cells isolated as described above. Bound host proteins were subsequently eluted by adding 200 μ L of lysis buffer (6 M urea, 5.6% n-octyl- β -D-glucopyranoside, 1 \times DPBS, 1 mM PMSF, 1 \times protease inhibitor cocktail) and incubating at room temperature for 10 min. Samples were sonicated briefly, centrifuged at 20,000 \times g for 3 min, and the resulting supernatant, designated as eluted proteins (EP), were used for western Blotting.

Lysates were separated by electrophoresis using the XCell SureLock Mini-Cell II system (Life Technologies) and subsequently transferred onto polyvinylidene difluoride (PVDF) membranes with the Invitrogen XCell II Blot Module, following the manufacturer's instructions. Membranes were then blocked in TBS-based blocking buffer (LI-COR) for 1 h at room temperature before being incubated with primary antibodies overnight. Rabbit anti INTGB4 (D8P6C) (Cell Signaling Technology, 14803), mouse anti beta actin (Cell Signaling Technology, 3700), rabbit anti GFP (D5.1) (Cell Signaling Technology, 2956) were used to probe human lysates. Rabbit anti INTGB4 (Proteintech, 25277-1) was used to probe murine lysates. On the following day, the membranes were

washed four times with TBS-t (1X TBS, 0.1% Tween 20) followed by 1 h incubation at room temperature with IRDye secondary antibodies. The proteins were then visualized using Odyssey CLx Imaging system and quantified with Image Studio software.

Tissue culture infection - Preparation of inoculum and infection of the cells

C. auris isolates were subcultured on PDA plates overnight, and several colonies were subsequently inoculated into 5 mL of YPD broth and grown overnight at 37 °C with agitation. Cells were harvested by centrifugation, the growth medium was removed, and pellets were washed three times with complete tissue culture medium. Cell density was determined using a hemocytometer and suspensions were diluted in complete tissue culture medium. For siRNA- or antibody-treated host cells, the prepared inoculum was added, and infection was synchronized by centrifugation at $1,000 \times g$ for 1 min. Infected monolayers were incubated for 2 h, washed three times with DPBS to remove non-adherent fungi, and lysed in 0.5% Triton X-100 prepared in deionized water. Cells were scraped and the lysates were serially diluted and plated on PDA plates. Fungal burden was quantified as colony-forming units (CFU) per well.

siRNA mediated INTG β 4 silencing in human and mouse keratinocytes

HaCaT cells were seeded at a density of 2.5×10^5 cells per well in 24-well plates. For murine XB-2 keratinocytes, mitomycin C-treated 3T3-J2 fibroblasts were first seeded at a density of 4×10^4 cells per well and allowed to adhere overnight after which XB-2 cells were seeded at 2.5×10^5 cells per well in 24-well plates. Following overnight incubation, the culture medium was replaced with Opti-MEM (Gibco, 31985062) serum-

free medium. Human keratinocytes were transfected with either 50 μ M targeting siRNA against *ITG β 4* (Santa Cruz Biotechnology, sc-53678) or an equivalent concentration of control siRNA (Santa Cruz Biotechnology, sc-37007). XB-2 cells were transfected with 30 μ M targeting siRNA (Santa Cruz Biotechnology, sc-35679) or control siRNA using the Xfect transfection reagent (TacaraBio, 631317), according to the manufacturer's instructions. After 24 h, the medium containing transfection complexes was replaced with complete growth medium, and cells were maintained for an additional 48 h to achieve effective *ITG β 4* silencing. Cells were then infected with *C. auris* isolates at a multiplicity of infection (MOI) of 1 and the fungal burden was determined as described above.

***ITG β 4* blockage using antibodies**

HaCaT and XB-2 cells were seeded at a density of 2.5×10^5 cells per well in 24-well plates, as described above, and cultured to near confluence. For HaCaT cells, rat anti-human *ITG β 4* antibody (eBioscience, 14-1049-82) was diluted 1:100 in complete culture medium and applied to the cells. Rat IgG isotype control (Invitrogen, 31933) was reconstituted in the same buffer as the targeting antibody, diluted 1:100 in culture medium, and added to control wells. For XB-2 cells, rabbit anti-mouse *ITG β 4* antibody (Proteintech, 2577-1) or rabbit IgG control were diluted 1:100 in culture medium and applied to the cells. After a 1 h incubation, cells were infected with *C. auris* at an MOI of 1 and the fungal burden was determined as described above.

Cytokine ELISA

HaCaT cells were seeded into 6-well plates at a density of 5×10^5 cells per well and subjected to ITG β 4 silencing using siRNA, as described above. After 48 h, cells were infected with *C. auris* isolates AR-0382 and AR-0387 at an MOI of 1, and infection was allowed to proceed for 24 h to maximize cytokine secretion. Following infection, cells were placed on ice for 15 min, and 1 mL of conditioned medium was collected into tubes containing 10 μ L of protease inhibitor cocktail. Samples were clarified by centrifugation at $10,000 \times g$ for 10 min at 4 °C, and the resulting supernatants were stored at -80 °C until use. Cytokine levels were subsequently quantified by the Cytokine Core Laboratory at the University of Maryland, Baltimore School of Medicine using ELISA-based assays.

Results and discussion

Whole-Cell Affinity Pulldown Identifies Integrin $\beta 4$ as a Host Protein Binding *Candida auris*

To identify keratinocyte-expressed surface proteins capable of directly interacting with *Candida auris*, we used a whole-cell *C. auris* affinity pulldown approach (Figure 2.1). In this method, HaCaT cell surface proteins were selectively biotinylated using a cell-impermeable, cleavable biotinylation reagent. Following biotinylation, membrane proteins were extracted employing an octyl- β -D-glucopyranoside-based detergent system, a mild nonionic detergent widely recognized for its ability to preserve the structural integrity and functional activity of membrane-associated proteins [111].

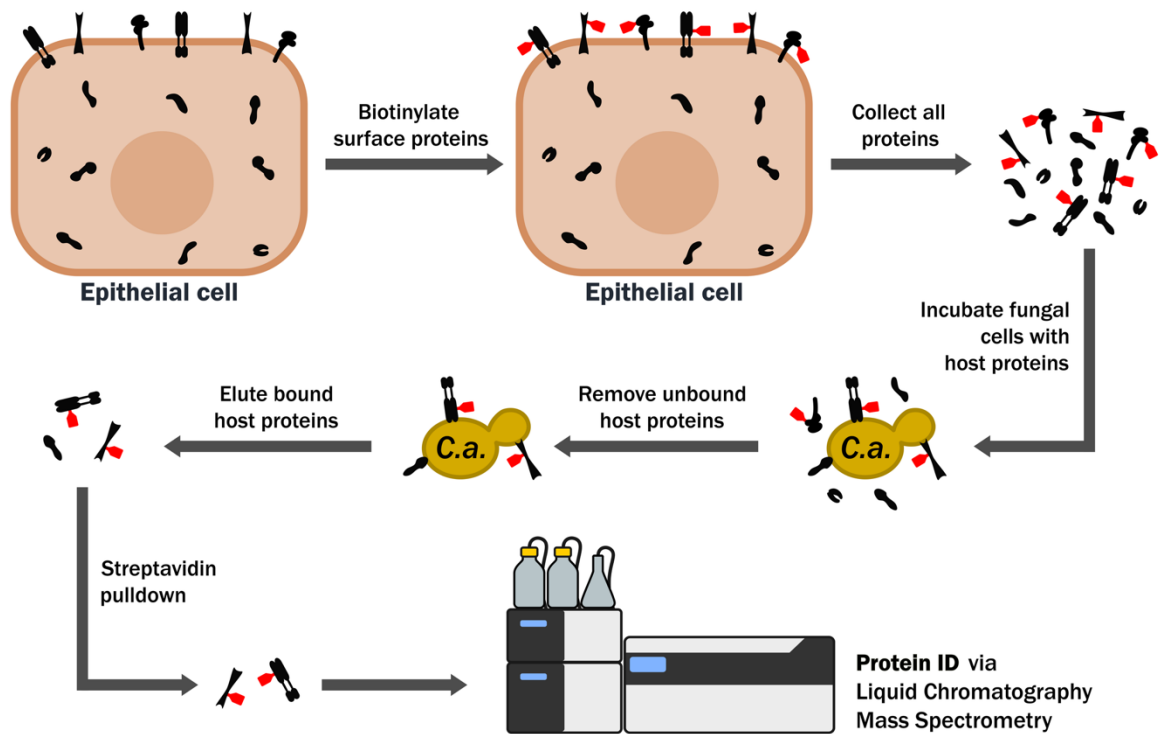


Figure 2.1. Schematic representation of the whole-cell affinity pulldown technique used to identify keratinocyte-derived host surface proteins that directly bind *Candida auris*. Surface proteins were biotinylated, isolated, incubated with fungal cells, and subsequently recovered through streptavidin pulldown for identification by liquid chromatography–mass spectrometry (LC-MS).

The biotinylated keratinocyte protein preparations were subsequently incubated with intact *C. auris* cells from two different isolates to enrich for host proteins that can physically associate with *C. auris*. Protein–fungal complexes were then recovered through streptavidin-mediated affinity purification and the bound host proteins were identified by liquid chromatography–coupled tandem mass spectrometry (LC–MS) [112]. This strategy enabled the unbiased identification of keratinocyte-derived surface peptides directly involved in fungal recognition and adhesion.

Proteomic analysis provided us with an extensive list of host proteins that were enriched in the *C. auris* bound preparations. Proteins were prioritized by detection of presence in both *C. auris* strains (AR-0382 and AR-0387) with ≥ 2 peptides, then enriching for cell-surface localization using curated annotation keywords (plasma membrane/cell surface, transmembrane, receptor, GPI-anchored). This yielded a high-confidence set of shared surface proteins (n=199; n=212 with a broader ECM-inclusive definition). The panel comprises adhesion and signaling molecules such as integrins, epidermal growth factor receptor (EGFR), tetraspanins, cadherins, transporters, and additional membrane receptors (**Table S1**). Moving forward, I decided to focus my attention on proteins (i) that are known to be expressed on the cell surface, (ii) for which at least 10 peptides were identified and (iii) with no known role in fungal pathogenesis. To this end, integrin $\beta 4$ (INTG $\beta 4$) was selected for follow-up experiments and functional validation.

INTG $\beta 4$ is a heterodimeric transmembrane adhesion receptor which contains a large extracellular domain that mediates interactions with components of the extracellular matrix, most notably laminins and vimentins [113-115]. INTG $\beta 4$ is uniquely

characterized by its unusually long cytoplasmic tail which anchors keratin intermediate filaments to the hemidesmosomal complex, thereby providing structural stability to epithelial layers [115]. Functionally, *INTGβ4* is involved in cell–matrix adhesion, maintenance of epithelial integrity, regulation of cell polarity, and signal transduction pathways governing proliferation, survival, and wound [113-116].

In order to verify that integrin $\beta4$ from keratinocytes can bind to *C. auris* cells, we used a commercially available anti-integrin $\beta4$ antibody to probe immunoblots containing HaCaT membrane proteins that were enriched for binding to fungal cells. This antibody recognized a *C. auris*-bound 210-kDa band derived from HaCaT cells (**Figure 2.2**). Furthermore, to rule out the possibility of strain-specific binding, we tested a diverse library of well-characterized *C. auris* isolates obtained from the Centers for Disease Control and Prevention (CDC), representing multiple phylogenetically distinct clades [68]. *ITGβ4* was detected as a ~210 kDa band in host membrane preparations that were enriched for binding to each of the nine *C. auris* isolates (**Figure 2.2**). These results indicate that integrin $\beta4$ is not strain-specific and is indeed conserved across clade-diverse *C. auris* isolates.

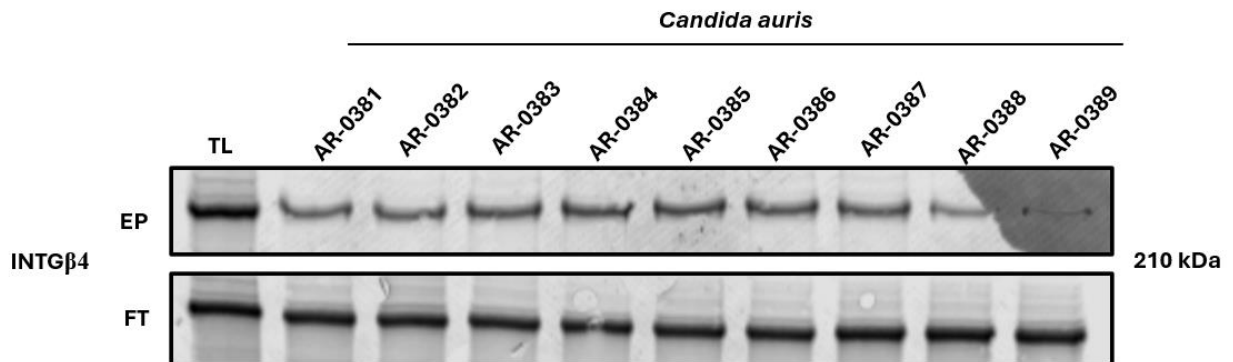


Figure 2.2. *Candida auris* isolates representing distinct genetic clades are capable of binding host *ITGβ4* derived from HaCaT cells. HaCaT cell lysates were subjected to whole-cell affinity pulldown with various *C. auris* isolates, and the resulting eluates (EP) and flow-through fractions (FT) were separated by SDS–PAGE. *ITGβ4* was detected using a specific primary antibody and corresponding secondary antibody. The total lysate (TL) lane represents the input control.

After establishing that ITG β 4 can bind, to *C. auris*, we next aimed to determine whether this interaction was specific to *C. auris* or could also extend to other yeast species. To address this, we assembled a library of phylogenetically diverse yeast species and subjected them to whole-cell affinity pulldown assays using HaCaT-derived lysates (**Figure 2.3**). ITG β 4 was able to bind all tested pathogenic yeast species (**Figure 2.3**). Robust ITG β 4 binding was detected across multiple *Candida* species, including *C. albicans*, *C. glabrata*, *C. tropicalis*, and *C. auris*. In addition, a interaction was also observed with *Cryptococcus neoformans* H99, a phylogenetically distinct basidiomycetous yeast. These findings indicate that ITG β 4 recognition is not restricted to *C. auris* or even the *Candida* genus but instead represents a broader host–fungal interaction mechanism conserved among clinically significant yeast pathogens.

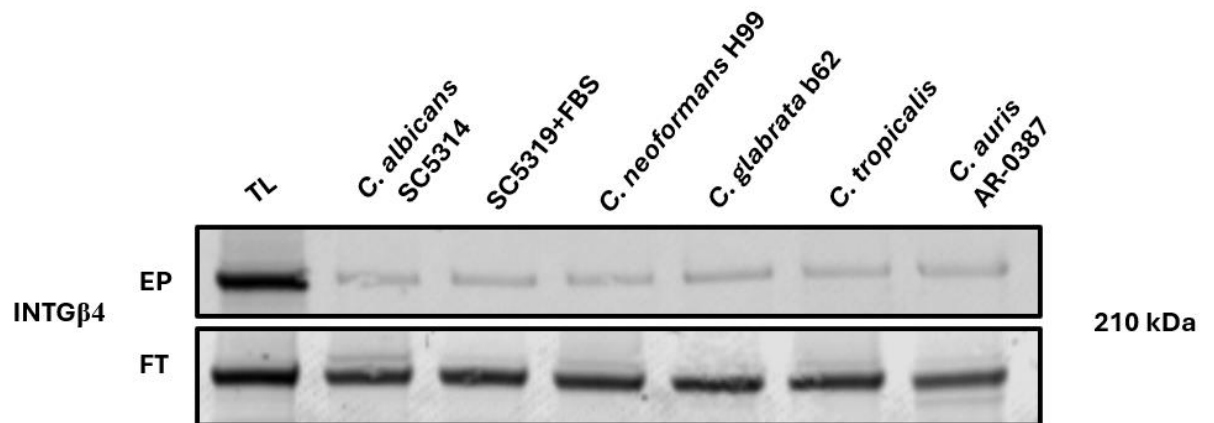


Figure 2.3. Integrin β 4 can associate with diverse pathogenic yeast species. Whole-cell affinity pulldown assays were performed using HaCaT-derived lysates incubated with a panel of yeast isolates, including *Candida albicans* SC5314, *C. albicans* SC5314 grown in the presence of FBS, *Cryptococcus neoformans* H99, *C. glabrata* b62, *C. tropicalis*, and *C. auris* AR-0387. Western blot analysis of eluates (EP) and flow-through fractions (FT) was carried out using ITG β 4-specific antibodies. A distinct ~210 kDa band corresponding to ITG β 4 was detected in the eluates of *C. neoformans*, *C. glabrata*, *C. tropicalis*, and *C. auris*. The total lysate (TL) lane served as a positive control.

ITG β 4 is well recognized to form complexes with multiple host proteins, including integrin α 6, growth factor receptors, and various extracellular matrix components, which together contribute to its structural and signaling functions [117, 118]. To assess whether heterologous expression of ITG β 4 can confer *C. auris* binding to cells that normally lack this phenotype, I generated a HEK293 cell line ectopically expressing a recombinant ITG β 4–GFP fusion protein and tested it in whole-cell affinity pulldown assays (**Figure 2.4**). Importantly, HEK293 cells normally do not exhibit binding to *C. auris*, but introduction of ITG β 4 was sufficient to confer this property, thereby adding rigor to our earlier findings in keratinocytes. As a control, GFP alone was expressed and subjected to the same pulldown and detection workflow to verify that binding was attributable to ITG β 4. Immunoblot analysis using GFP-specific antibodies revealed that ITG β 4–GFP, but not GFP alone, was consistently enriched in the eluates following incubation with *C. auris*, thereby demonstrating that ITG β 4 by itself is sufficient to mediate fungal binding (**Figure 2.4**).

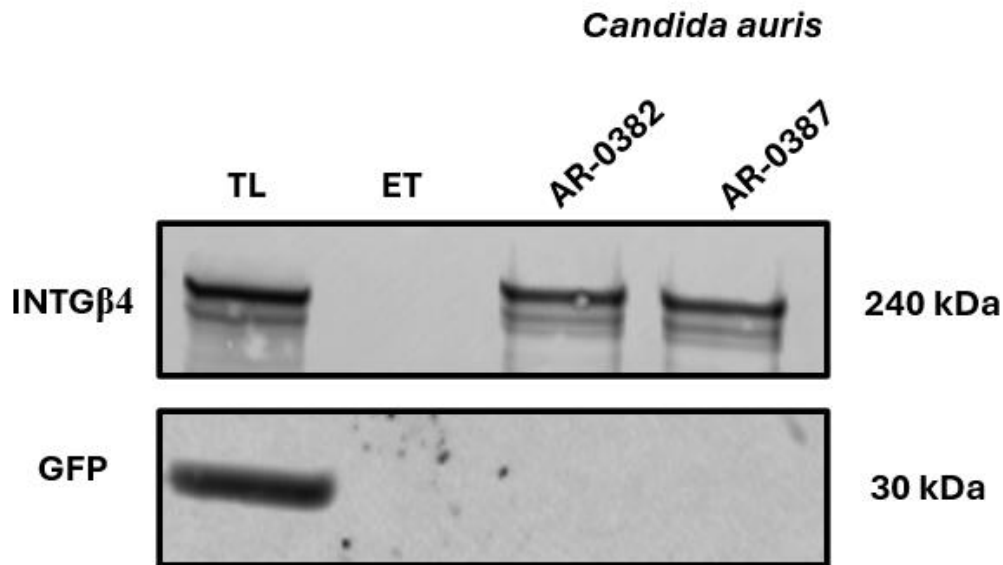


Figure 2.4. Recombinant ITGβ4–GFP fusion protein, but not GFP alone, was able to bind *Candida auris*. ITGβ4–GFP and GFP proteins were heterologously expressed in HEK293 cells and subsequently used in whole-cell affinity pulldown assays with *C. auris* isolates AR-0382 and AR-0387. Western blot analysis of eluates (EP) and flow-through fractions (FT) was performed using GFP-specific antibodies to detect either the ITGβ4–GFP fusion protein or GFP alone. While ITGβ4–GFP was specifically enriched in the eluates of both *C. auris* isolates, no enrichment was observed for GFP alone, confirming the requirement of ITGβ4 for binding. An empty-tube (ET) control, containing no fungal cells, was included to assess nonspecific binding.

Collectively, these data demonstrate that ITGβ4 is capable of binding various *C. auris* isolates in a clade-independent manner. Importantly, ITGβ4 recognition is not restricted to *C. auris* but extends to other clinically relevant pathogenic yeasts, including *Candida* species and *C. neoformans*. Furthermore, binding was also observed with ectopically expressed recombinant ITGβ4, indicating that the interaction does not rely on integrin-associated co-receptors or additional host proteins.

Integrin $\beta 4$ Facilitates *Candida auris* Binding to Keratinocytes

After confirming that ITG $\beta 4$ can associate with *Candida auris*, we next sought to characterize the functional role of this interaction during the early stages of infection. To achieve this, we employed two complementary strategies to disrupt ITG $\beta 4$ activity: RNA interference-mediated silencing of ITG $\beta 4$ expression and functional blockade using a monoclonal antibody. These approaches were applied to *in vitro* keratinocyte infection models utilizing both HaCaT human keratinocytes and XB-2 mouse keratinocytes, allowing cross-species validation of the findings. By quantifying *C. auris* adhesion under conditions of ITG $\beta 4$ suppression or inhibition, we were able to assess how modulation of this receptor influences fungal binding to epithelial cells.

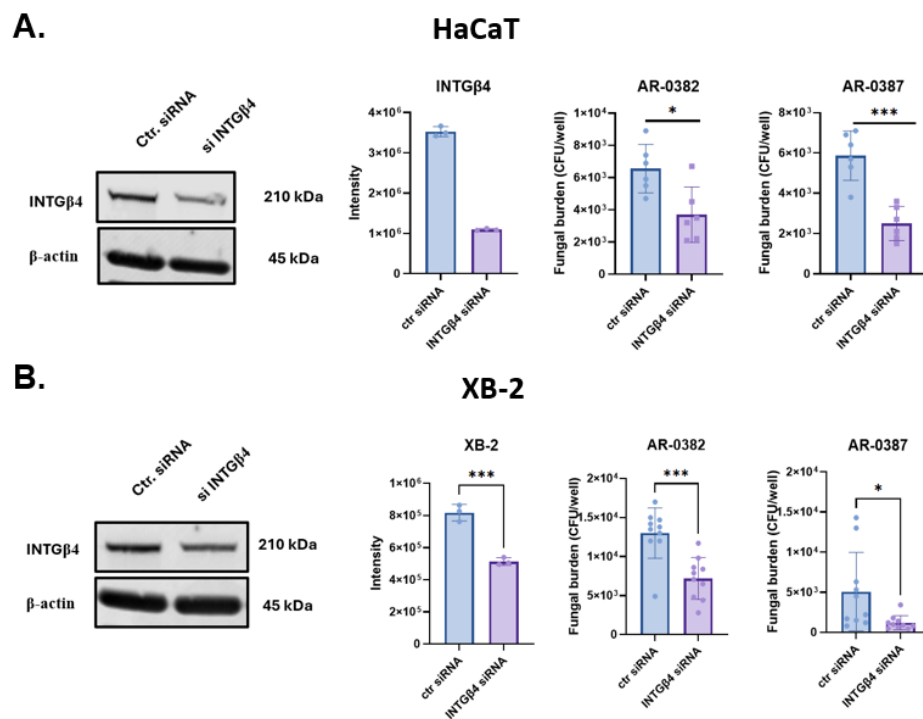


Figure 2.5. siRNA-mediated suppression of ITG $\beta 4$ in human HaCaT and mouse XB-2 keratinocytes significantly reduced *Candida auris* binding. (A) HaCaT and (B) XB-2 cells were transfected with ITG $\beta 4$ -targeting or non-targeting control siRNA. Following incubation, cells were infected with *C. auris* isolates AR-0382 and AR-0387, and fungal adhesion was quantified by determining the fungal burden (CFU/well) through serial dilution and plating. The data are presented as mean \pm SD. Statistical significance was determined using an unpaired Student's t-test. Significance is indicated as follows: * $p < 0.05$; *** $p < 0.001$.

The siRNA-mediated knockdown reduced ITG β 4 protein expression in both HaCaT and XB-2 keratinocytes (**Figure 2.5A-B**). Infection of HaCaT cells with ITG β 4-silenced cells resulted in a significant reduction ($p < 0.05$) in *C. auris* fungal burden for both AR-0382 and AR-0387 strains when compared to control siRNA-transfected groups. A comparable effect was observed in mouse XB-2 keratinocytes, where suppression of ITG β 4 expression likewise led to significantly decreased *C. auris* binding. These results collectively demonstrate that ITG β 4 plays a critical role in mediating *C. auris* adhesion to keratinocytes and that this function is conserved across host species, indicating that the contribution of ITG β 4 to fungal adhesion is not restricted to human keratinocytes but extends to murine cells as well.

In a complementary approach, I next sought to evaluate whether antibody-mediated blockade of ITG β 4 would recapitulate the phenotype observed with genetic knockdown. For this purpose, HaCaT and XB-2 keratinocytes were pre-incubated with a monoclonal antibody specifically targeting the ITG β 4 prior to *C. auris* infection (**Figure 2.6**). As a control, we included a species matched isotype control (IgG). Antibody-mediated blockade of ITG β 4 on HaCaT human keratinocytes resulted in a significant reduction of *C. auris* fungal burden for both tested isolates when compared to the isotype control (**Figure 2.6**). In contrast, when the same blocking strategy was applied to XB-2 mouse keratinocytes, a significant decrease in fungal burden was observed only with the *C. auris* AR-0387 isolate, while the AR-0382 strain showed no significant reduction (**Figure 2.6**). This differential phenotype may reflect variation in the stoichiometry or availability of *C. auris* ligands capable of recognizing ITG β 4 on XB-2 cells. Furthermore, since only a single antibody dilution was tested in these experiments, it is

possible that dose-escalation studies could yield a more pronounced effect and reveal strain-specific differences in ITG β 4-mediated fungal adhesion with greater resolution (Figure 2.6).

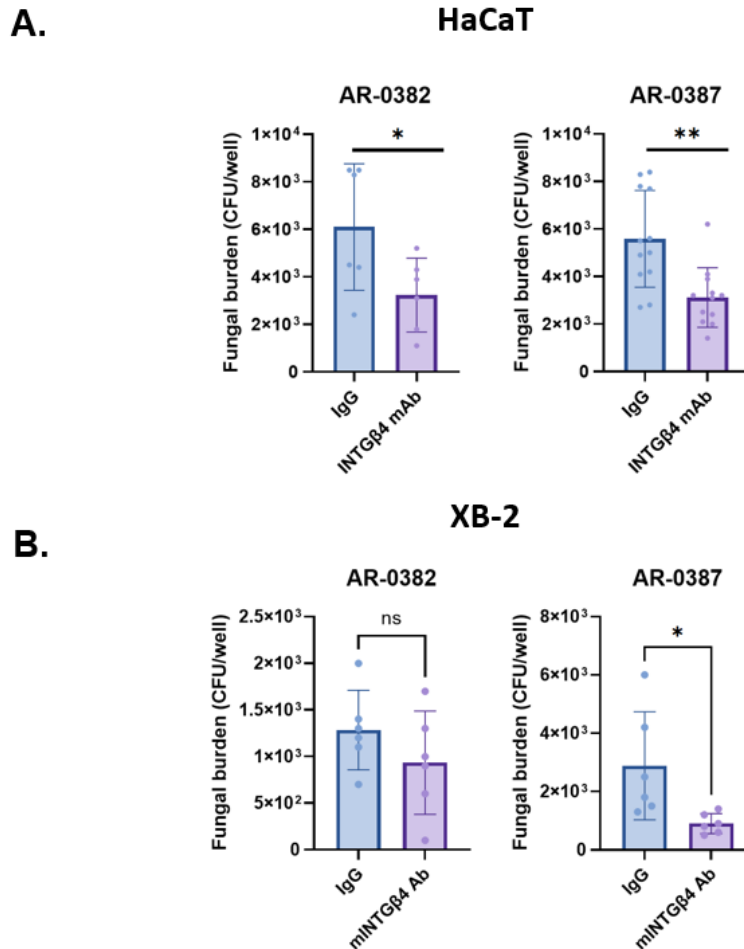


Figure 2.6. Antibody-mediated blockade of ITG β 4 reduced *Candida auris* binding to keratinocytes. (A) HaCaT and (B) XB-2 cells were pre-incubated for 1 h with a diluted monoclonal antibody targeting the extracellular domain of ITG β 4 or with a species-matched isotype IgG control prior to infection. Following incubation with *C. auris*, fungal adhesion was quantified by determining the fungal burden (CFU/well) through serial dilution and plating. The data are presented as mean \pm SD. Statistical significance was determined using an unpaired Student's t-test. Significance is indicated as follows: * p < 0.05; ** p < 0.01; ns- not significant.

We next hypothesized that the phenotype observed following ITG β 4 antibody blockade could potentially result from off-target effects of the antibody on either host

keratinocytes or *C. auris* cells. To test whether the observed inhibition of fungal binding was truly dependent on the interaction between *C. auris* and ITG β 4, we combined siRNA-mediated knockdown with antibody-mediated blocking in HaCaT keratinocytes (Figure 2.7).

Both ITG β 4-targeting siRNA and antibody-mediated blockade significantly reduced *C. auris* adhesion to HaCaT keratinocytes for both AR-0382 and AR-0387 isolates when compared with non-targeting siRNA or isotype IgG controls. In ITG β 4-silenced cells, fungal burden was markedly decreased, confirming the role of this integrin in mediating *C. auris* binding. Similarly, antibody treatment of control cells produced a comparable reduction in fungal adhesion, further validating ITG β 4 as the functional target. Importantly, when ITG β 4-targeting siRNA was combined with antibody treatment, no additional or synergistic reduction in fungal burden was observed, indicating that the inhibitory effect of the antibody is dependent on the presence of ITG β 4.

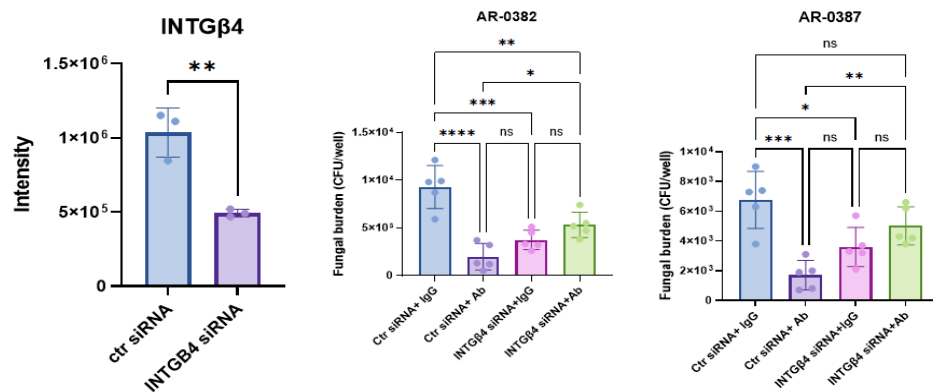


Figure 2.7. ITG β 4 is required for antibody-mediated suppression of *Candida auris* adhesion to HaCaT human keratinocytes. HaCaT cells were transfected with either ITG β 4-targeting siRNA or non-targeting control siRNA, followed by pre-incubation for 1 h with an ITG β 4-specific monoclonal antibody or a species-matched isotype IgG control. The cells were subsequently challenged with *C. auris*, and fungal adhesion was quantified by determining the fungal burden (CFU/well). The data are presented as mean \pm SD. Statistical significance was determined using an unpaired Student's t-test. Significance is indicated as follows: * p < 0.05; ** p < 0.01; *** p < 0.001, **** p < 0.0001; ns - not significant.

To provide an additional layer of evidence that ITG β 4 functions as a host receptor for *Candida auris* binding, we next sought to determine if ectopically expressed ITG β 4 can increase the association with *C. auris* binding to a model eukaryotic cell line which is not known to express ITGB4. HEK293 cells, which do not endogenously express ITG β 4 at detectable levels, were transfected with plasmids encoding either ITG β 4–GFP or GFP alone as a control. Following transfection, cells were incubated with *C. auris*, and adhesion was quantified to determine whether ectopic expression of ITG β 4 was sufficient to enhance fungal binding (**Figure 2.8**).

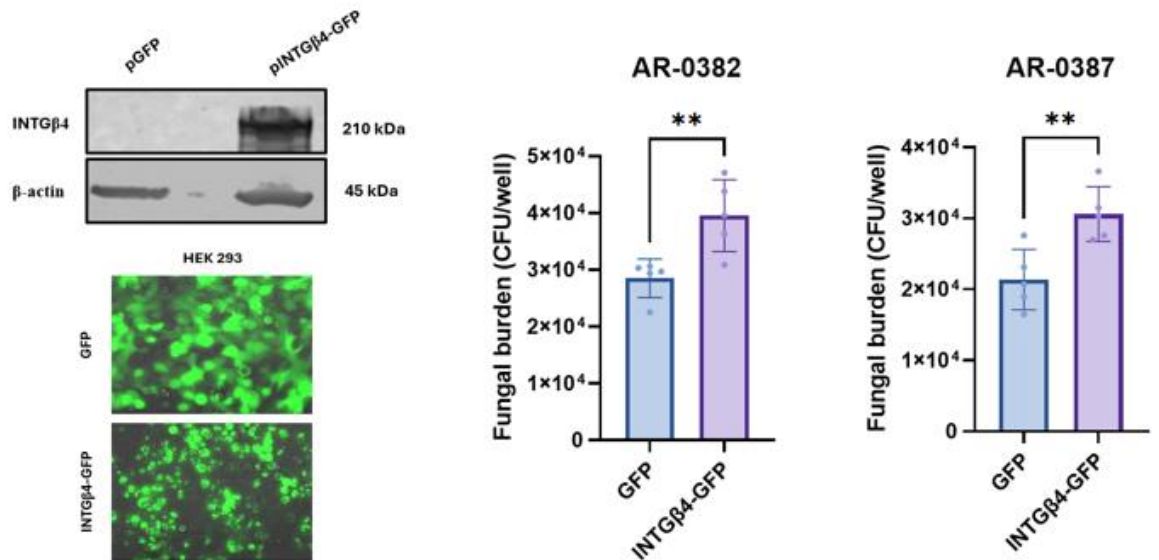


Figure 2.8. Overexpression of ITG β 4 in HEK293 cells results in increased *Candida auris* binding. HEK293 cells were transfected with plasmids encoding ITG β 4–GFP or GFP alone, which served as a control. Expression of the constructs was confirmed by immunoblot analysis using ITG β 4-specific antibodies and by fluorescence microscopy to verify GFP signal and cellular localization. Following validation, transfected cells were challenged with *C. auris*, and fungal adhesion was quantified by determining fungal burden (CFU/well). The data are presented as mean \pm SD. Statistical significance was determined using an unpaired Student’s t-test. Significance is indicated as follows: ** $p < 0.01$.

Transfection of HEK293 cells with plasmid encoding ITG β 4–GFP resulted in robust expression of the fusion protein, as confirmed by immunoblot analysis, which showed a clear ~240 kDa band corresponding to ITG β 4–GFP, and by fluorescence microscopy demonstrating strong GFP signal (**Figure 2.8**). In contrast, cells transfected with GFP alone had no ITG β 4 signal by immunoblot and displayed diffuse cytoplasmic fluorescence.

When these cells were challenged with *C. auris* isolates AR-0382 and AR-0387, expression of ITG β 4–GFP significantly enhanced fungal binding compared with GFP controls ($p < 0.05$), indicating that ectopic expression of ITG β 4 confers increased binding of *C. auris* to epithelial cells.

Despite this significant increase in binding, the experiment has several limitations. First, HEK293 cells are not keratinocyte-derived and therefore may not fully recapitulate the physiological context of skin epithelial ITG β 4 function. Second, immunoblot analysis detects both intracellular and surface-localized ITG β 4–GFP, making it impossible to directly estimate the relative proportion of ITG β 4 presented on the plasma membrane versus retained intracellularly. Thus, while these results strongly suggest a role for ITG β 4 in mediating *C. auris* adhesion, additional studies using keratinocyte-derived systems and surface-specific quantification methods (flow cytometry, surface biotinylation assays, cell fractionation) are needed to confirm the physiological relevance of these findings.

Collectively, these data demonstrate that disruption of ITG β 4 function, either through siRNA-mediated silencing or antibody-mediated blockade, significantly reduces the *Candida auris* burden in keratinocytes. Conversely, ectopic expression of ITG β 4 in a heterologous epithelial cell system confers increased fungal adhesion in vitro. Together,

these complementary approaches provide strong evidence that ITG β 4 functions as host receptor mediating *C. auris* binding to epithelial cells during the initial stages of infection.

Integrin β 4 Is Not Required for the Innate Immune Response of HaCaT Keratinocytes to *Candida auris*

Human keratinocytes, as the first line of defense against environmental insults and microbial colonization, express a wide repertoire of receptors that have evolutionarily evolved to detect pathogen-associated molecular patterns (PAMPs) [119]. In the case of fungi, recognition can be triggered by diverse pathogen-derived molecules, including cell wall components (mannans, β -glucans, chitin), secreted proteins, and small metabolites, all of which are capable of initiating innate immune responses and driving differential cytokine production [119]. Several fungal pathogens are known to exploit interactions with non-classical or non-immune receptors to indirectly modulate host immunity, often through non-canonical signaling pathways.

Currently, there is limited information regarding the involvement of ITG β 4 in innate immune regulation. However, evidence from the oncology literature suggests that ITG β 4 can influence cytokine production either directly through its own signaling capacity or indirectly via downstream pathways, including EGFR, PI3K/AKT, FAK, and c-MET [119-121]. These signaling cascades have been repeatedly implicated in shaping the cytokine milieu within tumor microenvironments [122]. Based on our findings that ITG β 4 mediates *C. auris* adhesion to keratinocytes and considering the established role of ITG β 4-associated signaling in modulating cytokine production in cancer biology, we

next sought to determine whether interaction between *C. auris* and ITGβ4 governs innate immune responses in HaCaT keratinocytes.

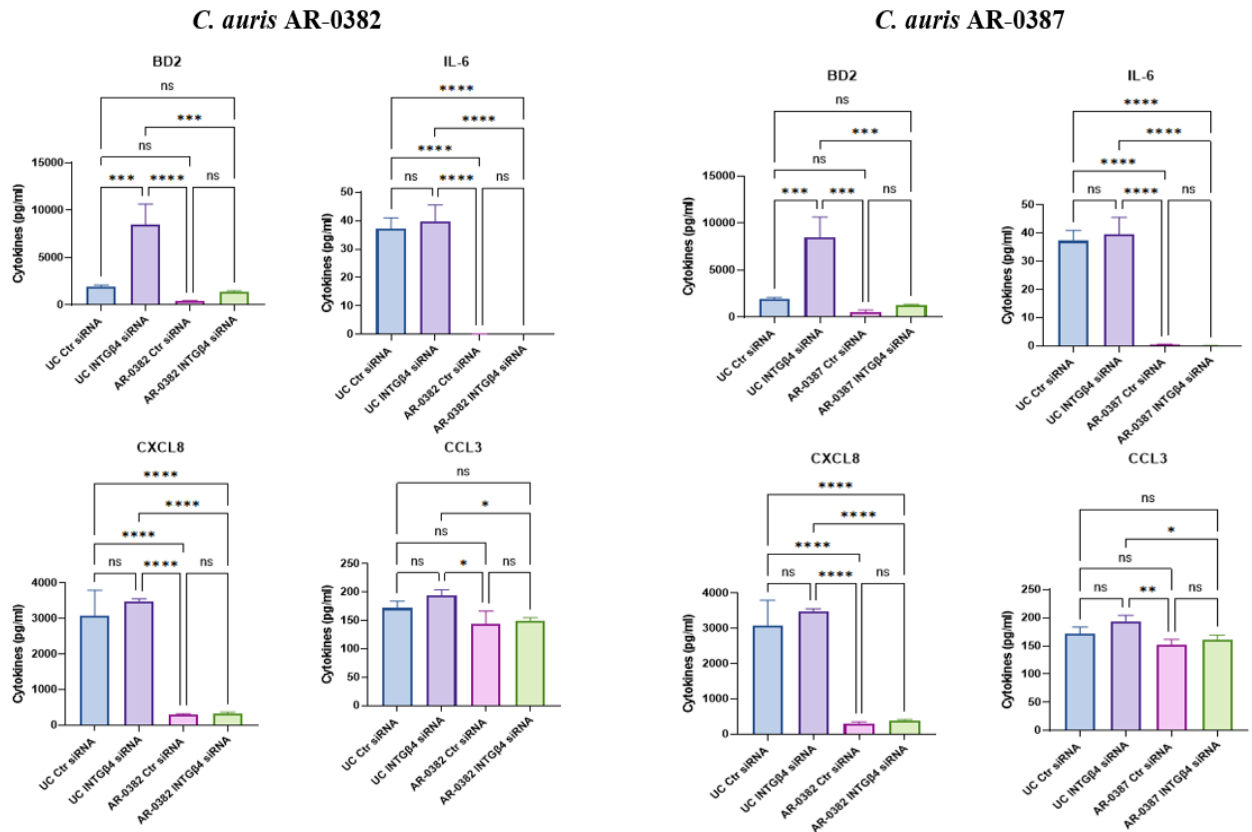


Figure 2.9. ITGβ4 is not involved in the innate immune response of HaCaT keratinocytes to *Candida auris*. HaCaT cells were transfected with either ITGβ4-targeting or non-targeting control siRNA and subsequently infected with *C. auris* isolates for 24 hours. Following infection, conditioned culture supernatants or media from uninfected control (UC) were collected, and secreted cytokines and antimicrobial peptides were quantified using ELISA. The data are presented as mean ± SD. Statistical significance was determined using an unpaired Student’s t-test. Significance is indicated as follows: *p<0.05;***p < 0.001; **** p<0.0001, ns- not significant.

To address this question, we employed siRNA-mediated silencing of ITGβ4 in HaCaT keratinocytes, followed by infection with *Candida auris* isolates AR-0382 and AR-0387 for 24 hours. Following infection, conditioned culture supernatants were

collected and analyzed for cytokine and chemokine production. Specifically, levels of β -defensin 2 (BD2), interleukin-6 (IL-6), CXCL8/IL-8, and CCL3/MIP-1 α . I chose to assay these specific proteins because of their documented involvement in the skin defense against various pathogens [123, 124].

Infection with both *C. auris* AR-0382 and AR-0387 isolates did not induce robust secretion of the tested cytokines or antimicrobial peptides, and these responses were not dependent on ITG β 4. In fact, HaCaT keratinocyte infection with *C. auris* was suppressive, resulting in reduced cytokine production compared to untreated controls. These findings are consistent with previous in vivo observations, where *C. auris* infection failed to elicit strong immune responses in mouse skin models. Collectively, these results indicate that *C. auris* suppresses keratinocyte immune responses through ITG β 4-independent mechanisms.

Integrin β 4 binding to *Candida auris* is not dependent on Als4112 but is mediated through ITG β 4 interaction with chitin

After establishing that ITG β 4 contributes to *Candida auris* pathogenesis by mediating fungal adhesion to keratinocytes, we next hypothesized that this interaction might involve the *C. auris* adhesin Als4112 [69]. Previous studies have identified Als4112 as an adhesion protein critical for *C. auris* attachment to extracellular matrix components, particularly laminin and collagen V [69]. Notably, ITG β 4 forms a heterodimeric complex with integrin α 6 to generate integrin α 6 β 4, a well-characterized receptor for laminin [125]. This functional overlap raised the possibility that Als4112 could serve as the fungal ligand for ITG β 4, thereby facilitating adhesion to keratinocytes.

To directly test this hypothesis, we investigated whether the interaction between *C. auris* and ITG β 4 is dependent on Als4112 by performing a whole-cell affinity pulldown with Wild type *C. auris*, an Als4112 deletion mutant, and an Als4112 deletion mutant that has been complemented with a wild-type copy of Als4112.

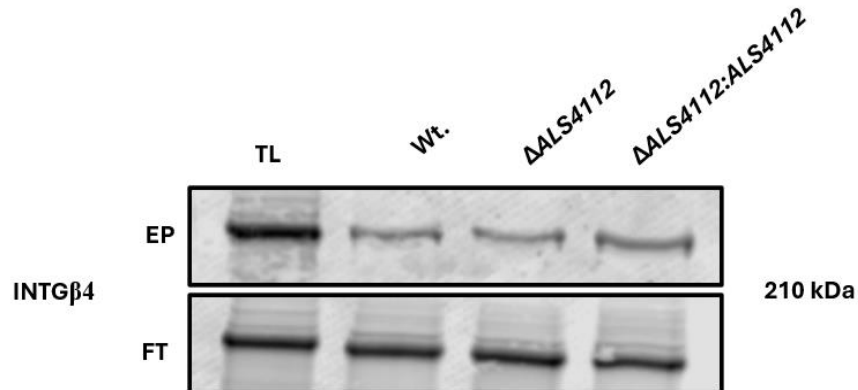


Figure 2.10. *C. auris* adhesin Als4112 is not involved in interaction with ITG β 4. The *C. auris* wild type strain (Wt.), Als4112 mutant (Δ ALS4112), and Als4112 complemented strain (Δ ALS4112:ALS4112) were used for whole cell affinity pulldown. Western blot analysis of eluates (EP) and flow-through fractions (FT) was carried out using ITG β 4-specific antibodies.

To our surprise, wild-type *C. auris*, the Δ ALS4112 deletion mutant, and the Δ ALS4112:ALS4112 complemented strain all demonstrated comparable binding to ITG β 4 (Figure 2.10). Deletion of Als4112 did not impair ITG β 4 interaction, nor was binding altered by genetic complementation of the adhesin. These findings indicate that ITG β 4 recognition of *C. auris* is independent of the Als4112 adhesin, suggesting that alternative fungal ligands are responsible for mediating this host–pathogen interaction.

To probe whether proteinaceous ligands mediate ITG β 4 binding to *Candida auris*, we applied two complementary approaches: heat inactivation to denature surface proteins and protease K digestion to enzymatically degrade them. Interestingly, ITG β 4 binding

was markedly reduced following heat inactivation at 95 °C, whereas even high concentrations of protease K had no detectable effect on binding (**Figure 2.11**). These contrasting results suggest that protein degradation *per se* does not impair ITG β 4 recognition. Instead, heat treatment likely alters the overall surface architecture of *C. auris*, leading to conformational changes or masking of cell wall components. It is plausible that heat-induced remodeling reduces accessibility of a cell wall component, thereby suppressing ITG β 4 binding. This finding points toward a non-proteinaceous cell wall component, such as chitin, as the key fungal ligand mediating ITG β 4 interaction.

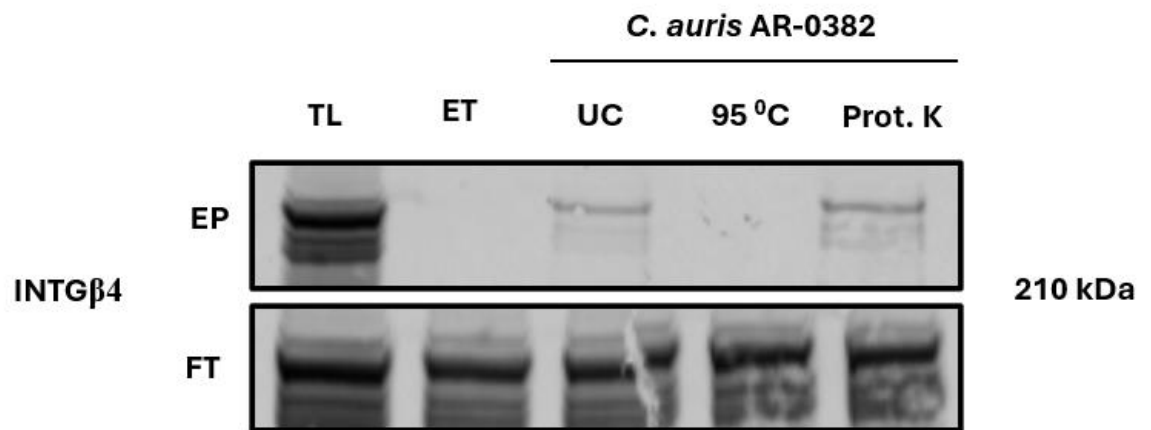


Figure 2.11. Heat inactivation, but not protease K digestion of *C. auris* suppressed ITG β 4 binding. The *C. auris* undergo no treatment (UC), heat inactivation at 95 °C for 1 hour, or protease K (Prot. K) digestion of surface proteins. The treated *C. auris* undergo whole cell affinity pulldown. Western blot analysis of eluates (EP) and flow-through fractions (FT) was carried out using ITG β 4-specific antibodies.

To explore the hypothesis that ITGB4 binds to chitin in the fungal cell wall, we performed a pulldown using purified, commercially available chitin. Varying amounts of

chitin were used for affinity pulldown of host cell membrane preparations followed by immunoblot detection of ITG β 4 (**Figure 2.12**).

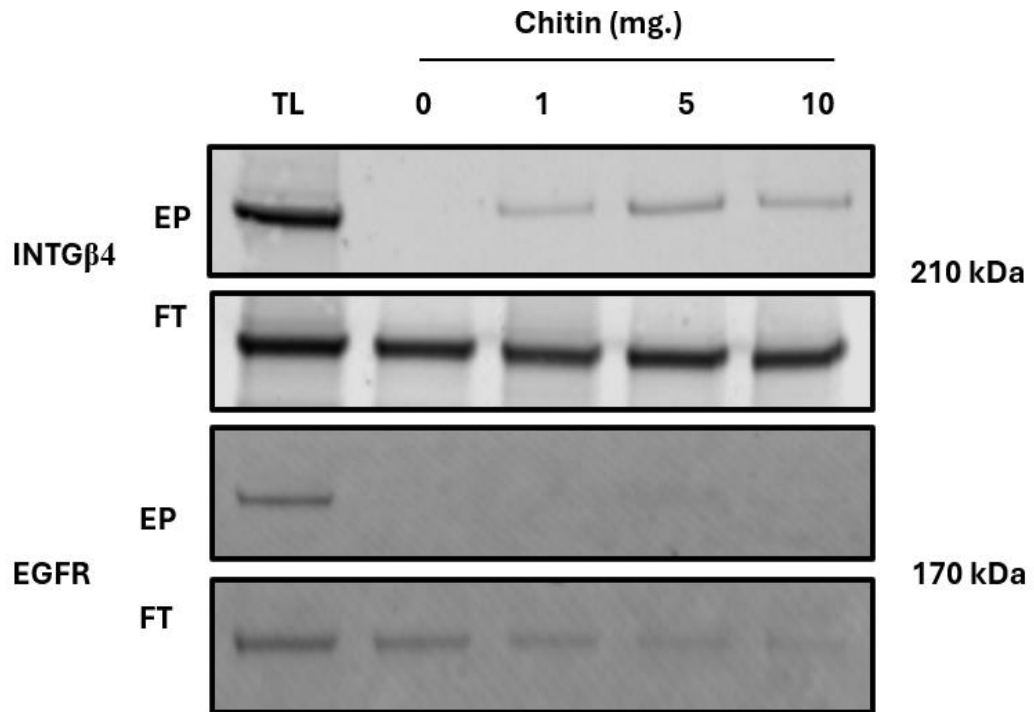


Figure 2.12. Purified chitin can bind ITG β 4 but not EGFR in pulldown assay. Immunoblots of the eluates were probed with specific antibodies against ITG β 4 and EGFR. EGFR was used as a negative control to eliminate a possibility of non-specific binding.

Probing with specific antibodies revealed a clear enrichment of ITG β 4 in the chitin-bound fractions (**Figure 2.12**). After establishing that ITG β 4 can bind to purified chitin, we next considered whether chitin might act as a nonspecific “sponge” capable of binding a broad range of host proteins. To address this, we selected EGFR as a secondary control protein, as EGFR has previously been reported to interact with *C. albicans* (**Figure 2.12**). Furthermore, LC-MS proteomic analysis identified EGFR as a *C. auris* interactor, providing additional confidence in its use as a chitin-binding control (**Table**

S1). Interestingly, ITG β 4 binding appeared to be specific, since no EGFR was detected in the chitin-bound protein fractions.

To further confirm that ITG β 4 is able to bind fungal chitin, we sought to test this hypothesis in a biologically relevant context using intact fungal cells. We first conducted a literature analysis to identify pharmacological agents capable of disrupting chitin synthesis in fungi. Among the available compounds, we selected Nikkomycin Z and Chitin Synthesis Inhibitor 4 (CSI-4), both of which target fungal chitin synthase and have been previously used to impair chitin biosynthesis in both experimental and pharmacological settings due to crucial role in fungal viability and survival [126-128]. We began by determining the minimum inhibitory concentrations (MICs) of these inhibitors against *C. auris* isolates using the CLSI broth microdilution protocol. Both compounds showed poor activity, as the *C. auris* isolates displayed high levels of resistance, with MIC values exceeding 500 μ M.

To overcome this limitation, we turned to *C. albicans* SC5314, a strain that demonstrated ITG β 4 binding in whole-cell pulldown assays. MIC testing revealed that CSI-4 inhibited *C. albicans* SC5314 growth at 400 μ M. Based on this, we selected a sub-inhibitory concentration (200 μ M) for subsequent experiments to avoid growth inhibition while selectively perturbing chitin biosynthesis. This approach enabled us to evaluate the role of fungal chitin in mediating ITG β 4 binding under biologically relevant conditions (**Figure 2.13**).

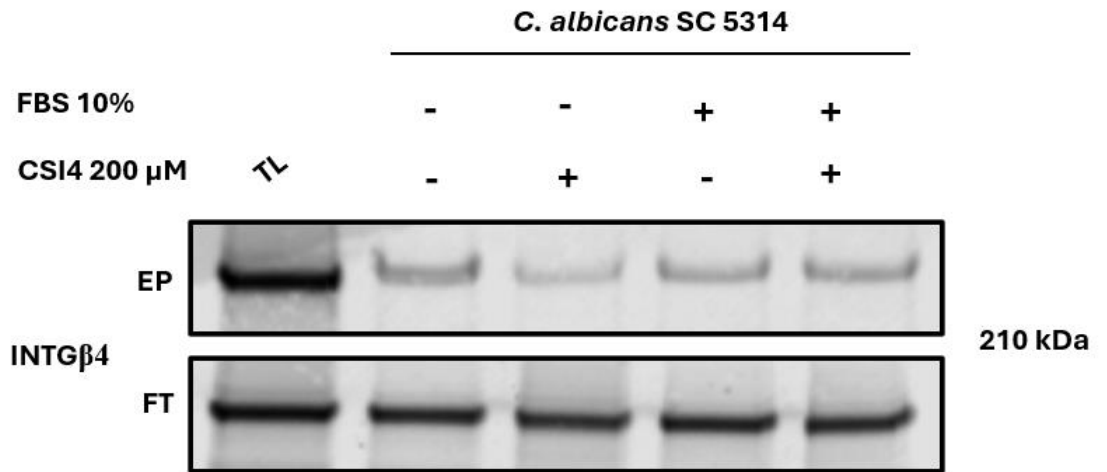


Figure 2.13. Chitin synthesis inhibition reduces ITG β 4 binding to *Candida albicans* SC5314 under FBS-free conditions. *C. albicans* SC5314 was cultured in YPD \pm sub-lethal CSI-4 and in parallel \pm 10% FBS. Cells were harvested and subjected to whole-cell affinity pulldown with HaCaT lysate. Eluates (EP) and flow-through (FT) fractions analyzed by Western blot using ITG β 4-specific antibodies.

By incubating *Candida albicans* SC5314 in the presence of 200 μ M CSI-4, we observed a marked reduction in ITG β 4 binding. However, this effect was suppressed when the assay was performed in medium supplemented with 10% FBS, a strong inducer of fungal hyphae formation in *C. albicans*. Chitin is enriched at fungal hyphal septa and tips, and its abundance increases during the dimorphic switch from the yeast to the hyphae [129, 130]. These apparently contradictory results may also be explained, at least in part, by the known phenomenon of serum protein binding, in which small-molecule inhibitors interact non-specifically with abundant serum proteins such as albumin. Albumin has a high binding capacity for hydrophobic and amphipathic molecules, and this interaction can significantly reduce the fraction of free, bioactive compound available to penetrate fungal cells. As a result, the effective intracellular concentration of CSI-4

would be diminished in FBS-containing medium, thereby reducing or eliminating its capacity to inhibit chitin synthesis.

Finally, to provide an additional layer of evidence supporting the interaction between ITG β 4 and chitin, we evaluated whether ITG β 4 overexpression in HEK293 cells confers enhanced adhesion to chitin- and chitosan-coated surfaces. For this purpose, tissue culture plates were coated with chitin or chitosan, which were covalently immobilized through Schiff base formation between poly-D-lysine and the amino groups of chitin/chitosan using glutaraldehyde crosslinking. In parallel, 1,3- β -D-glucan was passively adsorbed onto tissue culture plastic and used as a control. HEK293 cells expressing ITG β 4-GFP or GFP alone were seeded onto the modified surfaces, allowed to interact for one hour, washed, and subsequently grown to form colonies (**Figure 2.14**).

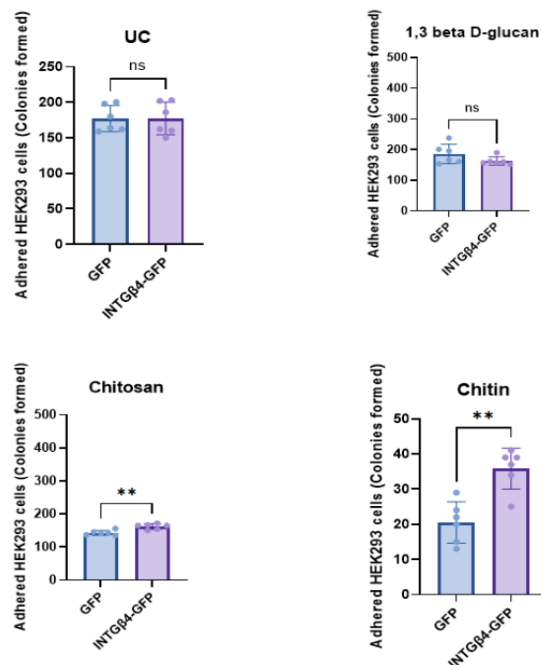


Figure 2.14. ITG β 4 overexpression enhances HEK293 cell adhesion to chitin and chitosan surfaces. HEK293 cells expressing ITG β 4-GFP or GFP were seeded on uncoated plastic (UC), 1,3- β -D-glucan-, chitosan-, or chitin-coated plates. Colony formation was quantified after one hour of adhesion followed by washing. Statistical significance was determined using an unpaired Student's t-test. Significance is indicated as follows: $p < 0.01$.

The adhesion assay revealed that ITG β 4 overexpression in HEK293 cells selectively results in increased binding to chitin- and chitosan-coated surfaces, whereas no significant differences were observed on uncoated plastic (UC) or 1,3- β -D-glucan. Specifically, ITG β 4-GFP-expressing cells exhibited a significant increase in colony formation relative to GFP controls on both chitosan and chitin, with the most pronounced effect detected on chitin-coated plates. In contrast, adhesion to uncoated and β -glucan-coated surfaces remained comparable between groups, indicating that ITG β 4 does not confer nonspecific adhesion (**Figure 2.14**).

Collectively, these data suggest that ITG β 4 binding to *C. auris* is independent of the Als4112 adhesin and resistant to protease K digestion. Pulldown experiments using purified chitin further demonstrated that ITG β 4, but not EGFR, specifically associates with chitin. Functional inhibition of chitin biosynthesis using CSI-4, a small-molecule chitin synthase inhibitor, revealed that ITG β 4 binding was reduced when *Candida albicans* SC5314 cells were cultured with CSI-4 under serum-free conditions.

Conclusions

C. auris is an emerging, multidrug-resistant fungal pathogen associated with high morbidity and mortality worldwide. Clinical isolates of *C. auris* frequently display intrinsic resistance to multiple classes of antifungal agents, including azoles, polyenes, and, in some cases, echinocandins, making these infections exceptionally difficult to treat and contributing to poor patient outcomes [131]. Despite the growing clinical threat and the extensive research devoted to antifungal resistance mechanisms, our understanding of *C. auris* host-pathogen interactions remains limited. In particular, the molecular

determinants of adhesion, epithelial colonization, and long-term persistence within the host are poorly defined. Since adhesion to host cells is the critical first step toward colonization and subsequent infection, elucidating the mechanisms that mediate *C. auris* attachment to epithelial surfaces is essential for understanding its pathogenesis and for identifying potential therapeutic targets.

In this chapter, using an omics-guided unbiased approach, we identified ITG β 4 as a novel host surface-expressed protein capable of binding *C. auris* and other pathogenic yeasts, suggesting that ITG β 4 has the potential to be a pan-fungal receptor. Modulation of ITG β 4, either through molecular silencing methods or blockade with ITG β 4-specific antibodies, significantly reduced *C. auris* binding to both human and murine keratinocytes in an Als4112 adhesin-independent manner. Further screening demonstrated that ITG β 4 selectively binds purified chitin, and pharmacological inhibition of chitin synthase with small molecules diminished ITG β 4 binding in *C. albicans*.

Despite the experimental evidence provided, this study has several limitations that also presents opportunities for future research. First, although we successfully demonstrated that *C. auris* binds to human and mouse keratinocytes in an ITG β 4-dependent manner, it remains unclear whether this mechanism operates *in vivo*. This question is particularly challenging to address because genetic knockout of ITG β 4 in mice is lethal, with homozygous deletion resulting in death shortly after birth [132, 133]. Additionally, antibody-based approaches are difficult to translate to skin infection models, as the pharmacokinetics and tissue penetration of monoclonal antibodies in skin layers are difficult to predict [134]. As an alternative, lentiviral-mediated delivery of ITG β 4-targeting siRNA to skin could represent a promising avenue, given that lentiviral

or adeno-associated virus vectors have previously been applied for stable gene delivery to cutaneous tissues [135, 136].

Through biochemical and pharmacological experiments, we identified chitin as the most likely fungal ligand mediating ITG β 4 recognition. However, detailed characterization of the ITG β 4–chitin interaction remains technically challenging due to the insoluble and crystalline nature of chitin. Unlike soluble ligands, chitin is not easily amenable to modern biophysical approaches such as dynamic surface plasmon resonance (SPR), isothermal titration calorimetry (ITC), or cryo-electron microscopy (cryo-EM), which typically require soluble, well-defined molecular complexes. To overcome these limitations, alternative strategies could be employed, such as immunogold labeling coupled with transmission electron microscopy to localize ITG β 4–chitin interactions at the host–fungal interface, or atomic force microscopy (AFM)–based force mapping to quantify the strength of ITG β 4 binding to chitin. Development of soluble chitooligosaccharide analogs may also allow for the application of traditional protein–ligand binding assays, providing a more detailed molecular understanding of this interaction.

This work identifies ITG β 4 as a previously unrecognized host receptor that mediates *Candida auris* adhesion to keratinocytes in a manner independent of classical adhesins such as Als4112. These findings extend the role of ITG β 4 beyond its established functions in epithelial integrity and cancer biology, positioning it as a potential pan-fungal receptor involved in the earliest stages of colonization. While technical and biological limitations remain, this work lays the foundation for future studies aimed at

dissecting ITG β 4–chitin interactions *in vivo* and evaluating their potential as targets for therapeutic intervention against multidrug-resistant fungal pathogens such as *C. auris*.

Chapter 3. Multi-omics–Guided Identification of EGFR and *c*-MET as Host Receptors Mediating *Lomentospora prolificans* Adhesion to Human Lung Epithelial Cells

Introduction

Lomentospora prolificans (*L. prolificans*) is an emerging opportunistic mold that poses a significant therapeutic challenge due to its broad intrinsic resistance to antifungal agents and its capacity to cause invasive disease in immunocompromised hosts [137]. Clinical manifestations range from localized pulmonary or soft tissue involvement to rapidly progressive disseminated infections, particularly in patients with hematological malignancies or those undergoing solid organ or hematopoietic stem cell transplantation. Mortality rates are exceedingly high, often exceeding 70–80% in disseminated disease, reflecting both the limited efficacy of existing antifungal regimens and the aggressive nature of the pathogen [14, 100].

L. prolificans exhibits minimal susceptibility to triazoles, echinocandins, and polyenes, and no standardized therapeutic protocols have been established [27]. In addition to its pharmacological challenges, *L. prolificans* demonstrates robust adherence to epithelial surfaces, invasion of pulmonary tissue, and evasion of innate immune responses, all of which contribute to its pathogenesis and systemic dissemination, especially to central nervous system [102]. These characteristics underscore the urgent need to elucidate the molecular determinants of host–pathogen interactions, particularly the mechanisms mediating epithelial adhesion and colonization, to enable the development of targeted diagnostic and therapeutic interventions [102].

Modern molecular and omics-guided approaches, including transcriptomics, proteomics, phosphoproteomics, and functional genomics, hold great potential to dissect the poorly understood biology of *L. prolificans*. These tools can be used to uncover, in an unbiased and comprehensive manner, the molecular determinants of adhesion, invasion, and immune evasion, thereby filling fundamental gaps in knowledge while also identifying candidate targets for therapeutic or diagnostic development. By bridging basic science with translational applications, such approaches hold promise to guide innovative strategies against this highly drug-resistant pathogen.

Omics-guided host-pathogen characterization strategies have been previously employed in understand host-pathogen interactions for several fungal pathogens. Among them, growth factor receptors have recently been identified as important host determinants modulated by pathogenic fungi during early infection and epithelial invasion [138]. In mucormycosis, caused by emerging pathogenic mold, *Rhizopus delemar* has been shown to exploit the epidermal growth factor receptor (EGFR) to adhere to and invade nasal and lung epithelial cells [139]. Furthermore, pharmacological blockade of EGFR signaling attenuates invasion and reduces mortality in animal models of pulmonary mucormycosis [139]. In *Candida albicans*, EGFR and hepatocyte growth factor receptor (*c*-MET) form a complex that contributes to hyphal endocytosis, where receptor activation by *C. albicans* orchestrates actin cytoskeletal remodeling that facilitates epithelial penetration and intracellular invasion [71]. In contrast, *c*-MET, a receptor tyrosine kinase implicated in bacterial, and viral adhesion, cytoskeletal dynamics, and epithelial barrier modulation, has not yet been fully systematically examined in fungal infections, especially in context of rare and emerging molds [140].

By applying an unbiased multi-omics approach, we characterized host responses to *L. prolificans* infection in HSAEC1-KT human airway epithelial cells and in a murine pulmonary infection model. Transcriptomic profiling combined with integrated pathway analysis revealed signaling networks engaged during infection, highlighting growth factor receptor pathways as central nodes. Subsequent phosphoproteomic analyses and whole-cell affinity pulldown assays identified multiple host surface proteins capable of directly binding *L. prolificans*, leading to the discovery of EGFR and c-MET as epithelial receptors. Functional validation demonstrated that these receptors mediate fungal adhesion and modulate epithelial innate immune responses, establishing EGFR and c-MET as key determinants of early host–pathogen interactions in pulmonary lomentosporiosis.

Materials and methods

Ethics statement

All experimental procedures were conducted in accordance with institutional and federal biosafety regulations. Work involving *Lomentospora prolificans* and related pathogens was carried out under protocol IBC-00003284, approved by the Institutional Biosafety Committee at the University of Maryland, Baltimore. All animal experiments were reviewed and authorized by the Institutional Animal Care and Use Committee (IACUC) of the Los Angeles Biomedical Research Institute at Harbor-UCLA Medical Center (protocol no. 21125) and performed in compliance with NIH guidelines for the care and use of laboratory animals.

Fungal strains and culture conditions

Clinical isolates of *L. prolificans* (DI16-482, DI16-483, and DI16-484) were employed in this study. The strains were grown on peptone–dextrose agar (PDA) plates and incubated for 7-12 days at 37 °C prior to use. Conidia were collected in endotoxin-free Dulbecco’s phosphate-buffered saline (DPBS) supplemented with 0.5% Tween 80, washed thoroughly in sterile DPBS, and counted with a hemocytometer to standardize inoculum concentrations. For *in vitro* assays, freshly harvested spores were resuspended in Small Airway Epithelial Cell Growth Medium Basal Medium (SAGM; Lonza, Cat. #CC-3118) without rhEGF and pre-incubated for 3 h at 37 °C to promote spore swelling.

Cell lines and culture conditions

HSAEC1-KT cells (ATCC CRL-4050) were cultured in SABM Basal Medium (Lonza, CC-3119) supplemented with the SAGM SingleQuots kit (Lonza, CC-4124), 1X Penicillin–Streptomycin (Pen-Strep) (Gibco, 15140122). A549 cells were cultured in Dulbecco’s Modified Eagle Medium (DMEM) (Gibco, 11965092) supplemented with 10% heat-inactivated fetal bovine serum (FBS) (SigmaAldrich, F4135) and 1% Penicillin–Streptomycin (Pen-Strep) (Gibco, 15140122). Cells were maintained at 37 °C in a humidified atmosphere containing 5% CO₂. Cultures were replenished with fresh medium every 2–3 days and routinely subcultured once per week.

***L. prolificans* induced damage to HSAEC1-Kt cells**

A chromium-51 (⁵¹Cr) release assay was performed to evaluate epithelial cell damage as described previously [141]. Human small airway epithelial cells (HSAECs)

were seeded into 96-well tissue culture plates and labeled overnight (16 h) with 1 μCi of sodium chromate ($\text{Na}_2^{51}\text{CrO}_4$; ICN) per well in SAGM medium. Prior to infection, monolayers were rinsed twice with pre-warmed Hank's balanced salt solution (HBSS) to remove unincorporated tracer. For challenge experiments, cells were exposed to *L. prolificans* spores (5×10^4 conidia per well) suspended in 200 μl of fresh SAGM. Control wells containing uninfected HSAECs were maintained under identical conditions to determine baseline (spontaneous) ^{51}Cr release. At 6, 12, 24, 36, and 48 h post-inoculation, half of the supernatant from each well was collected and transferred to gamma-counting tubes, while the remaining supernatant and cell monolayer were harvested separately. Total incorporated radioactivity was calculated as the sum of counts from the released fraction and the corresponding cell-associated fraction.

***Galleria mellonella* infection model**

Galleria mellonella larvae were purchased from Carolina Biologics and maintained under standard conditions prior to experimentation. Twenty larvae of comparable weight (150-300 mg each) were selected for each assay, transferred to 90-mm plastic Petri dishes, and anesthetized on ice for 10 min. Conidia of *L. prolificans*, prepared as described above, were enumerated and adjusted to 1×10^9 spores/ml in endotoxin-free DPBS. Each larva received an injection of 10 μl of the suspension ($\approx 1 \times 10^7$ spores) into the hemocoel via the last left proleg using a sterile Hamilton syringe. Control groups were inoculated with 10 μl of endotoxin-free DPBS alone. Infections were conducted at both 25 °C and 37 °C, and larvae were monitored over 48 h. Mortality

was scored daily, defined by the presence of complete melanization and absence of response to gentle tactile stimulation.

Actin filamentation staining

HSAEC1-KT cells were cultured on poly-L-lysine-coated round glass coverslips (Electron Microscopy Sciences, Cat. #72292-01) placed in 6-well plates and maintained at 37 °C in a humidified atmosphere containing 5% CO₂. For infection assays, swollen *L. prolificans* conidia were added at a multiplicity of infection (MOI) of 1:5 (1.2×10^6 spores per well) in Small Airway Basal Medium (SABM), centrifuged to synchronize the infection and incubated for 3 h. When needed, cells were pre-treated with cytochalasin D (ChD) at 25 μ M for 1-hour prior infection and maintained during infection period. After incubation, culture medium was aspirated, and cells were rinsed three times with PBS before fixation in 4% paraformaldehyde for 10 min. Permeabilization was performed using 0.5% Triton X-100 in DPBS for 10 min. Actin cytoskeleton was visualized with TRITC-phalloidin (100 μ M in DPBS) for 1 h at room temperature, and nuclei were counterstained with Hoechst 33342 (Thermo Fisher Scientific). Coverslips were mounted using ProLong Gold Antifade reagent (Thermo Fisher Scientific), and imaging was performed with an EVOS confocal microscope (Invitrogen MT700 system). Z-stacks were acquired and reconstructed with EVOS software (Invitrogen MT7000).

RNA sequencing (RNA-seq)

RNA sequencing was carried out to characterize *L. prolificans* DI16-483 –induced transcriptional responses at 3, 6, and 16 h post-infection. Total RNA was extracted from HSAEC1-KT cells using the PureLink RNA isolation kit (Invitrogen, Cat. #12183020).

Strand-specific, paired-end libraries were generated with the TruSeq RNA Sample Preparation Kit (Illumina) and sequenced on the NovaSeq platform (Illumina), producing 150 bp reads from both ends of each cDNA fragment. Raw reads were aligned to the human reference genome (GRCh38, release 101) using HISAT2, and gene-level read counts were obtained from the alignment files. Differential gene expression analysis was performed with the DESeq Bioconductor package. Genes were classified as significantly differentially expressed when they exhibited an absolute \log_2 fold change ≥ 1 with a false discovery rate (FDR) < 0.01 . All experiments were conducted in biological triplicate.

Pathway-level changes were explored using the upstream regulator analysis (URA) module in Ingenuity Pathway Analysis (IPA; Qiagen, <http://www.ingenuity.com>). This algorithm evaluates overlap between the differentially expressed gene set and a curated regulator–target interaction database, incorporating the directionality of gene expression changes to infer upstream regulator activity. Predicted activation or inhibition of signaling pathways was determined based on z-scores, with thresholds of > 2 for activation and < -2 for repression.

Proteomic and phosphoproteomic analysis

For proteomic profiling, HSAEC1-KT cells were infected with *L. prolificans* DI16-483 spores for 3, 6, and 16 h, washed extensively with ice-cold PBS, 1mM, and lysed in 8 M urea supplemented with phosphatase and protease inhibitors. The lysates were submitted to proteomic and metabolomics core facility, at Weill Cornell Medicine of Cornell university for analysis. Equal amounts of protein from each sample were reduced with dithiothreitol (DTT), alkylated with iodoacetamide, and digested overnight with

sequencing-grade trypsin at 37 °C. Resulting peptides were desalted on C18 columns and dried prior to liquid chromatography–tandem mass spectrometry (LC–MS/MS) analysis. Phosphoproteomic enrichment was performed in parallel using TiO₂ chromatography to isolate phosphorylated peptides before LC–MS/MS acquisition.

Preparation of biotinylated HSAEC1-KT protein lysates

HSAEC1-KT cells were seeded into 100-mm tissue culture dishes at a density of 5×10^6 cells per plate and grown until near confluence. Monolayers were placed on ice for 10 min and rinsed three times with 10 mL of ice-cold DPBS. Surface proteins were labeled with the cell-impermeable reagent Sulfo-NHS-SS-biotin (BroadPharm, Cat. #325143), which was first dissolved in DMSO and then diluted in PBS (pH 8.0) to a final concentration of 0.5 mg/mL. The biotinylation solution was added to the cultures and incubated for 1 h on ice with gentle rocking. After incubation, excess reagent was removed, and unbound biotin was quenched with PBS (pH 8.0) containing 100 mM glycine for 10 min on ice. Cells were then washed three times with ice-cold DPBS supplemented with 1 mM PMSF. For lysis, 2 mL of buffer containing 5.6% n-octyl- β -D-glucopyranoside, 1 \times DPBS, 1 mM PMSF, and a protease inhibitor cocktail was added. Cells were scraped, collected, briefly sonicated, and centrifuged at 10,000 \times g for 10 min at 4 °C to remove debris. Recovered protein concentrations were quantified using the Pierce BCA Protein Assay Kit (Thermo Scientific, Cat. #23225) or the Qubit Protein Quantification Kit (Invitrogen, Cat. #Q33211). Lysates were aliquoted into microcentrifuge tubes and stored at –80 °C until analysis.

Whole-cell affinity purification using *L. prolificans* and biotinylated HSAEC1-KT proteins

L. prolificans clinical isolates were cultured on peptone–dextrose agar plates as described above. Spores were collected, washed, swollen for 3 hours and suspended in ice-cold 1× DPBS containing 1 mM PMSF. Following enumeration by hemocytometer, 8.5×10^8 spores were incubated overnight at 4 °C with 5 mg of surface-biotinylated HSAEC1-KT proteins under gentle rotation. After incubation, fungal cells were pelleted by centrifugation at $10,000 \times g$ for 5 min, and the supernatant was retained as flow-through (FT). The spore pellets were washed three times with 600 μ L of ice-cold wash buffer (1× DPBS, 1 mM PMSF, and protease inhibitor cocktail). Host proteins bound to the fungal surface were then eluted by adding 200 μ L of lysis buffer (6 M urea, 5.6% n-octyl- β -D-glucopyranoside, 1× DPBS, 1 mM PMSF, protease inhibitor cocktail) and incubating at room temperature for 10 min. Samples were briefly sonicated, centrifuged at $20,000 \times g$ for 3 min, and the resulting eluates (EP) were collected and stored at –80 °C until analysis.

Streptavidin Enrichment and Proteomic Analysis

Proteins recovered from whole-cell affinity purification were dialyzed extensively against 1× DPBS prior to enrichment. Biotin-labeled host proteins were captured using streptavidin-coated magnetic beads (Pierce, Cat. #88816) according to the manufacturer’s protocol. After binding and washing steps, bead-associated proteins were submitted to the Proteomics and Metabolomics Core Facility at Weill Cornell Medicine (Cornell University) for identification by liquid chromatography–tandem mass spectrometry (LC–

MS/MS). Human protein identities were assigned based on database searches of the acquired MS spectra.

Tissue culture infection experiments

To assess EGFR and c-MET phosphorylation, HSAEC1-KT cells were seeded at a density of 2.5×10^5 cells per well in six-well plates and cultured to near confluence. The growth medium was aspirated, and cells were washed three times with Dulbecco's phosphate-buffered saline (DPBS). Subsequently, growth factor-depleted SAGM medium lacking recombinant human EGF and bovine pituitary extract was added, and the cells were incubated overnight to induce growth factor starvation. The following day, cells were infected with swollen *L. prolificans* conidia at a multiplicity of infection (MOI) of 5 (2×10^6 spores per well). Synchronization of infection was achieved by centrifugation at $1,000 \times g$ for 1 min, and infection was allowed to proceed for 3 or 6 h. At the indicated time points, plates were transferred to ice, the medium was removed, and cells were washed with ice-cold DPBS supplemented with 1 mM sodium orthovanadate and 20 mM sodium fluoride. Cells were then lysed with 1× lysis buffer (Cell Signaling Technology, Cat. #9803) containing phosphatase inhibitor cocktails II and III, protease inhibitor cocktail mix, and 1 mM PMSF. Lysates were collected by scraping, followed by sonication on ice and centrifugation at $3,000 \times g$ for 10 min at 4 °C. The resulting supernatants were used for immunoblotting analyses.

Immunoblotting

Lysates were obtained using during tissue culture infection or pulldowns were separated by electrophoresis using the XCell SureLock Mini-Cell II system (Life Technologies) and subsequently transferred onto polyvinylidene difluoride (PVDF) membranes with the Invitrogen XCell II Blot Module, following the manufacturer's instructions. Membranes were then blocked in TBS-based blocking buffer (LI-COR) for 1 h at room temperature before being incubated with primary antibodies overnight (**Table S3.1**).

Table 3.1. List of primary antibodies used for Immunoblot detection.

Antibody	Catalog number	Manufacturer
Beta-Actin (13E5) Rabbit mAb	#4970	Cell Signaling Technologies
Beta-Actin (8H10D10) Mouse mAb	#3700	Cell Signaling Technologies
EGF receptor (D38B1) XP Rabbit mAb	#4267	Cell Signaling Technologies
Met (D1C2) XP Rabbit mAb	#8190	Cell Signaling Technologies
Phospho-c-Met (Tyr1003) Mouse mAb	#44-882G	Invitrogen
Phospho-EGFR (Tyr1197) Rabbit mAb	#600-401-928	Rockland

On the following day, the membranes were washed four times with TBS-t (1X TBS containing 0.1% Tween 20) followed by 1 h incubation at room temperature with IRDye secondary antibodies. The proteins were then visualized using Odyssey CLx Imaging system and quantified with Image Studio software.

siRNA mediated c-MET and EGFR silencing in HSAEC1-Kt cells and adhesion assay

HSEC1-Kt cells were seeded at a density of 2.5×10^5 cells per well in 24-well plates and incubated for 4-5 days until they reached 80% confluency. Following

incubation, the culture medium was replaced with Opti-MEM (Gibco, 31985062) serum-free medium. HSAEC1-kt were transfected with either 50 μ M targeting siRNA against *cMET* (Santa Cruz Biotechnology, sc-29397), *EGFR* (Santa Cruz Biotechnology, sc-44340) or an equivalent concentration of control siRNA (Santa Cruz Biotechnology, sc-37007). After 24 h, the medium containing transfection complexes was replaced with complete growth medium, and cells were maintained for an additional 48 h to achieve effective silencing that was confirmed by immunoblot. Cells were then infected with *L. prolificans* isolates at MOI 1, infection was synchronized by centrifugation at 1,000 \times g for 1 min. and infection was maintained for 3 hours. washed three times with DPBS to remove non-adherent fungi, and lysed in 0.5% Triton X-100 prepared in deionized water. Cells were scraped, and the lysates were serially diluted and plated on PDA plates. Fungal burden was quantified as colony-forming units (CFU) per well.

Pharmacological manipulation of EGFR and cMET in HSAEC1-Kt cells and adhesion assay

HSAEC1-KT cells were seeded into 24-well plates at a density of 5×10^5 cells per well and cultured for 48 h until confluent. To inhibit receptor signaling, cells were pretreated for 1 h in SAGM medium lacking rhEGF and containing 0.1% DMSO with either gefitinib (50 μ M; EGFR inhibitor) or crizotinib (10 μ M; c-MET inhibitor). Following pretreatment, cells were infected with *Lomentospora prolificans* isolates at an MOI of 1 in the continued presence of inhibitors for 3 h. Fungal burden was quantified as colony-forming units (CFU) per well as described above.

For selective degradation of c-MET, a PROTAC-based approach was applied. The c-MET degrader SJF-8240 (MedChemExpress, Cat. #HY-123961) was prepared in complete SAGM medium supplemented with rhEGF and 0.1% DMSO to a final concentration of 50 μ M. HSAEC1-KT cells were exposed to SJF-8240 for 24 h, after which the medium was removed, and cells were washed with DPBS prior to infection with *L. prolificans* as described above. Post-infection, fungal burden was assessed by CFU quantification.

Cytokine analysis by ELISA

HSAEC1-Kt cells were seeded into 6-well plates at a density of 5×10^5 cells per well and subjected to EGFR and c-MET silencing using siRNA, as described above. After 48 h, cells were infected with *L. prolificans* at an MOI of 1, and infection was allowed to proceed for 24 h to maximize cytokine secretion. Following infection, cells were placed on ice for 15 min, and 1 mL of conditioned medium was collected into tubes containing 10 μ L of protease inhibitor cocktail. Samples were clarified by centrifugation at $10,000 \times g$ for 10 min at 4 °C, and the resulting supernatants were stored at -80 °C until use. Cytokine levels were subsequently quantified by the Cytokine Core Laboratory at the University of Maryland, Baltimore School of Medicine using ELISA-based assays.

Murine model of pulmonary lomentosporiasis

To test the effects of crizotinib and gefitinib on mouse survival following infection, male ICR mice (20 to 25 g [from Envigo]) were immunosuppressed by cyclophosphamide (200 mg/kg administered intraperitoneally [i.p.]) and cortisone acetate

(500 mg/kg administered subcutaneously) given on days -2, -3, and 8 relative to infection. This treatment resulted in 16 days of pancytopenia and neutropenia. To control for bacterial infection, immunosuppressed mice received 50 mg/liter enrofloxacin (Baytril; Bayer, Leverkusen, Germany) *ad libitum* on day -3 through day 0, after which the enrofloxacin was replaced with daily ceftazidime (5 mg/mouse) treatment administered subcutaneously through day 13 relative to infection. Mice were infected with 1.4×10^4 spores of *L. prolificans* DI16-483 in 25 μ l PBS given intratracheally. Treatment with crizotinib (50 mg/kg), gefitinib (40 and 120 mg/kg) was initiated 24 hours after infection and continued daily. Placebo-treated mice received vehicle solution only by p.o. Survival of mice served as the primary endpoint, with moribund mice humanely euthanized.

Results and discussion

***Lomentospora prolificans* exhibits pathogenicity in *Galleria mellonella* and neutropenic murine models**

We first sought to evaluate the virulence of *L. prolificans* isolates using the *Galleria mellonella* infection model, which has been widely employed to investigate the pathogenicity of various fungal organisms, including *Aspergillus fumigatus*, *Candida albicans*, and *Cryptococcus neoformans* [142]. Although *G. mellonella* lacks the adaptive immune system and complex anatomical barriers characteristic of vertebrates, it possesses innate immune components such as hemocytes with functional similarities to mammalian macrophages and neutrophils. This makes it a valuable platform for studying host-pathogen interactions at the level of innate immunity [143, 144]. In addition, the ability to maintain larvae at different incubation temperatures enabled us to examine how

environmental conditions, specifically at 25 °C and 37 °C, influence the virulence potential of *L. prolificans* (Figure 3.1).

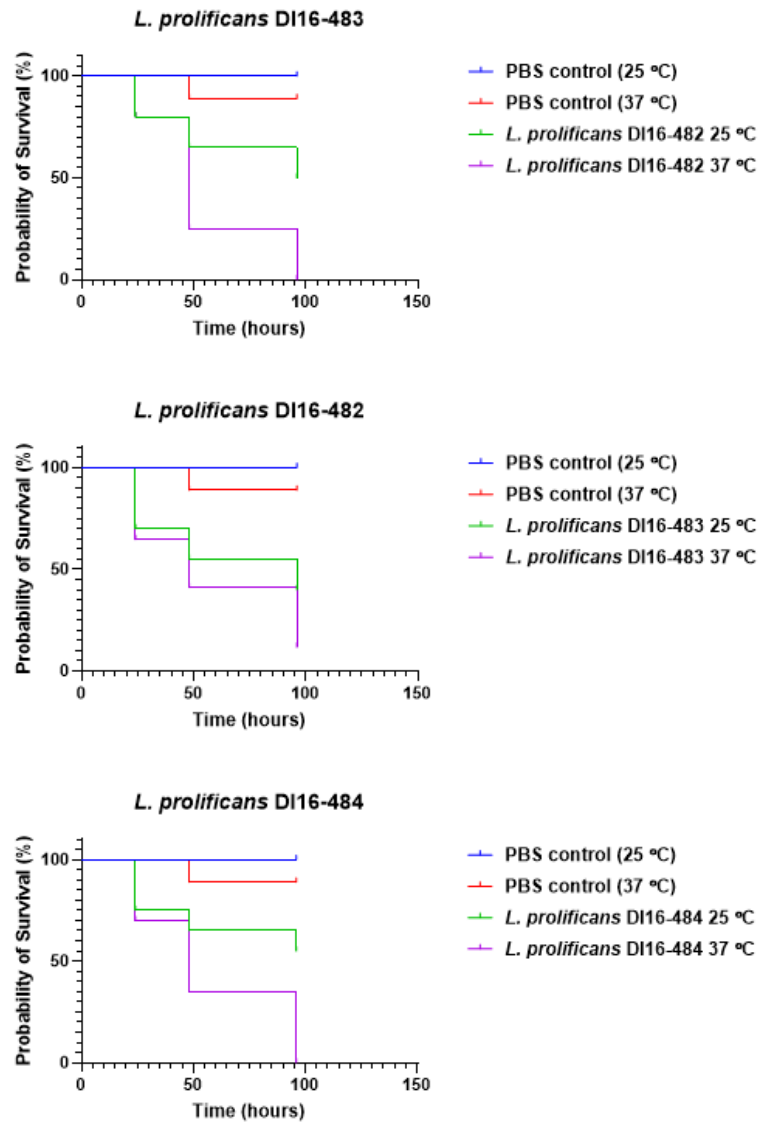


Figure 3.1. Virulence of *Lomentospora prolificans* isolates in the *Galleria mellonella* infection model. Twenty *G. mellonella* larvae were inoculated with *L. prolificans* isolates and maintained at either 25 °C or 37 °C. Survival was monitored over time to assess temperature-dependent differences in virulence.

The *G. mellonella* infection model revealed that *L. prolificans* isolates DI16-483, DI16-482, and DI16-484 are capable of causing progressive and lethal infections, with survival outcomes influenced by temperature. Larvae infected and incubated at 37 °C exhibited markedly accelerated mortality compared to those maintained at 25 °C (**Figure 3.1**). PBS-injected controls showed minimal mortality at either temperature, confirming that larval death was attributable to fungal infection rather than procedural stress. These observations are consistent with prior studies in which pathogenic fungi demonstrated increased lethality in *G. mellonella* at 37 °C, reflecting adaptation to mammalian host environments. The fact that *L. prolificans* exhibits a similar temperature-dependent virulence profile highlights its pathogenic potential and aligns with clinical reports of its ability to cause invasive infections in immunocompromised and immunocompetent patients.

After establishing the temperature-dependent virulence potential of *L. prolificans* in the invertebrate *Galleria mellonella* model, we next sought to characterize the pathogenicity of a representative isolate, *L. prolificans* DI16-483, using a neutropenic murine pulmonary infection model [145]. This vertebrate model provides a translational and clinically relevant context to assess fungal virulence under conditions of host immune suppression mimicking *L. prolificans* infections in neutropenic patients (**Figure 3.2**).

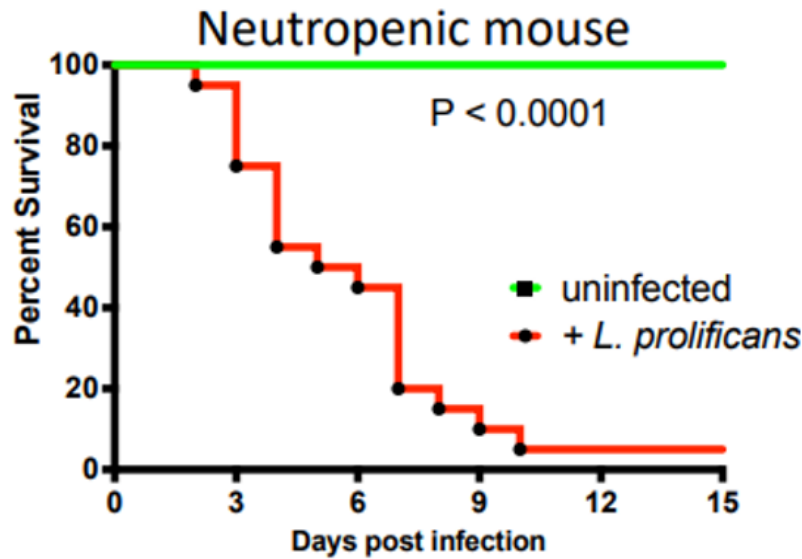


Figure 3.2. *Lomentospora prolificans* DI16-483 induces lethality in a neutropenic murine pulmonary model. Neutropenia was induced with cyclophosphamide, and mice were challenged intratracheally with the *L. prolificans* isolate. Survival was monitored daily.

In the neutropenic murine pulmonary infection model, infection with *L. prolificans* DI16-483 resulted in rapid and progressive mortality, with animals succumbing by day 12 post-infection (**Figure 3.2**). In contrast, uninfected control mice remained fully viable throughout the 15-day observation period, confirming that mortality was directly attributable to fungal challenge and not immunosuppression or breakout of bacterial infections. The survival difference between infected and uninfected groups was significant ($p < 0.0001$), underscoring the strong pathogenic potential of *L. prolificans* in immunocompromised mammalian hosts. These findings demonstrate the clinical scenario, where *L. prolificans* infections are most frequently associated with

severe and often fatal disease in neutropenic or otherwise immunosuppressed patients (Figure 3.2).

These results demonstrate that *L. proliferans* exhibits robust virulence across diverse biological systems, with particularly aggressive disease outcomes under conditions of impaired host immunity.

Interaction of *L. proliferans* with human airway epithelial cells

To build upon the results obtained from invertebrate and murine infection models and establish a platform for dissecting the molecular interactions of *L. proliferans* within the human lung environment, we employed HSAEC1-KT human airway epithelial cells as a host model. In contrast to frequently used pulmonary carcinoma-derived cell lines such as A549 or Calu-3, which harbor oncogenic alterations that can confound host responses, HSAEC1-KT cells originate from normal, non-neoplastic human small airway epithelium and have been immortalized through transfection with human telomerase reverse transcriptase (hTERT) [96]. This immortalization strategy preserves key physiological and structural features of primary airway epithelial cells while enabling long-term propagation in culture. Consequently, HSAEC1-KT cells more closely approximate the responses of healthy lung tissue, providing a relevant system for investigating the early events of host–pathogen interactions, cytoskeletal dynamics, and cellular signaling during *L. proliferans* infection [146].

We first aimed to determine whether interaction of *L. proliferans* with HSAEC1-KT cells leads to host cell death over time. To address this, we employed a highly

sensitive ^{51}Cr release assay, in which HSAEC1-KT cells were infected with the *L. prolificans* DI16-483 isolate (Figure 3.3).

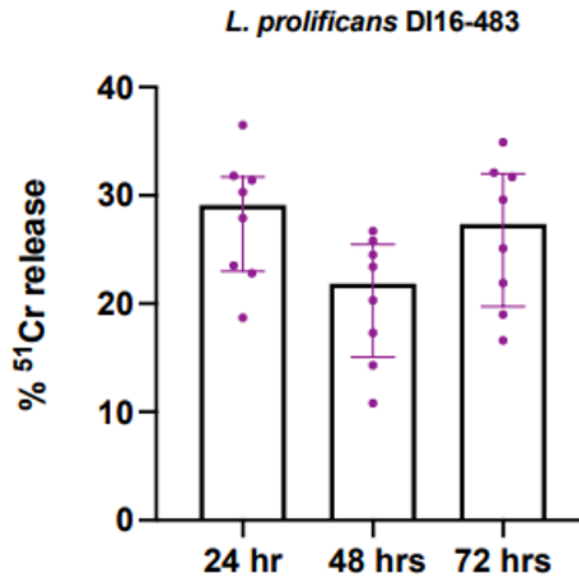


Figure 3.3. The HSAEC1-Kt infection with *L. prolificans* does not induces significant cell death over 72 hours period of infection. HSAEC1-Kt cells were infected with *L. prolificans* DI16-483 and the pathogen-induced cell death was measured by ^{51}Cr release assay.

To our surprise, the chromium release assay demonstrated that infection of HSAEC1-KT cells with *L. prolificans* DI16-483 did not result in substantial cytotoxicity over a 72-hour period (Figure 3.3). Levels of ^{51}Cr release remained relatively stable, with only modest variation between 24, 48, and 72 hours post-infection (approximately 20–30%). These values are consistent with baseline membrane damage expected in long-term cell culture conditions and did not indicate progressive host cell lysis over time. The absence of significant increases in cytotoxicity suggests that *L. prolificans* is able to establish a non-cytolytic interaction with HSAEC1-KT airway epithelial cells. These

findings imply that epithelial cell death is not the primary outcome of infection *in vitro*, but rather that *L. prolificans* may adopt strategies that promote persistence within the host epithelium.

After establishing that interaction of *L. prolificans* with HSAEC1-KT cells does not induce significant host cell death, we next sought to visualize the cellular interface in order to probe the underlying host–pathogen interactions. Microscopy-based studies were employed to examine the potential of *L. prolificans* to invade airway epithelial cells, as many pathogenic fungi are known to breach epithelial barriers either by direct hyphal penetration or through receptor–ligand mediated internalization (**Figure 3.4**). For example, conidia of *Rhizopus delemar* and *Aspergillus fumigatus* have been shown to undergo epithelial uptake, enabling intracellular persistence and dissemination [74, 147]. However, comparable data regarding the epithelial interactions of *L. prolificans* are lacking. To address this gap, we performed infections of HSAEC1-KT cells with *L. prolificans* DI16-483 and visualized actin dynamics to show pathogen-induced cytoskeletal remodeling and potential invasion. Actin recruitment to fungal contact sites was assessed as a hallmark of host cell engagement in the infection process.

Fluorescence microscopy revealed that *L. prolificans* DI16-483 germlings establish direct contact with HSAEC1-KT cells, which was accompanied by marked actin cytoskeletal rearrangements forming concentric ring-like structures around the fungal elements (**Figure 3.4**). In uninfected controls, actin filaments displayed the expected cortical distribution, whereas cytochalasin D (ChD) treatment alone disrupted filament organization, resulting in diffuse phalloidin staining and a loss of well-defined actin structures. Following infection with *L. prolificans*, robust actin recruitment was observed

at fungal contact sites, forming tubular–concentric ring assemblies that are consistent with localized cytoskeletal remodeling and indicative of pathogen-driven invasion mechanisms (**Figure 3.4**). Strikingly, pre-treatment for 1 hour of epithelial cells with ChD markedly reduced the frequency and intensity of actin ring formation, although occasional residual structures were still detected. This suggests that *L. prolificans*–induced cytoskeletal remodeling is largely dependent on active actin polymerization but may also involve reorganization of pre-existing filaments or partially ChD-insensitive pathways (**Figure 3.4**).

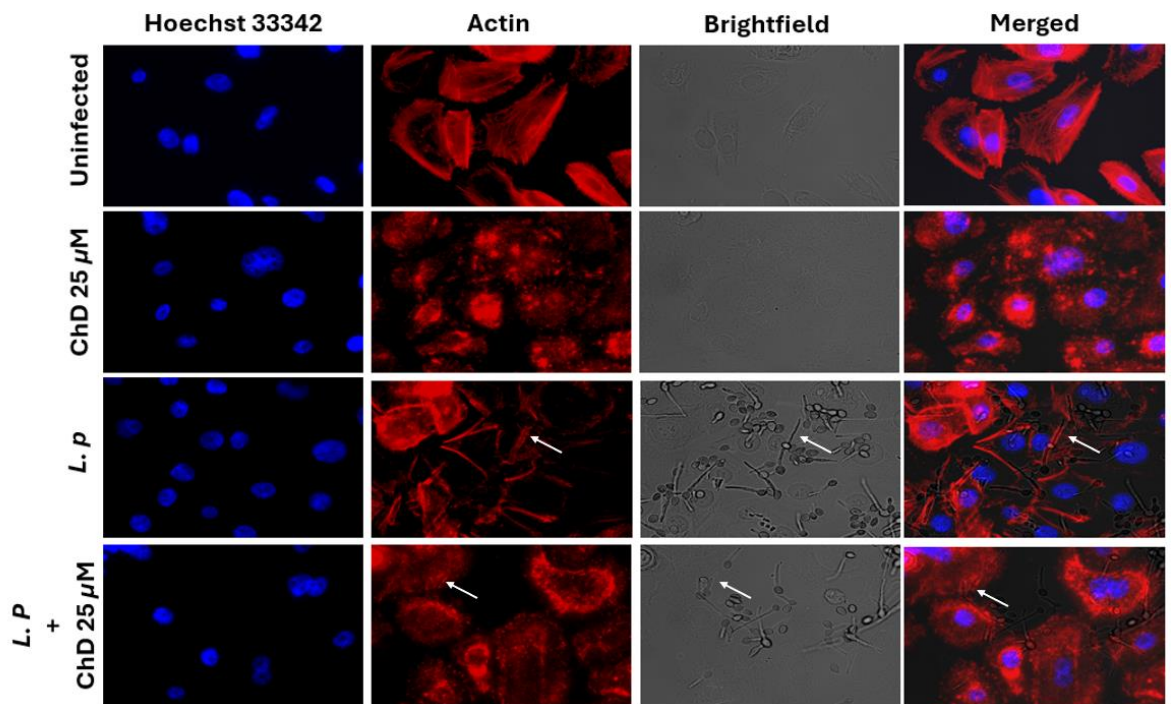


Figure 3.4. Invasion of HSAEC1-KT human small airway epithelial cells by *Lomentospora prolificans* requires actin cytoskeleton rearrangement and it is partly blocked by cytochalasin D. The HSAEC1-KT cells were infected with *L. prolificans* DI16-483 (*L.p*) for 3 hours and actin microelectron was visualized by using TRIC-phalloidin (white arrow). When needed, cells were preincubated with cytochalasin D (ChD) for one hour prior infection.

Together, these observations demonstrate that invasion of human airway epithelial cells by *L. prolificans* requires dynamic actin rearrangement yet may exploit multiple host cytoskeletal mechanisms to engage the epithelium. These findings demonstrate that invasion of airway epithelial cells by *L. prolificans* requires dynamic reorganization of the actin cytoskeleton.

Together, these results suggest that *L. prolificans* exploits actin-dependent processes to engage with and potentially penetrate host epithelial barriers.

Multi-omic analysis of *L. prolificans* infected HSAEC1-KT cells

To investigate the transcriptomic epithelial response to *L. prolificans* infection, we performed transcriptomic profiling of human small airway epithelial cells (HSAEC1-KT) exposed to *Lomentospora prolificans* for 3, 6, and 16 hours, alongside uninfected controls. Furthermore, we included two *Scedosporium* species, *S. boydii* and *S. apiospermum*. Samples from each condition were collected in triplicate to ensure reproducibility. Because poly(A)-enriched RNA was used for library preparation, both host and fungal transcripts were in principle captured. However, since no mechanical disruption step was included during RNA extraction, recovery of fungal RNA was minimal. As a result, the sequencing data predominantly reflected host-derived transcripts, allowing us to specifically analyze epithelial gene expression changes in response to infection [141].

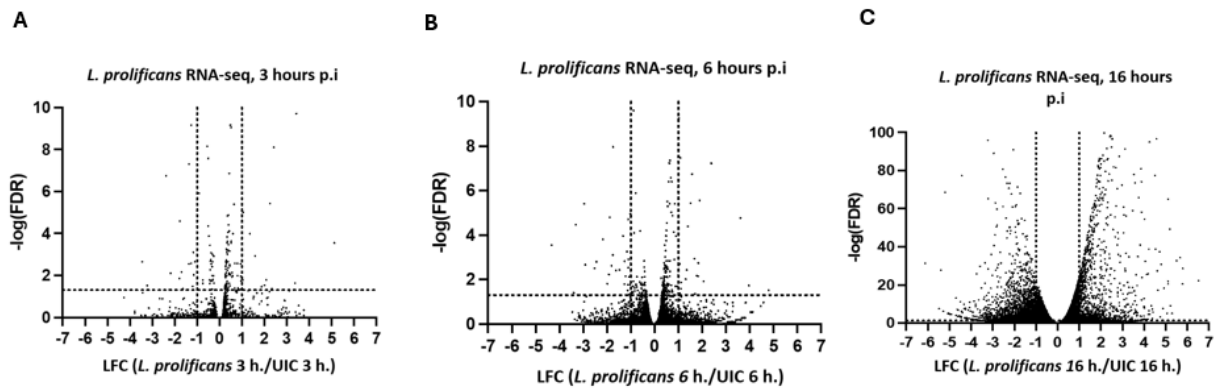


Figure 3.5. The changes of gene expression in HSAEC1-Kt cells following infection with *L. prolificans* DI16-483 at 3 (A), 6 (B), and 16 (C) hours post infection (*p.i.*). The volcano plots display the distribution of differentially expressed genes, where the x-axis represents the \log_2 fold change (LFC) between infected and uninfected control cells, and the y-axis represents the $-\log_{10}$ adjusted *p*-value (FDR).

Transcriptomic profiling of HSAEC1-KT cells infected with *Lomentospora prolificans* revealed a time-dependent pattern of host gene expression changes (**Figure 3.5**). At 3 hours post-infection (**Figure 3.5A**), only a limited number of transcripts were significantly differentially expressed compared with uninfected controls, indicating that early host responses were modest. By 6 hpi (**Figure 3.5B**), differential expression became more pronounced, with a broader set of genes exhibiting both up- and down-regulation, suggesting progressive activation of host signaling pathways as the infection established. The strongest transcriptional changes occurred at 16 hpi (**Figure 3.5C**), where a large cohort of genes showed significant changes, including many with high fold-changes and strong statistical support. This indicates that prolonged exposure to *L. prolificans* drives a robust host transcriptional response.

We next examined proteomic changes in HSAEC1-KT cells following infection with *L. prolificans*. Because RNA-seq analysis revealed that the most pronounced transcriptional changes occurred at 16 hours post-infection, we chose instead to focus our

proteomic analysis on the earlier stages of infection (3 and 6 hours post-infection) in order to capture host signaling events that underlie the initial response to fungal contact.

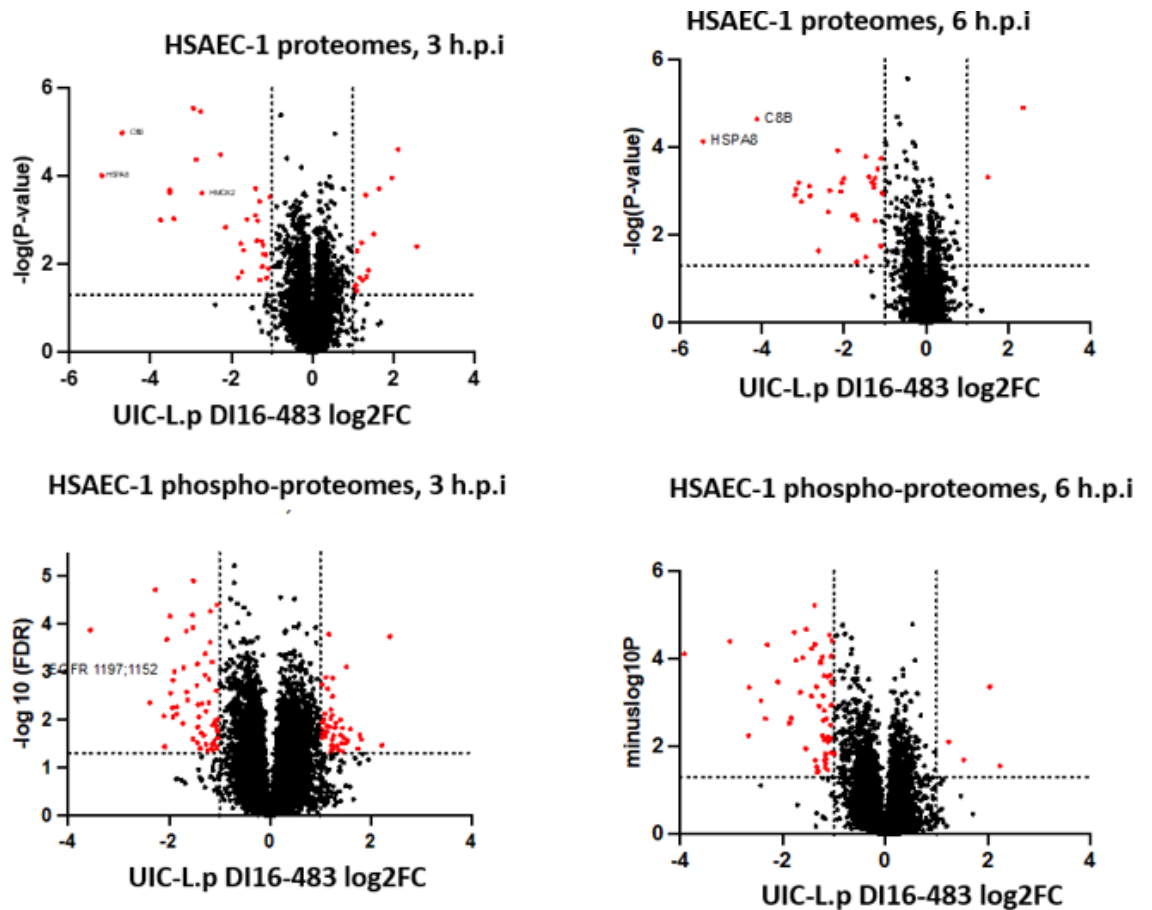


Figure 3.6. The changes in proteome and phospho-proteome profiles of HSAEC1-Kt cells following infection with *Lomentospora prolificans* DI16-483. Volcano plots display the distribution of differentially expressed proteins (top row) and phospho-proteins (bottom row) at 3 (left) and 6 (right), while red dots represents significantly different changes in proteins or their phosphorylation at specific hours post infection (h.p.i.). The x-axis shows the \log_2 fold change (\log_2FC) between infected and uninfected control cells, while the y-axis represents the $-\log_{10}$ transformed statistical significance.

Our proteomic analyses included both quantitative measurements of both the simple abundance of specific proteins and the phosphorylation states of specific proteins. Analysis of protein abundance in HSAEC1-KT cells during early *L. prolificans* infection

revealed dynamic host protein remodeling at both 3 and 6 hours post-infection compared to time-matched uninfected control (**Figure 3.6**). At 3 hpi, several stress-associated factors were significantly modulated, including heat shock proteins (HSP90, HSPA8) and the molecular chaperone CCT [148]. By 6 hpi, these shifts became more pronounced, with HSPA8 and CCT components remaining significantly altered, indicating that *L. prolificans* infection imposes stress signaling in HSAEC1-Kt cells. At 3 hpi, phosphorylation events were observed on epidermal growth factor receptor (EGFR), notably at tyrosine residues Y1197 and Y1152, sites associated with receptor activation and downstream signaling through MAPK and PI3K/AKT pathways [149]. The activation of EGFR signaling in airway epithelial cells aligns with previous studies showing that Mucorales, *A. fumigatus* and *C. albicans* exploit host receptor tyrosine kinases, including EGFR and ErbB family members, to facilitate adhesion, internalization, and invasion [73, 139, 150]. EGFR-mediated actin remodeling has been described as a prerequisite for fungal entry, and its phosphorylation here suggests that *L. prolificans* possibly engages similar epithelial signaling mechanisms to promote invasion.

To further validate these observations, we revisited the RNA-seq dataset and conducted pathway enrichment analysis using Ingenuity Pathway Analysis (IPA). This approach enabled us to integrate transcriptomic signatures with biological networks, thereby predicting upstream regulators and signaling pathways that are likely driving the observed gene expression changes during *L. prolificans* infection (**Figure 3.7**). The analysis of HSAEC1-KT cells infected with *L. prolificans* revealed selective activation of host signaling regulators that differed in both magnitude and kinetics from those induced by the closely related species *S. apiospermum* and *S. boydii* (**Figure 3.7A**). At early

infection stages (3–6 hpi), *L. prolificans* strongly engaged growth factor receptor pathways, including EGFR, and possibly downstream MAPK/ERK signaling, consistent with our proteomic evidence of EGFR phosphorylation. These regulators are tightly linked to actin cytoskeletal remodeling, supporting our observation of actin ring formation around fungal germlings. In contrast to *Scedosporium* species, which elicited broader pro-inflammatory regulators such as TNF, IL1B, and NF-κB, *L. prolificans* induced a comparatively muted inflammatory transcriptional response. By 16 hpi, *L. prolificans* continued to maintain growth factor–associated signaling (EGFR, PDGF-BB, ERK1/2), while pro-inflammatory nodes remained less pronounced (**Figure 3.7A**).

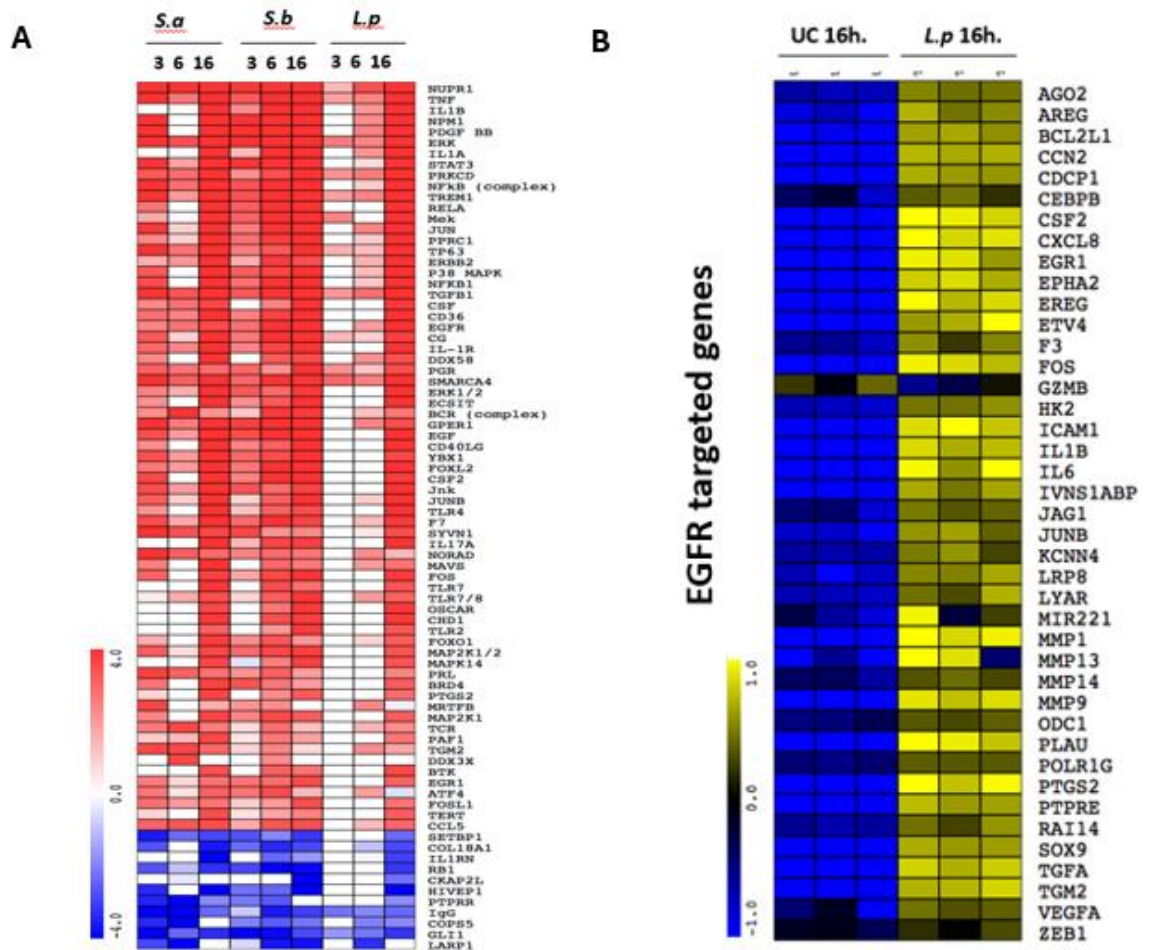


Figure 3.7. Integrated pathway analysis (IPA) predicts activation of growth factor receptor signaling in HSAEC1-KT cells following *Lomentospora prolificans* (*L.p*) infection, with comparative profiling against the closely related species *Scedosporium apiospermum* (*S.a*) and *Scedosporium boydii* (*S.b*). (A) Heatmap showing differential expression of genes associated with growth factor receptor signaling pathways at 3, 6, and 16 hours post infection.+ (B) Heatmap of EGFR-targeted genes at 16 hours post infection. Compared to uninfected control cells (UC, 16h).

L. prolificans infected cells displayed broad upregulation of canonical EGFR-regulated transcripts, including growth factors (AREG, TGFA, EREG), transcription factors (FOS, JUNB, EGR1), cytokines (IL1B, IL6, CXCL8), and extracellular matrix-modifying enzymes (MMP1, MMP9, MMP13, MMP14) (**Figure 3.7B**). This suggests that *L. prolificans* relies on epithelial remodeling and cytoskeletal engagement rather than robust immune activation to establish infection, a strategy that may help explain its persistence in airway tissue despite limited host cell death.

EGFR and c-MET growth factor receptors mediate host interaction with *Lomentospora prolificans*

After characterizing the transcriptional and proteomic responses of airway epithelial cells to *L. prolificans* and identifying the first candidate host receptors, we next established a novel affinity pulldown strategy to directly probe host-pathogen interactions (**Figure 3.8**). This approach enabled the capture and identification of preferentially biotinylated epithelial cell surface proteins using cell-impermeable biotin chemistry, capable of binding *L. prolificans*, thereby providing direct evidence of receptor-level engagement at the host-fungal interface (**Figure 3.8**).

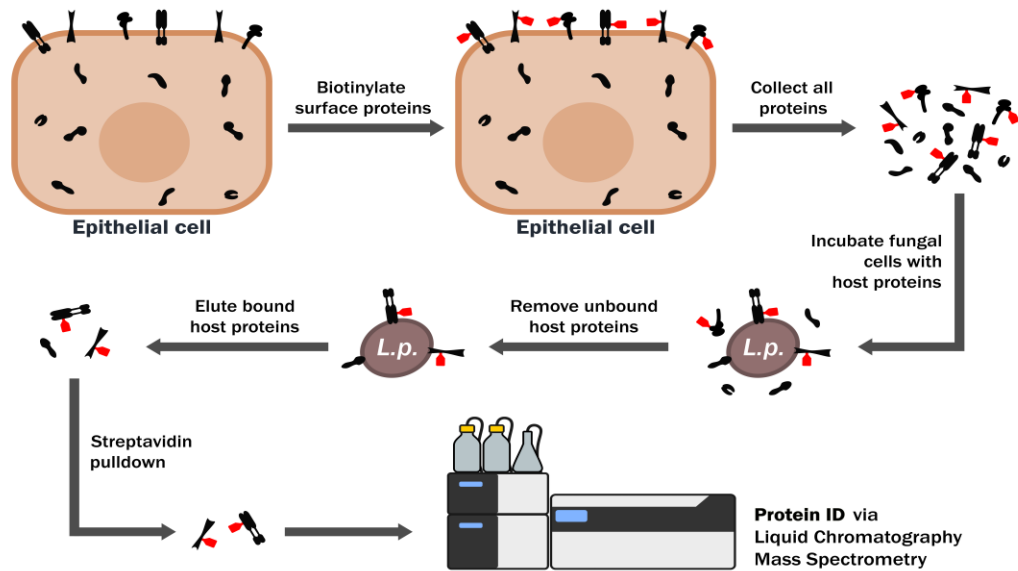


Figure 3.8. Schematic representation of the whole-cell affinity pulldown technique used to identify human small airway epithelium-derived host surface proteins that bind *L. proliferans*. Cell surface proteins were biotinylated, incubated with fungal cells, and bound proteins were isolated by streptavidin pulldown. Interacting host proteins were then identified by liquid chromatography–mass spectrometry (LC–MS).

To minimize the possibility of cell line-specific bias associated with the use of HSAEC1-KT cells, we extended our affinity pulldown experiments to include biotinylated lysates from A549 lung epithelial cells. Proteins that were consistently detected in both cell lines were prioritized as high-confidence candidates for functional analysis (Table S2). Among detected proteins, various surface expressed proteins, such as integrins, growth factor receptors, extracellular matrix proteins were detected. Notably, this analysis confirmed the presence of EGFR previously implicated through RNA-seq and proteomic data, as well as c-MET, which had been identified by proteomics in HSAEC1-KT cells infected with *L. proliferans* (Figure 3.9). Furthermore, this provided

the first evidence that EGFR can directly bind fungal pathogen, rather than interacting indirectly.

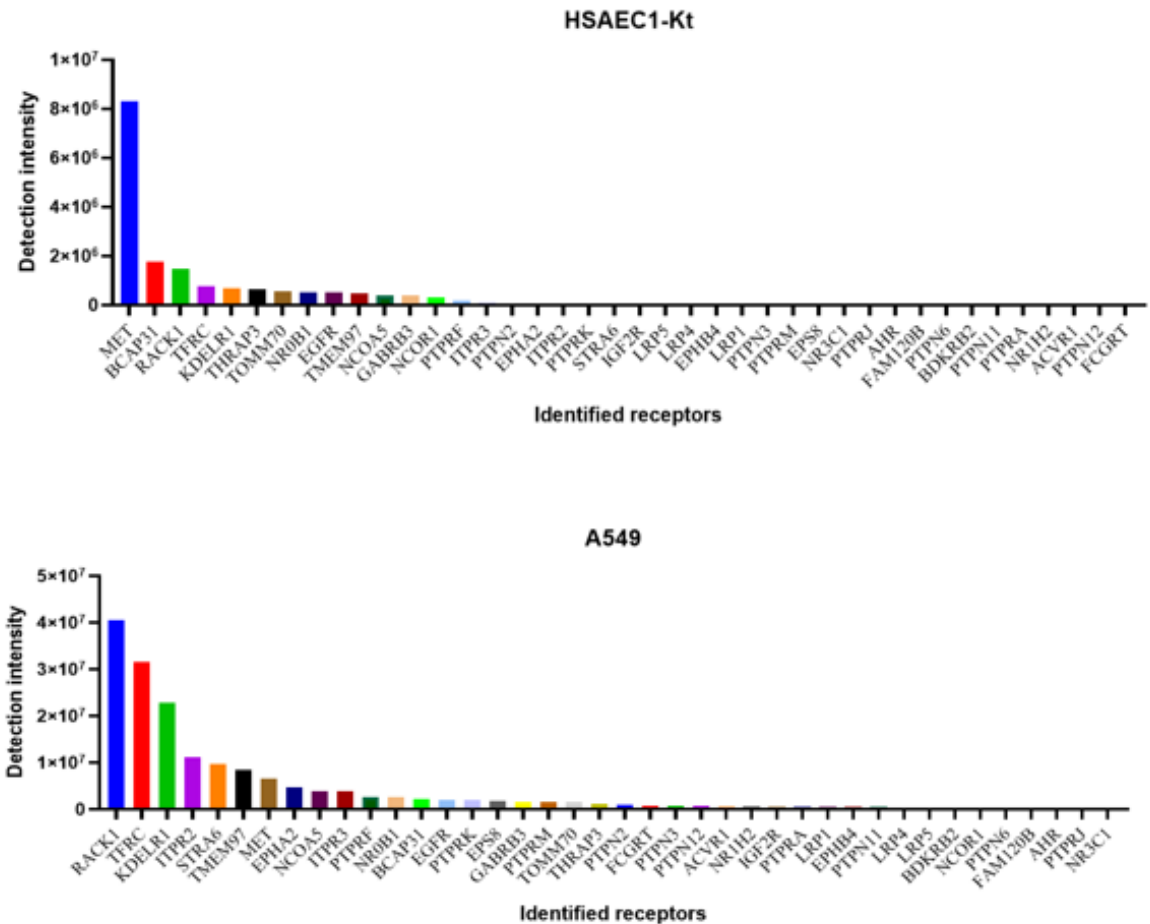


Figure 3.9. Proteomic LC-MS pulldown experiments identified multiple host cell surface proteins that directly interact with *Lomentospora prolificans* conidia. Bar graphs show detection intensity of identified receptors in HSAEC1-Kt cells (top) and A549 cells (bottom). Several high-abundance receptors, including MET, RAC1, and EGFR family members, were detected, indicating potential host–fungal interaction partners.

After identifying EGFR and *c*-MET as candidate host receptors capable of directly binding *L. prolificans* through proteomic approaches in two lung-derived epithelial cell lines, we next sought to validate these interactions by immunoblot analysis.

For this, pulldown assays were performed using non-biotinylated HSAEC1-KT cell lysates, followed by probing for EGFR and *c*-MET. In addition, to assess whether the fungal developmental stage influences receptor binding, we compared interactions mediated by harvested spores (HS), swollen spores (SS), and germlings (GS). This approach allowed us to determine stage-specific differences in protein binding by *L. prolificans* (Figures 3.10-3.11).

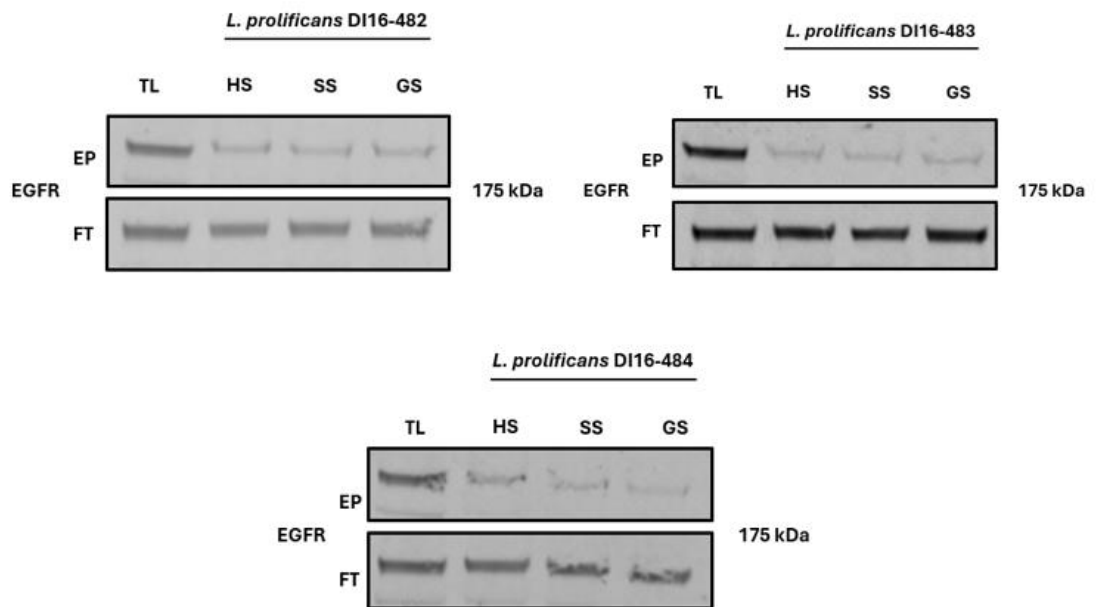


Figure 3.10. EGFR directly binds *Lomentospora prolificans* conidia and germlings in affinity pulldown assays. Harvested spores (HS), swollen spores (SS), and germlings (GS) were subjected to whole-cell affinity pulldown with HSAEC1-KT lysates. Eluted proteins (EP) and flow-through fractions (FT) were analyzed by immunoblot and probed for EGFR.

EGFR was consistently detected in eluates across all three clinical isolates (DI16-482, DI16-483, and DI16-484), confirming its ability to directly associate with fungal cells (Figure 3.10).

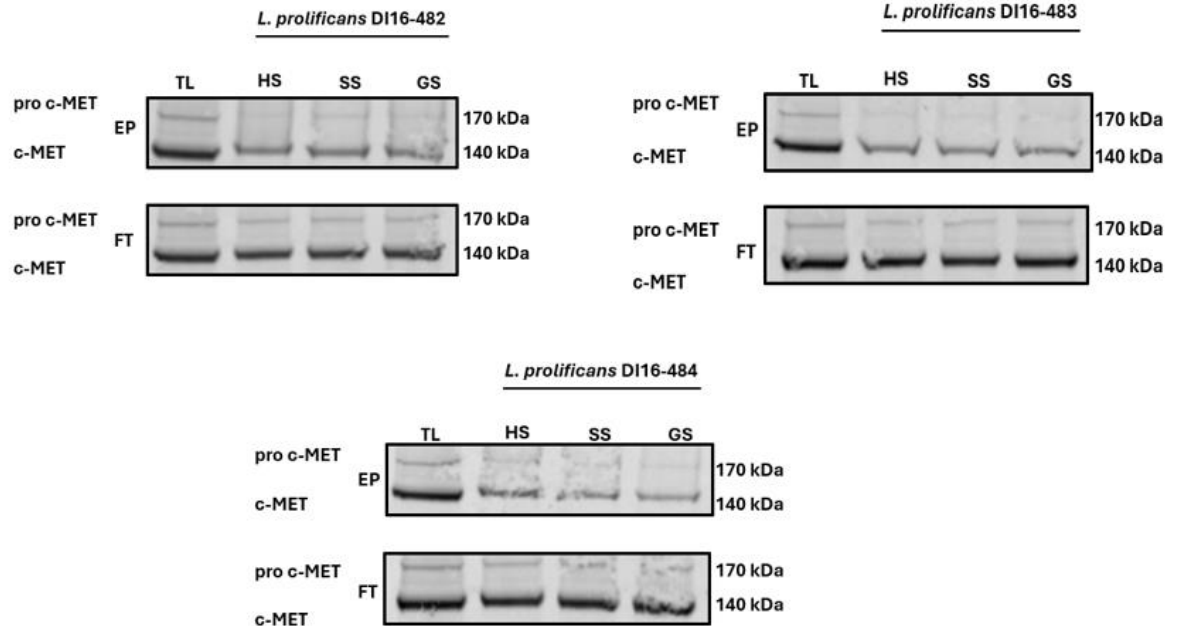


Figure 3.11. c-MET directly binds *Lomentospora prolificans* conidia and germlings in affinity pulldown assays. Harvested spores (HS), swollen spores (SS), and germlings (GS) were subjected to whole-cell affinity pulldown with HSAEC1-KT lysates. Eluted proteins (EP) and flow-through fractions (FT) were analyzed by immunoblot and probed for c-MET.

A similar pattern was observed for c-MET, where both the precursor (170 kDa) and mature (140 kDa) forms were recovered in eluates. Again, germlings mediated the interaction, followed by swollen spores, whereas harvested spores bound only weakly. These findings demonstrate that *L. prolificans* can directly interact with both EGFR and c-MET, and that receptor binding is enhanced during fungal morphogenesis, particularly at the germling stage when host invasion processes are initiated.

EGFR and c-MET are phosphorylated in HSAEC1-KT cells following *Lomentospora prolificans* infection

After establishing that EGFR and c-MET can directly bind *L. prolificans* conidia, we next investigated whether fungal interaction with HSAEC1-KT cells leads to phosphorylation of these receptors, thereby supporting the hypothesis that receptor engagement triggers downstream signaling cascades. We next analyzed the phosphoproteomic dataset to assess EGFR and c-MET phosphorylation in response to *L. prolificans* infection at 3 and 6 hours post-infection (**Figure 3.12**).

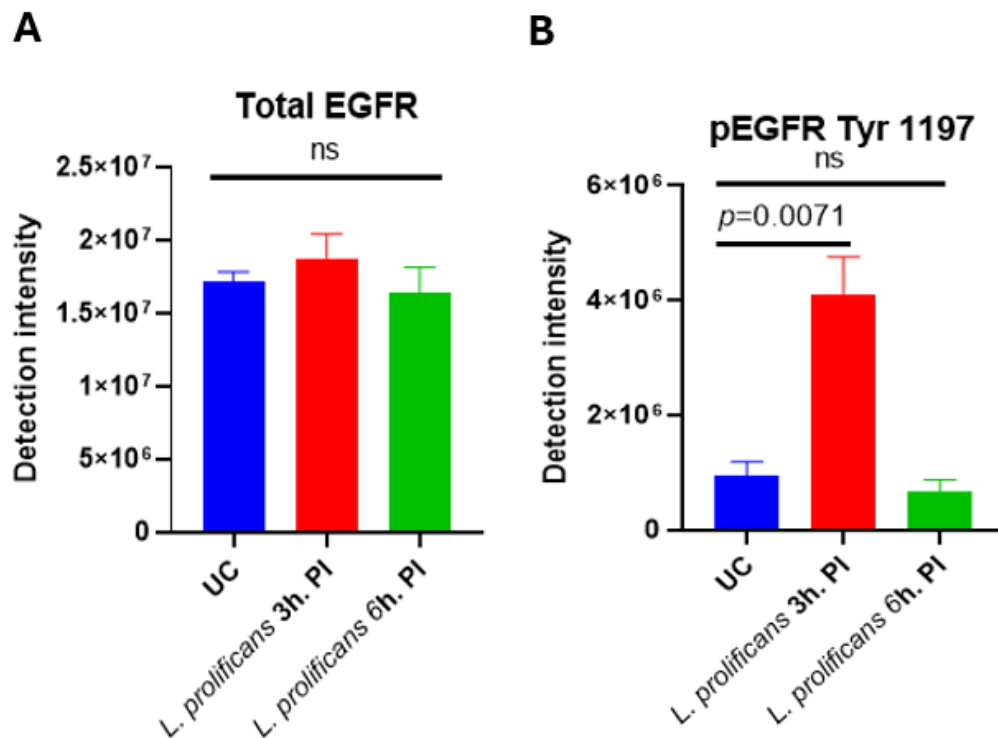


Figure 3.12. Proteomic-based analysis of EGFR Tyr1197 phosphorylation dynamics in HSAEC1-Kt cells during *Lomentospora prolificans* infection. Panel A shows that total EGFR protein abundance remained unchanged at 3 and 6 hours post infection compared with uninfected controls. Panel B demonstrates a significant, transient increase in phosphorylation of EGFR Tyr1197 at 3 hours post infection, as detected by quantitative phospho-proteomics.

A significant increase in phosphorylation of EGFR at the conserved Tyr1197 residue was observed, while the total abundance of EGFR remained unchanged,

indicating that the effect was due to receptor activation rather than altered protein levels. Functionally, phosphorylation of EGFR at Tyr1197 is associated with the recruitment of adaptor proteins such as Shc and Grb2, leading to activation of the RAS–RAF–MEK–ERK signaling cascade, which drives transcriptional responses involved in cell proliferation, differentiation, and cytoskeletal remodeling [151-153]. Importantly, Tyr1197 phosphorylation has also been implicated in EGFR endocytosis and receptor sorting, suggesting that *L. prolificans* may exploit this modification to trigger receptor internalization and trafficking. Such receptor dynamics could potentially facilitate actin-dependent cytoskeletal remodeling and promote fungal adhesion or invasion of airway epithelial cells.

We next evaluated c-MET phosphorylation in HSAEC1-KT cells during *L. prolificans* infection at 3- and 6-hours post-infection (**Figure 3.13**).

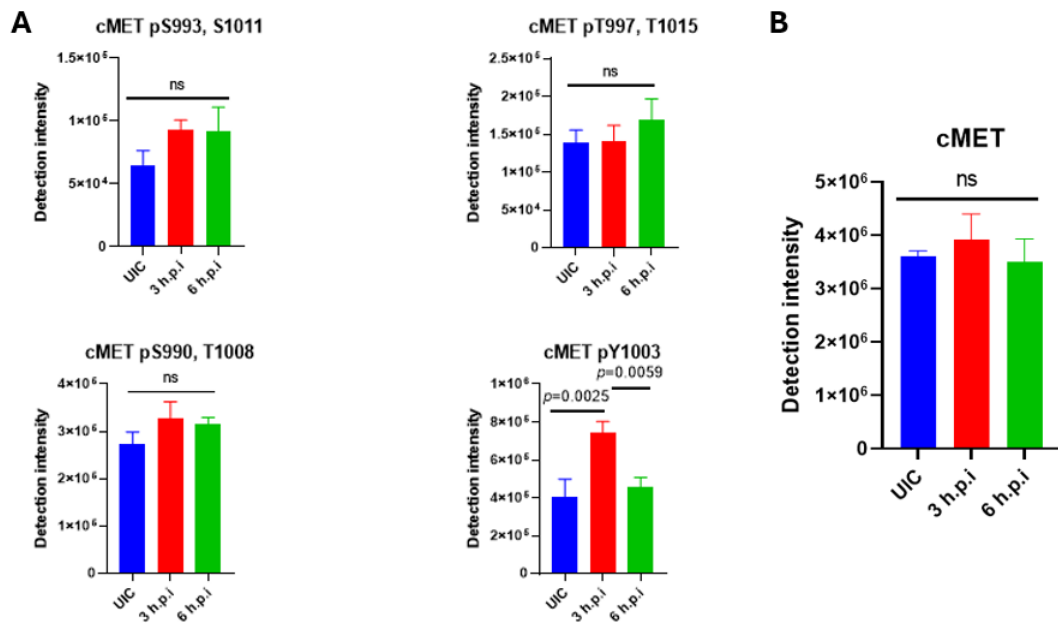


Figure 3.13. Proteomics-based profiling of c-MET phosphorylation during *Lomentospora prolificans* infection of HSAEC1-Kt cells. Panel A shows phosphoproteomic analysis of identified c-MET phosphorylation sites at 3 and 6 hours post infection compared with uninfected controls. Panel B demonstrates that total c-MET protein abundance remained unchanged across the same time points.

Analysis of multiple phosphosites revealed that most residues, including Ser993/Ser1011, Thr997/Thr1015, and Ser990/Thr1008, showed no significant changes compared with uninfected controls. However, we observed a significant increase in phosphorylation at Tyr1003, a conserved regulatory site within the juxtamembrane domain of *c*-MET. Importantly, total *c*-MET protein abundance remained unchanged across conditions. Functionally, phosphorylation of *c*-MET at Tyr1003 is known to regulate receptor ubiquitination and internalization through recruitment of the E3 ubiquitin ligase CBL, thereby controlling receptor turnover and signaling dynamics. This suggests that *L. proliferans* engagement induces selective phosphorylation of *c*-MET at a site critical for receptor endocytosis and degradation, potentially fine-tuning receptor signaling outputs during infection [154-156].

Immunoblot validation further demonstrated that *L. proliferans* infection induces transient EGFR phosphorylation in HSAEC1-KT cells (**Figure 3.14**). At 3 hours post-infection, all three isolates (DI16-482, DI16-483, and DI16-484) showed elevated pEGFR levels compared with uninfected controls, while total EGFR expression remained stable (**Figure 3.14**). Consistent with our LC-MS based results (**Figure 3.12**), we did not observe an infection-induced increase in phosphorylation at 6 hours post-infection.

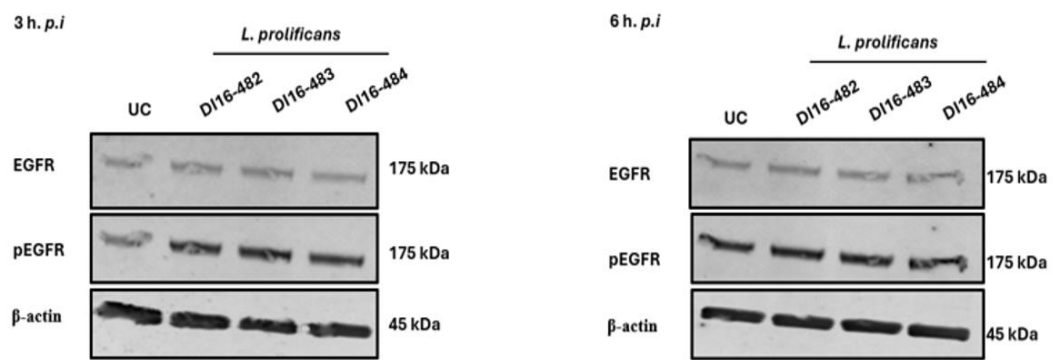


Figure 3.14. EGFR Tyr 1197 phosphorylation is induced by *Lomentospora prolificans* infection of HSAEC1-KT cells. Immuno blot analysis at 3 and 6 hours post-infection demonstrating increased phosphorylation of EGFR (pEGFR) at Tyr 1197 across isolates DI16-482, DI16-483, and DI16-484, while total EGFR levels remained unchanged.

The confirmation of EGFR Tyr1197 and c-MET Tyr1003 phosphorylation in airway epithelial cells following *L. prolificans* infection is of particular significance. Given the intrinsic multidrug resistance of *L. prolificans* to nearly all available antifungal agents, these findings open new avenues for host-directed therapeutic strategies. Targeting host growth factor receptor signaling with clinically approved tyrosine kinase inhibitors, such as the EGFR inhibitor gefitinib and the c-MET inhibitor crizotinib, may provide a novel approach to limit fungal invasion and mitigate infection progression [157].

EGFR and c-MET govern *L. prolificans* adhesion and immune responses in HSAEC1-KT human airway epithelial cells

After confirming that *L. prolificans* can interact with EGFR and c-MET and their interaction results in phosphorylation signaling, we then aimed to functionally determine role of EGFR and c-MET during the infection. Building upon our previous finding where we observed that actin recruitment during the infection, we hypothesized that EGFR and c-MET could act as a *L. prolificans* receptors on human small airway epithelial cells.

We first employed siRNA-mediated knockdown of EGFR and c-MET in HSAEC1-KT cells, followed by a fungal adhesion assay to assess the impact of receptor silencing on *L. prolificans* binding (**Figure 3.15-3.16**).

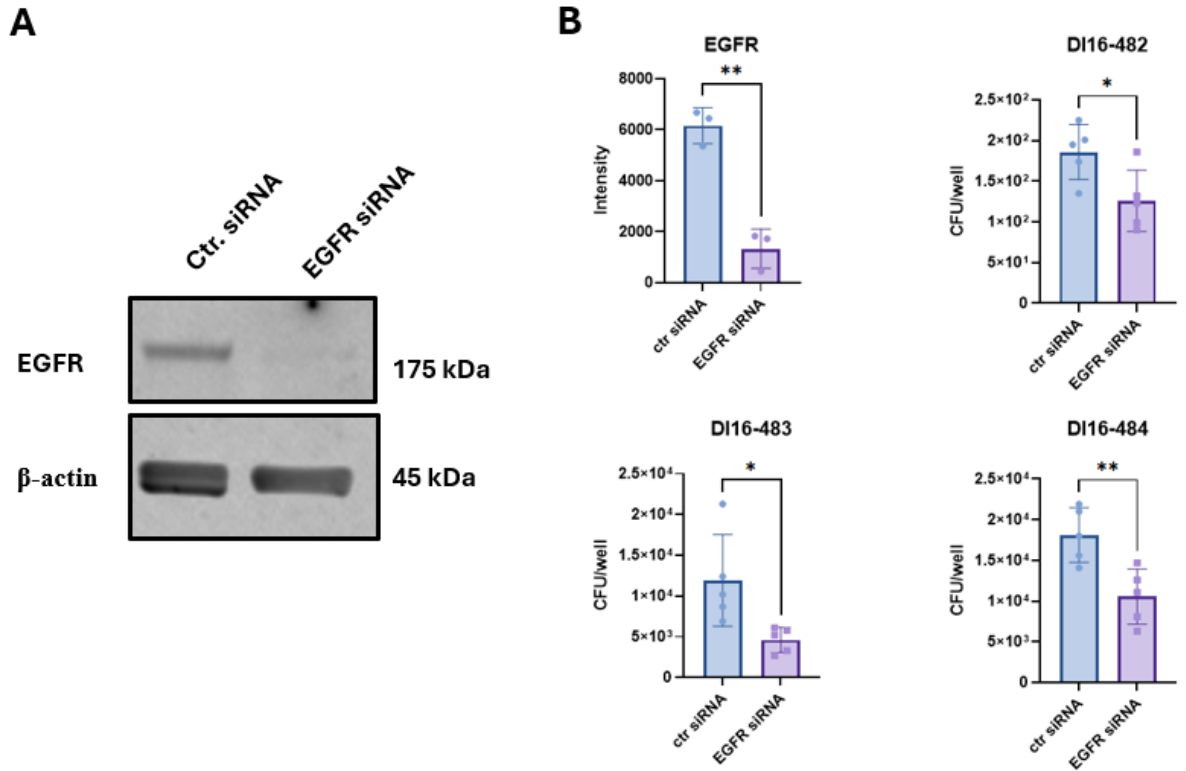


Figure 3.15. EGFR silencing by siRNA in HSAEC1-KT human airway epithelial cells reduces the adhesion of *Lomentospora prolificans*. (A) Immunoblot confirmation of knockdown of EGFR in HSAEC1-KT cells following siRNA transfection compared with control siRNA-treated cells. (B) Quantification of EGFR protein levels and functional adhesion assays showed that EGFR knockdown significantly decreased fungal adhesion for isolates DI16-482, DI16-483, and DI16-484 compared with control cells. Data are shown as mean \pm SEM, with statistical significance indicated (* $p < 0.05$, ** $p < 0.01$).

Efficient silencing of EGFR expression in HSAEC1-KT cells was confirmed by immunoblot analysis following siRNA transfection (**Figure 3.15A**). Intensity quantification further demonstrated a significant reduction in EGFR levels compared to control siRNA-treated cells (**Figure 3.15B**). Functional assessment using adhesion assays revealed that silencing EGFR markedly reduced *L. prolificans* binding across all three clinical isolates tested (**Figure 3.15B**).

In parallel with EGFR, we next assessed the role of c-MET in mediating *L. prolificans* adhesion to airway epithelial cells. siRNA-mediated knockdown efficiently reduced both the precursor (170 kDa) and mature (140 kDa) forms of c-MET, as confirmed by immunoblot and quantification (**Figure 3.16A–B**). Similar to EGFR silencing, loss of c-MET expression led to a significant decrease in fungal adhesion across all three clinical isolates (DI16-482, DI16-483, and DI16-484) compared with control siRNA-treated cells (**Figure 3.16B**).

In parallel with EGFR, we next assessed the role of c-MET in mediating *L. prolificans* adhesion to airway epithelial cells. siRNA-mediated knockdown efficiently reduced both the precursor (170 kDa) and mature (140 kDa) forms of c-MET, as

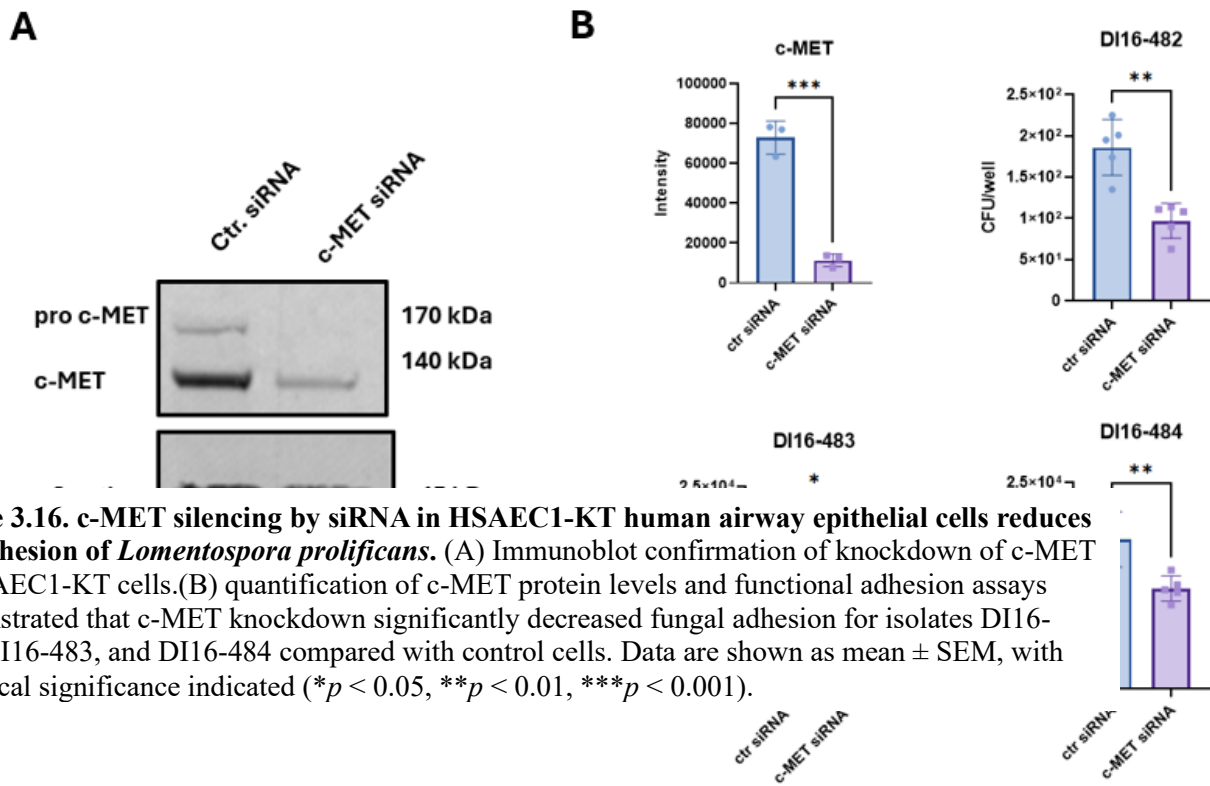


Figure 3.16. c-MET silencing by siRNA in HSAEC1-KT human airway epithelial cells reduces the adhesion of *Lomentospora prolificans*. (A) Immunoblot confirmation of knockdown of c-MET in HSAEC1-KT cells.(B) quantification of c-MET protein levels and functional adhesion assays demonstrated that c-MET knockdown significantly decreased fungal adhesion for isolates DI16-482, DI16-483, and DI16-484 compared with control cells. Data are shown as mean ± SEM, with statistical significance indicated (* $p < 0.05$, ** $p < 0.01$, *** $p < 0.001$).

confirmed by immunoblot and quantification (**Figure 3.16A–B**). Similar to EGFR

silencing, loss of c-MET expression led to a significant decrease in fungal adhesion across all three clinical isolates (DI16-482, DI16-483, and DI16-484) compared with control siRNA-treated cells (**Figure 3.16B**).

After establishing that knockdown of EGFR and c-MET reduced fungal adhesion, we next sought to determine whether pharmacological inhibition of these receptors would produce a similar effect. For EGFR inhibition, we employed gefitinib, a clinically approved ATP-competitive tyrosine kinase inhibitor that has been widely used to modulate EGFR signaling in *vivo in* both preclinical models and patients. To block c-MET signaling, we used crizotinib, an orally bioavailable dual c-MET/ALK tyrosine kinase inhibitor approved for clinical use.

Pharmacological inhibition of growth factor receptor signaling reduced *L. prolificans* adhesion to HSAEC1-KT cells (**Figure 3.17**). Treatment with the EGFR inhibitor gefitinib (25 μ M) significantly decreased fungal burden for isolates DI16-482 and DI16-484 in HSAEC1-KT, while no significant reduction was observed for isolate DI16-483 (**Figure 3.17A**). Similarly, inhibition of c-MET with crizotinib (10 μ M) led to a significant decrease in adhesion across all three isolates, with the strongest effect observed in DI16-484 (**Figure 3.17B**).

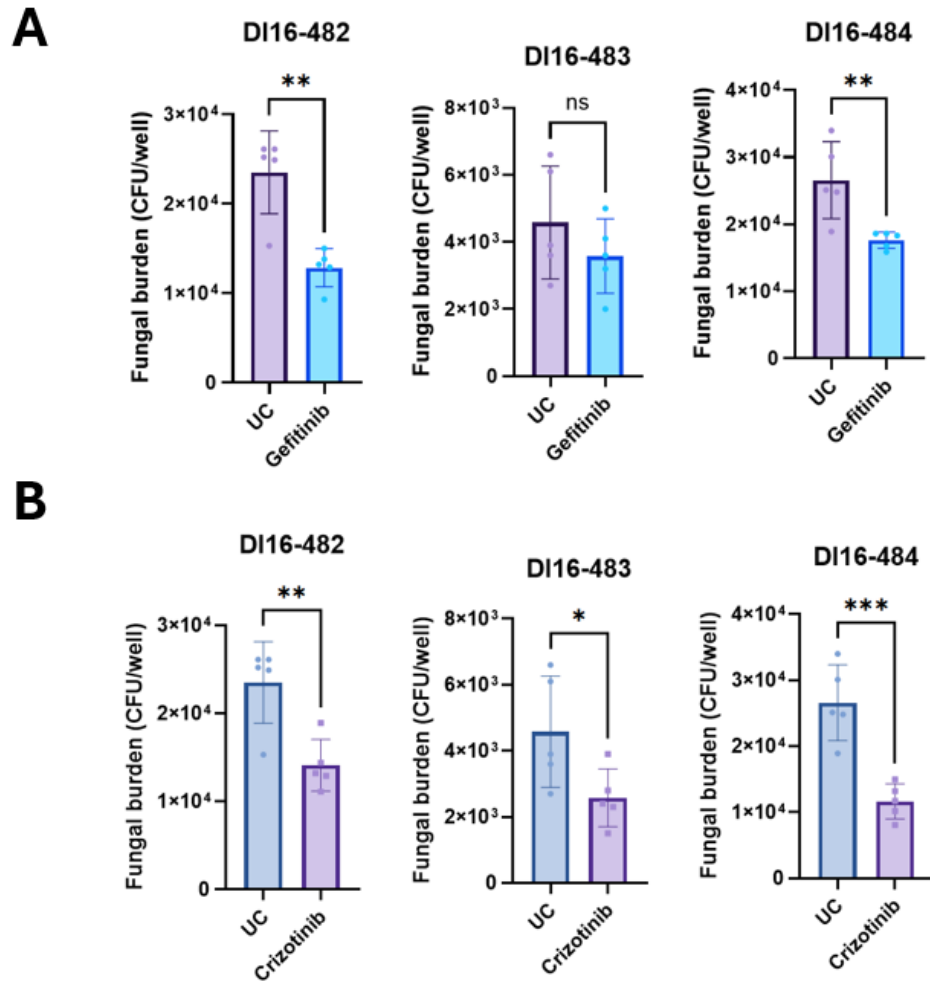


Figure 3.17. Pharmacological inhibition of EGFR and c-MET with FDA approved inhibitors reduces *Lomentospora prolificans* adhesion to HSAEC1-KT human airway epithelial cells. (A) Treatment of HSAEC1-KT cells with the EGFR inhibitor gefitinib significantly decreased fungal adhesion for isolates DI16-482 and DI16-484, while no significant reduction was observed for isolate DI16-483. (B) Treatment with the c-MET inhibitor crizotinib significantly reduced adhesion across all three isolates. Data are presented as mean \pm SEM, with statistical significance indicated (* $p < 0.05$, ** $p < 0.01$, *** $p < 0.001$).

Finally, to further dissect the functional role of EGFR and c-MET during *L. prolificans* infection and given that growth factor receptors are known to modulate immune responses through the MAPK/ERK signaling axis (20832498, 36037968), we investigated whether silencing these receptors altered cytokine secretion by HSAEC1-KT cells (Figures 3.18–3.19).

modulate IL-6 and IL-8, revealing potential for host-directed therapies targeting growth factor receptor signaling.

Collectively, these results demonstrate that EGFR and c-MET expressed on human pulmonary epithelial cells govern *L. proliferans* adhesion and epithelial immune responses through direct receptor engagement and downstream signaling. This dual role highlights EGFR and c-MET as potential therapeutic targets, opening avenues to explore pharmacological inhibition of growth factor receptor signaling as a strategy to counteract the pulmonary pathogenesis of *L. proliferans*.

The effect of EGFR and c-MET inhibition on survival in a neutropenic murine model of pulmonary lomentosporiasis

After identifying and confirming EGFR and c-MET as receptors exploited by *L. proliferans* on human airway epithelial cells, we next sought to evaluate whether pharmacological inhibition of these receptors *in vivo* could alter the outcome of infection. To this end, we employed a neutropenic murine model of pulmonary lomentosporiasis, in which mice were intratracheally challenged with the *L. proliferans* DI16-483 isolate. To block EGFR signaling, animals received oral treatment with gefitinib at either a low dose (40 mg/kg) or a high dose (120 mg/kg), beginning shortly after infection. In parallel, inhibition of c-MET signaling was achieved by administering crizotinib (50 mg/kg) (**Figure 3.20**).

Animals treated with vehicle alone exhibited a progressive decline in survival, with approximately one-third of animals alive by day 8 post-infection, after which survival plateaued. In contrast, animals receiving gefitinib or crizotinib succumbed more

rapidly, with median survival reduced to approximately 5–6 days. No long-term survivors were observed in any of the inhibitor-treated groups (Figure 3.20).

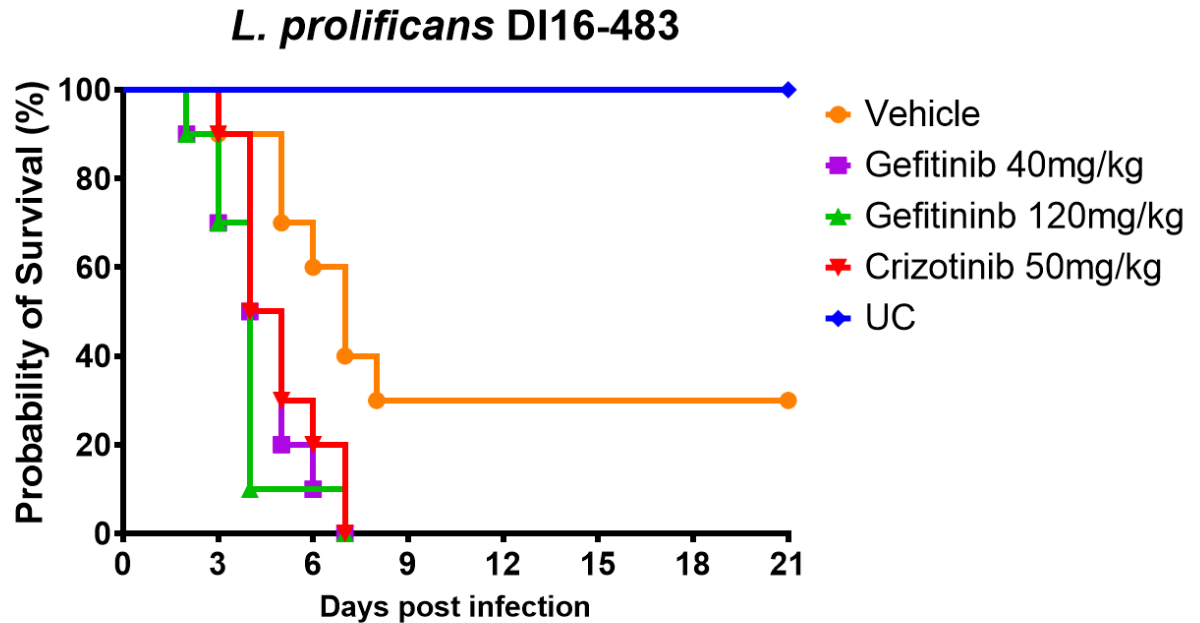


Figure 3.20. Effect of EGFR and c-MET inhibition on survival in a neutropenic murine model of pulmonary *Lomentospora prolificans* infection. CD-1 mice were rendered neutropenic and intratracheally infected with the *L. prolificans* DI16-483 isolate, followed by treatment with gefitinib (40 or 120 mg/kg), crizotinib (50 mg/kg), or vehicle.

These results suggest that while EGFR and c-MET inhibition can reduce fungal adhesion and cytokine secretion *in vitro*.. Previous work in murine models of invasive pulmonary aspergillosis has demonstrated that EGFR signaling supports host defense by promoting epithelial cytokine production, including IL-6 and chemoattractants such as CXCL1 and CXCL2, by maintaining epithelial barrier integrity and repair. Consistent with these findings, our epithelial model demonstrated that EGFR and c-MET silencing attenuated IL-6 and IL-8 secretion, thereby potentially impairing lung residing macrophage activation and recruitment and inflammatory signaling *in vivo*.

Conclusions

L. prolificans is an emerging opportunistic mold that causes disseminated and pulmonary infections with extremely high mortality, primarily due to its intrinsic resistance to nearly all available antifungal agents. Despite its increasing clinical relevance, little is known about its pathogenic mechanisms, host–pathogen interactions, or the molecular determinants that enable invasive disease [158].

In this chapter, we employed a multi-omics approach coupled with orthogonal functional validation to identify and characterize, for the first time, host lung epithelial cell receptors that mediate interaction with *L. prolificans*. Through a series of RNA-seq experiments followed by integrated pathway analysis and upstream regulator prediction, we identified EGFR and c-MET as key signaling hubs activated in HSAEC1-KT cells during *L. prolificans* infection. Proteomic and phosphoproteomic analyses further revealed infection-specific phosphorylation signatures in both receptors, which were subsequently validated in vitro through direct binding assays and Western blotting. Among these, EGFR Tyr1197 was identified as a major phosphorylation site. This residue lies within the receptor's C-terminal tail and is a docking site for adaptor proteins such as Shc and Grb2, linking EGFR activation to downstream MAPK/ERK signaling and receptor internalization [159].

Previous studies have demonstrated that c-MET can form multi-receptor complexes with other tyrosine kinase receptors, facilitating cytoskeletal rearrangements and endocytosis of fungal elements such as *Candida albicans* germlings. Our data suggest that *L. prolificans* exploits similar epithelial signaling pathways, where EGFR and c-MET not only act as adhesion receptors but also undergo pathogen-driven

phosphorylation events that may promote fungal uptake and modulation of host responses.

Consistent with these findings, pharmacological inhibition of EGFR and c-MET using gefitinib and crizotinib reduced fungal burden *in vitro*. However, this effect did not translate into improved survival *in vivo*. Instead, neutropenic mice infected with *L. prolificans* and treated with either gefitinib or crizotinib succumbed more rapidly, suggesting that the EGFR/c-MET signaling axis contributes not only to fungal adhesion but also plays a pivotal immunomodulatory role in sustaining innate antifungal defenses during pulmonary infection.

Despite these promising findings, further investigation is required to elucidate the precise roles of EGFR and c-MET during *L. prolificans* infection of lung epithelial cells. An important unresolved question is whether these receptors engage the fungus independently or whether they form multi-receptor complexes, as has been described for *C. albicans* and *A. fumigatus*. Clarifying this point is particularly relevant for translational applications, since combined inhibition of multiple receptor pathways could potentially yield synergistic protective effects. In addition, future work should focus on identifying the fungal ligand responsible for EGFR and c-MET activation.

Although direct pharmacological targeting of host receptors did not confer survival benefits in neutropenic mice, blockade of the corresponding fungal adhesins or ligands—through small molecules or monoclonal antibodies—may provide an alternative strategy to disrupt early epithelial interactions and limit the initiation of pulmonary infection. Therefore, future work should be aimed at addressing these key questions.

Collectively, these results demonstrate that although EGFR and c-MET represent receptors for *L. prolificans* on airway epithelial cells, their pharmacological inhibition *in vivo* using gefitinib and crizotinib under conditions of severe immunosuppression is detrimental and results in increased mortality among infected animals.

Chapter 4. Integrin β 4 is a receptor for emerging fungal pathogens

Introduction

Lomentospora prolificans is a filamentous, dematiaceous, emerging fungal pathogen responsible for infections in both immunocompromised and immunocompetent individuals [100, 160]. These infections can occur at various anatomical sites, with disseminated and pulmonary infections being the most prevalent and deadly forms of the disease [160-162]. Infections caused by *Lomentospora prolificans* are highly resistant to most licensed antifungal agents with a paucity of therapeutic options [5]. The respiratory tract is the main portal of entry for disseminated infections that occur in immunocompromised patients. In immunocompetent individuals, the invasive cases often occur as a consequence of direct traumatic inoculation into musculoskeletal tissue [163, 164]. In the respiratory tract, airway epithelial cells line the mucosa and act as a physical barrier against inhaled fungal particles. These cells also produce and secrete antimicrobial peptides that can serve as a biochemical barrier to fungal invasion as well as recruit innate immune cells to clear the infection via their ability to produce cytokines and chemokines [165]. Most studies of *L. prolificans* have examined interaction with neutrophils, monocytes, or macrophages [166]. However, with the exception of one study [90], the interaction between *L. prolificans* and lung epithelial cells has not been thoroughly explored. Herein, we examine the interaction between *L. prolificans* and a normal, Tert-immortalized, small human airway epithelial cell line (HSAEC1-KT).

Materials and methods

Fungal strains and culture conditions

Clinical isolates of *L. prolificans* (DI16-482, DI16-483, and DI16-484) and *Scedosporium apiospermum*, *Scedosporium boydii* were employed in this study. The strains were grown on peptone–dextrose agar (PDA) plates and incubated for 7-12 days at 37 °C prior to use. Conidia were collected in endotoxin-free Dulbecco’s phosphate-buffered saline (DPBS) supplemented with 0.5% Tween 80, washed thoroughly in sterile DPBS, and counted with a hemocytometer to standardize inoculum concentrations. For *in vitro* assays, freshly harvested spores were resuspended in Small Airway Epithelial Cell Growth Medium Basal Medium (SAGM; Lonza, Cat. #CC-3118) without rhEGF and pre-incubated for 3 h at 37 °C to promote spore swelling.

Cell lines and culture conditions

HSAEC1-KT cells (ATCC CRL-4050) were cultured in SABM Basal Medium (Lonza, CC-3119) supplemented with the SAGM SingleQuots kit (Lonza, CC-4124), 1X Penicillin–Streptomycin (Pen-Strep) (Gibco, 15140122). A549 cells were cultured in Dulbecco’s Modified Eagle Medium (DMEM) (Gibco, 11965092) supplemented with 10% heat-inactivated fetal bovine serum (FBS) (SigmaAldrich, F4135) and 1% Penicillin–Streptomycin (Pen-Strep) (Gibco, 15140122). Cells were maintained at 37 °C in a humidified atmosphere containing 5% CO₂. Cultures were replenished with fresh medium every 2–3 days and routinely subcultured once per week.

Whole-cell affinity purification using *L. prolificans* and biotinylated HSAEC1-KT and A549 proteins

L. prolificans clinical isolates were cultured on peptone–dextrose agar plates as described above. Spores were collected, washed, swollen for 3 hours and suspended in ice-cold 1× DPBS containing 1 mM PMSF. Following enumeration by hemocytometer, 8.5×10^8 spores were incubated overnight at 4 °C with 5 mg of surface-biotinylated HSAEC1-KT proteins under gentle rotation. After incubation, fungal cells were pelleted by centrifugation at $10,000 \times g$ for 5 min, and the supernatant was retained as flow-through (FT). The spore pellets were washed three times with 600 µL of ice-cold wash buffer (1× DPBS, 1 mM PMSF, and protease inhibitor cocktail). Host proteins bound to the fungal surface were then eluted by adding 200 µL of lysis buffer (6 M urea, 5.6% n-octyl- β -D-glucopyranoside, 1× DPBS, 1 mM PMSF, protease inhibitor cocktail) and incubating at room temperature for 10 min. Samples were briefly sonicated, centrifuged at $20,000 \times g$ for 3 min, and the resulting eluates (EP) were collected and stored at –80 °C until analysis.

Immunoblotting

Lysates were obtained using during tissue culture infection or pull-downs were separated by electrophoresis using the XCell SureLock Mini-Cell II system (Life Technologies) and subsequently transferred onto polyvinylidene difluoride (PVDF) membranes with the Invitrogen XCell II Blot Module, following the manufacturer's instructions. Membranes were then blocked in TBS-based blocking buffer (LI-COR) for 1 h at room temperature before being incubated with primary antibodies overnight. On the following day, the membranes were washed four times with TBS-t (1X TBS containing 0.1% Tween 20) followed by 1 h incubation at room temperature with IRDye

secondary antibodies. The proteins were then visualized using Odyssey CLx Imaging system and quantified with Image Studio software.

Results and discussion

Integrin β 4 from airway epithelial cells can bind to *L. proliferans*

Pulmonary infection is initiated when airborne conidia are inhaled, or aspirated into the lungs, and then deposited into the airways. The initial adhesion of fungal pathogens to airway epithelial cells plays a crucial role in subsequent steps of pathogenesis [167]. Therefore, we set out to identify host cell surface proteins that can physically interact with *L. proliferans* (DI16-483) by performing whole fungal cell pulldowns with biotinylated HSAEC1-KT surface proteins, followed by proteomic analysis using liquid chromatography-mass spectrometry. Using a conservative prioritization scheme, we identified 5 proteins that were listed as “high confidence” hits in the Cell Surface Protein Atlas [168], annotated as “Receptor” in the UniProt database (<https://www.uniprot.org>), and for which at least 10 peptides were identified (**Table S3**). For further investigation, we selected integrin β 4 which is known to be expressed in the lungs of both humans and mice [169-171].

In order to verify that integrin β 4 from airway epithelial cells can bind to *L. proliferans* conidia, we used a commercially available anti-integrin β 4 antibody to probe immunoblots containing HSAEC1-KT membrane proteins that were enriched for binding to conidia. This antibody recognized a conidium bound 210-kDa band derived from HSAEC1-KT cells. We also observed an association between integrin β 4, derived from

HSAEC1-KT cells and conidia of two additional isolates of *L. prolificans* (DI16-482 and DI16-484) (**Figure 4.1A**). Heat killing or pre-treatment of conidia with Proteinase K did not inhibit association with integrin $\beta 4$ (**Figure 4.1B**).

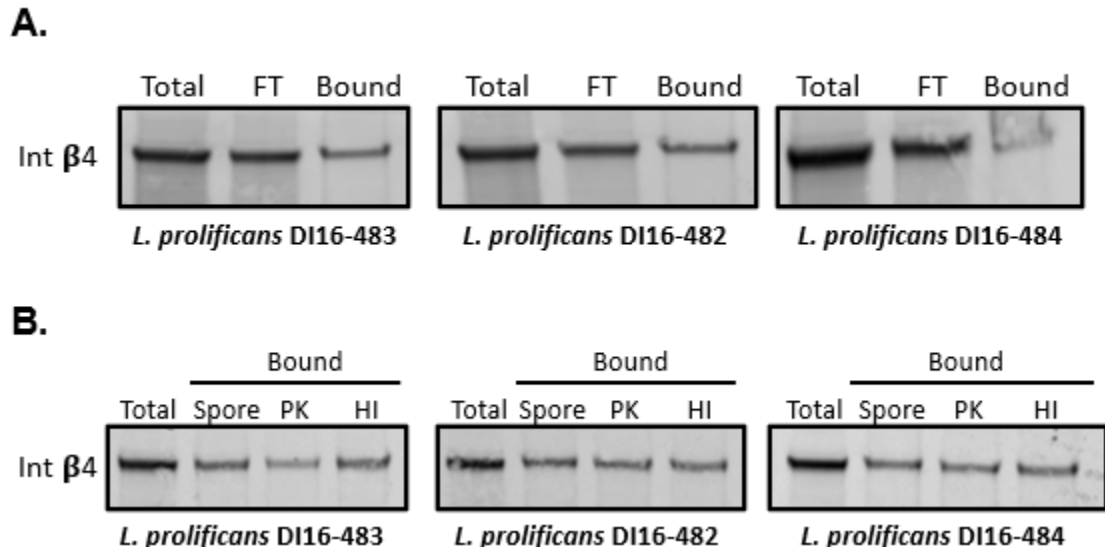


Figure 4.1. *L. prolificans* can bind integrin $\beta 4$ across all tested isolates in Protease K and heat inactivation non-dependent manner. A panel shows that integrin $\beta 4$ is able to bind tree tested isolates. Panel B demonstrates that heat inactivation or protease K digestion of surface proteins of *L. prolificans* does not suppress the integrin $\beta 4$ binding.

Moreover, integrin $\beta 4$ derived from A549 cells was also able to bind *L. prolificans* (**Figure 4.2A**). We did not recover integrin $\beta 4$ protein in negative control, empty tube samples in which the fungus was left out of the reaction (**Figure 4.2B**).

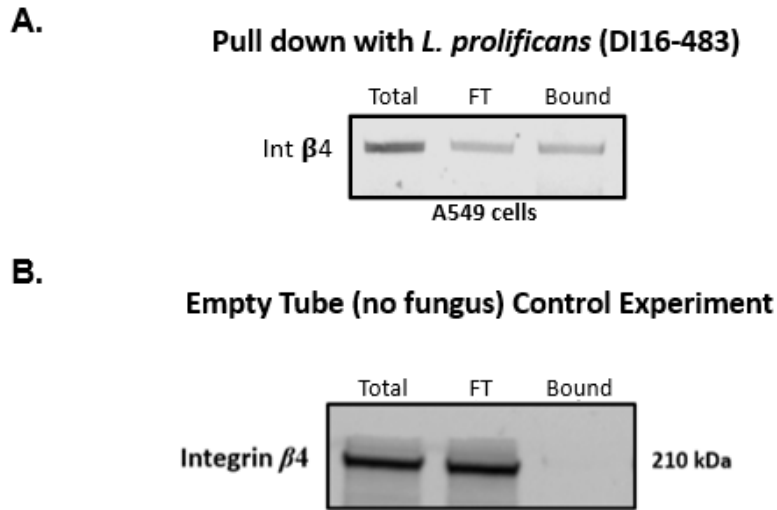


Figure 4.2. *L. proliferans* binds integrin β 4 derived from A549 cell lysates but not no fungi empty tube controls. Panel A shows A549 derived integrin β 4 binding to *L. proliferans*. Panel B demonstrates that integrin β 4 does not bind empty tube.

demonstrated specific binding to all three clinical isolates of *L. proliferans*, whereas no binding was detected to the non-fungal control. In contrast, GFP alone failed to bind any of the tested *L. proliferans* isolates (**Figure 4.3**).

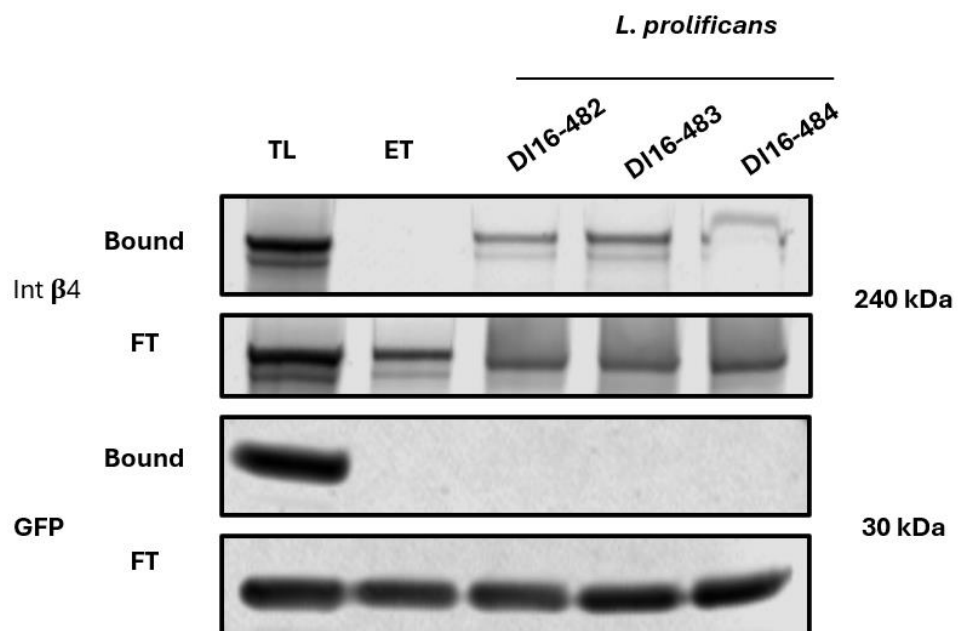


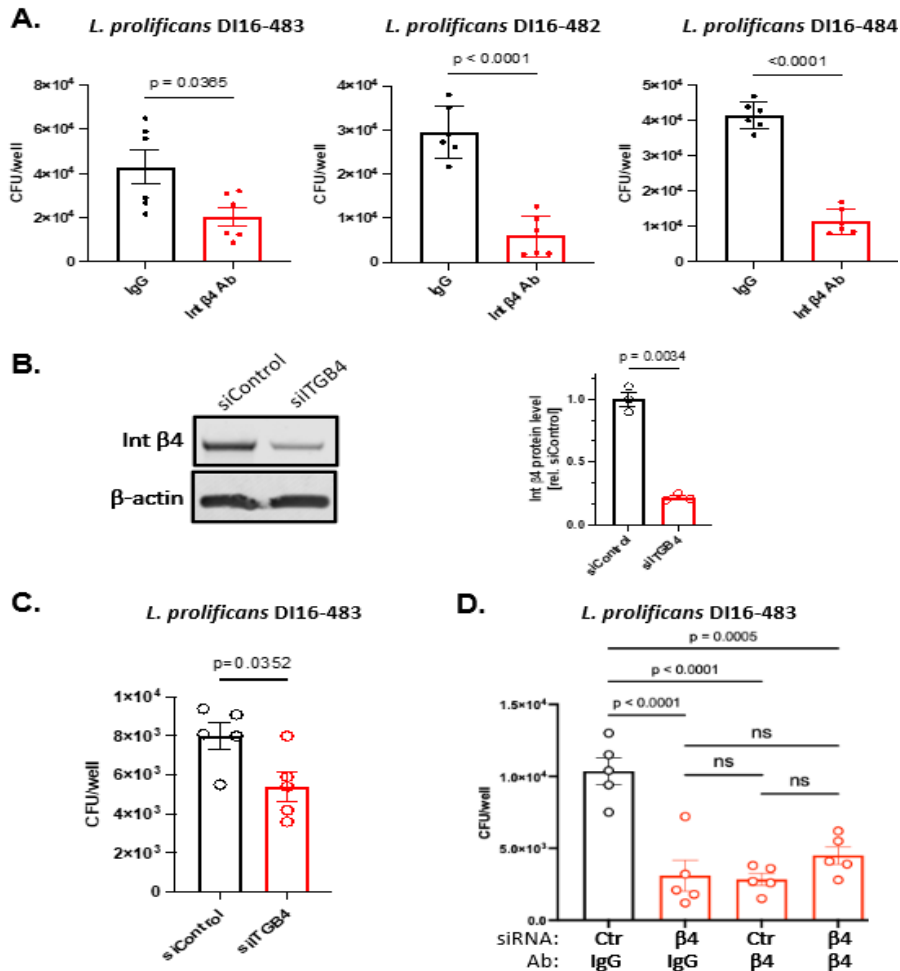
Figure 4.3. Binding of recombinant integrin β 4–GFP fusion protein to *Lomentospora prolificans* clinical isolates. Pulldown assays were performed using recombinant integrin β 4–GFP or GFP expressed in HEK293 cells and incubated with three *L. prolificans* clinical isolates (DI16-482, DI16-483, DI16-484) or a non-fungal control (ET). Bound and flow-through fractions were analyzed by immunoblotting with an integrin β 4–specific antibody.

These results indicate that integrin β 4 binding is not strain-specific and that integrin β 4 is most likely not binding to a protein on the conidial surface of *L. prolificans* due to insensitivity to heat and protease K treatments.

Integrin β 4 promotes *L. prolificans* adherence to airway epithelial cells

We next sought to determine whether blocking the function of integrin β 4 would prevent adherence of *L. prolificans* to airway epithelial cells. HSAEC1-KT cells were pre-treated with an anti-integrin β 4 antibody or an isotype control, then infected with *L. prolificans* for 3 hours. Compared to pre-treatment with an isotype-matched control IgG, the anti-integrin β 4 antibody reduced the adherence of all three *L. prolificans* isolates by

more than 50% (**Figure 4.4A**).



We also examined whether knocking-down the expression of integrin $\beta 4$ in epithelial cells would reduce fungal adhesion. Treatment of HSAEC1-KT cells with integrin $\beta 4$ -directed siRNA resulted in a $\sim 75\%$ inhibition of integrin $\beta 4$ protein expression (**Figure 4.4B**) and a significant reduction in the ability *L. prolificans* to adhere to the host cells (**Figure 4.4C**). In a complementary approach, we examined the effects of combining antibody blockade and siRNA inhibition on fungal adhesion. As observed in other experiments (**Figure 4.4A-C**), pre-treatment with anti-integrin $\beta 4$ antibody or

siRNA alone each significantly reduced fungal adhesion (**Figure 4.4D**). Notably, treating the host cells with both the anti-integrin $\beta 4$ antibody and siRNA resulted in equivalent levels of inhibition as each individual treatment (**Figure 4.4D**), confirming the specificity of the antibody-based inhibition in our experiments. Together, these results suggest that integrin $\beta 4$ promotes adherence of *L. prolificans* to small airway epithelial cells.

Integrin $\beta 4$ promotes adherence of *S. apiospermum* and *S. boydii* to airway epithelial cells

We next sought to determine if integrin $\beta 4$ can also bind to pathogenic isolates of two closely related species of emerging fungal pathogens, *Scedosporium apiospermum* and *Scedosporium boydii*. From the time of its initial discovery until 2014, *L. prolificans* was considered a *Scedosporium* species [172, 173]. Immunoblotting of HSAEC1-KT membrane proteins that were enriched for binding to two different *S. apiospermum* isolates (DI16-476 and DI16-477) and 2 different *S. boydii* isolates (DI16-479 and DI16-480) demonstrated binding to integrin $\beta 4$ to all four isolates (**Figure 4.5A**). The adherence of each of these isolates to HSAEC1-KT cells was significantly reduced by blocking with an anti-integrin $\beta 4$ antibody (**Figure 4.5B**).

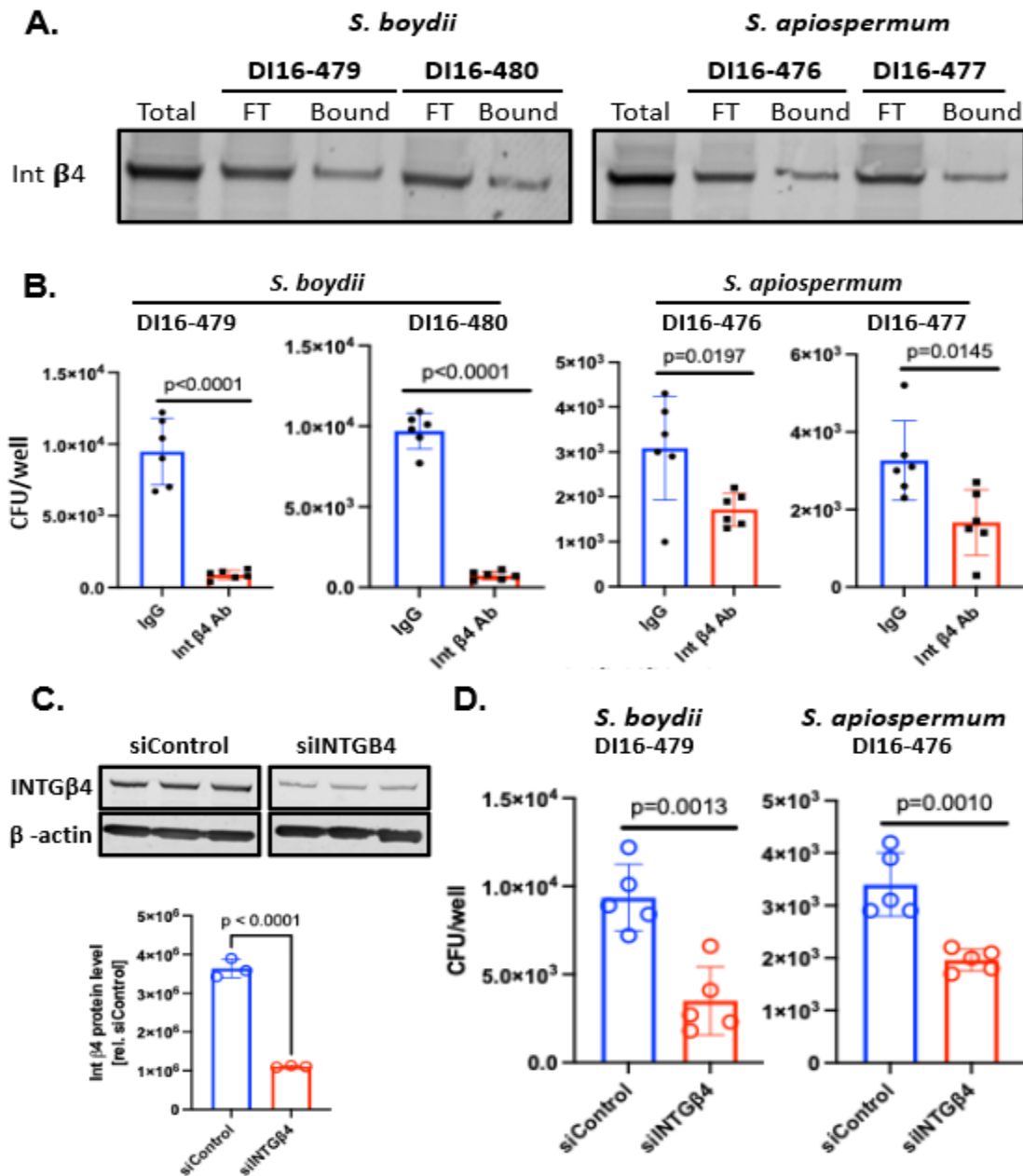


Figure 4.8. Integrin β 4 mediates adherence of *Scedosporium boydii* and *Scedosporium apiospermum* to airway epithelial cells. (A) Pull-down assays using HSAEC1-KT cell lysates demonstrated that endogenous integrin β 4 bound to multiple *S. boydii* and *S. apiospermum* isolates. (B) Antibody blocking of integrin β 4 significantly reduced adherence of all tested *S. boydii* and *S. apiospermum* isolates compared with IgG controls. (C) Western blot validation of integrin β 4 knockdown by siRNA in HSAEC1-KT cells. (D) siRNA-mediated silencing of integrin β 4 significantly reduced adherence of *S. boydii* DI16-479 and *S. apiospermum* DI16-476.

integrin β 4-directed siRNA resulted in a ~70% inhibition of integrin β 4 protein

expression (Figure 4.5C) and a significant reduction in the ability *S. boydii* and *S.*

apiospermum to adhere to the host cells (**Figure 4.5D**). These data suggest that the ability to associate with integrin $\beta 4$ and promote fungal adherence is not a property that is unique to *L. prolificans* but also applies to at least two additional closely related species.

Conclusions

In this work, we investigated the *in vitro* interaction between *L. prolificans* and human airway epithelial cells to identify host proteins that promote this interaction. The most salient findings of our study are (1) integrin $\beta 4$ can bind to conidia of *L. prolificans*; (2) this binding can occur with both heat-killed and protease K treated conidia; (3) pre-treatment of airway epithelial cells with an anti-integrin $\beta 4$ antibody reduces fungal adhesion; and (4) integrin $\beta 4$ also binds to the conidia of, and promotes the adhesion of, *S. apiospermum* and *S. boydii*, two species that are closely related to *L. prolificans*.

Integrin $\beta 4$ forms a complex with integrin $\alpha 6$ to serve as a receptor for laminin and as a cellular adhesion molecule [174-176]. Signaling from the integrin $\alpha 6\beta 4$ complex regulates various cellular processes, including cell migration, survival, and angiogenesis [175, 176]. Integrin $\beta 4$, alone or in complex with integrin $\alpha 6$, can also mediate host cell attachment and infection of Zika virus [177]. Notably, our LC-MS analysis did not detect any integrin $\alpha 6$ peptides among our enriched surface proteins. Furthermore, immunoblot pulldown experiments with *L. prolificans* did not confirm any detectable binding to recombinant integrin $\alpha 6$, indicating that this receptor is not involved in the interaction under the tested conditions (**Figure 4.6**).

L. prolificans DI16-489

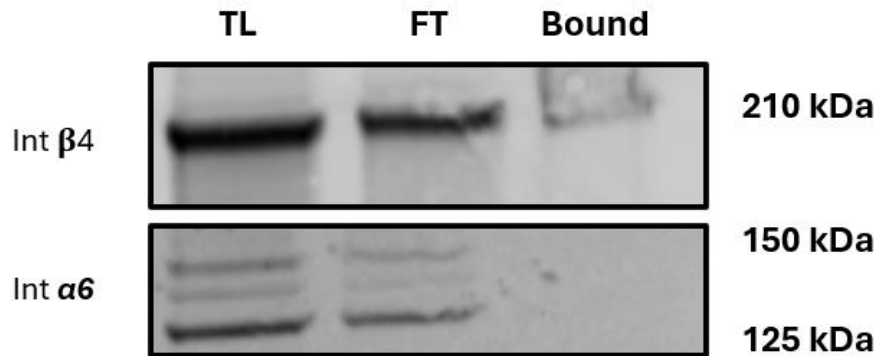


Figure 4.6. Pulldown of endogenous integrins β4 and α6 from HSAEC1-KT cells with *Lomentospora prolificans* isolate DI16-489. Pulldown assays were performed using total lysates from HSAEC1-KT cells incubated with *L. prolificans* DI16-489. Bound and flow-through fractions were analyzed by immunoblotting with integrin-specific antibodies.

and our analysis suggests that integrin β4 binding to conidia likely does not involve a fungal protein due to binding not being affected by heat or protease K treatment. Furthermore, the interaction between *L. prolificans* and integrin β4 could not be inhibited by the addition of excess laminin to the binding reaction (**Figure 4.7**). These observations suggest that integrin β4 binds to conidia in a manner that is independent of both integrin α6 and the integrin β4 laminin-binding domain.

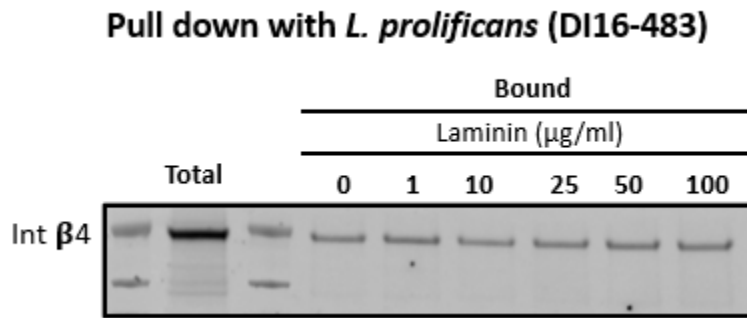


Figure 4.7. Integrin $\beta 4$ binding to *Lomentospora prolificans* is not inhibited by laminin. Pulldown assays were performed using HSAEC1-KT lysates incubated with *L. prolificans* isolate DI16-483 in the presence of increasing concentrations of laminin (0–100 $\mu\text{g/ml}$). Immunoblotting with an integrin $\beta 4$ –specific antibody revealed consistent levels of bound integrin $\beta 4$ across all laminin concentrations, indicating that fungal binding to integrin $\beta 4$ is not competitively inhibited by laminin.

The ability of integrins to function as fungal adhesion molecules has been documented among evolutionarily diverse fungi. The CalA protein of *Aspergillus fumigatus* binds to host integrin $\alpha 5 \beta 1$ expressed on pulmonary epithelial cells to facilitate host cell invasion [178]. Similarly, *Candida albicans* hyphae can bind to integrin $\alpha X \beta 2$ in a β -glucan-sensitive manner demonstrating a multiple roles of integrins in fungal pathogenesis [179]. Furthermore, Mucorales fungi bind to integrin $\alpha 3 \beta 1$ on lung epithelial cells through the action of the fungal spore coat protein encoded by CotH7 [74]. Notably, a role for integrin $\beta 4$ in fungal-host interactions has not been previously described.

Our siRNA and antibody-mediated receptor blocking studies (**Figure 2**) suggest a role for integrin $\beta 4$ in the initial interaction between *L. prolificans* airway epithelial cells, specifically as a fungal adhesion receptor. At the moment, the fungal ligand(s) that interacts with integrin $\beta 4$ remains unknown. Additional experiments are required to (i) identify the fungal ligand(s), (ii) identify other host factors that might be involved in the

integrin β 4-mediated binding, (iii) characterize the fungal associated downstream signaling events of integrin β 4-mediated adhesion, and (iv) understand the broader role (*e.g.* fungal invasion and host immune response) of integrin β 4 in the pulmonary host defense and development of fungal infections caused by isolates of the genera *Lomentospora* and *Scedosporium*.

Chapter 5. Future directions

The present work establishes a set of host receptors, integrin $\beta 4$ (ITG $\beta 4$), EGFR, and c-MET, that are exploited by emerging fungal pathogens to adhere to epithelial cells and modulate host signaling. These discoveries highlight novel aspects of fungal pathogenesis but also raise important questions regarding their *in vivo* relevance, the identity of the corresponding fungal ligands, and their translational potential as therapeutic targets. Addressing these gaps will require the integration of advanced animal models, molecular approaches for receptor manipulation, and the development of targeted therapeutic strategies.

ITG $\beta 4$ in *C. auris* colonization and persistence

The demonstration that ITG $\beta 4$ mediates adhesion of *C. auris* to keratinocytes suggests a key role in the establishment of persistent skin colonization, which underlies hospital outbreaks and transmission. However, its role *in vivo* has not been validated. ITG $\beta 4$ knockout mice die shortly after birth due to the critical role of the receptor in epithelial hemidesmosome formation, necessitating alternative approaches [180]. Keratinocyte-specific knockout models, using keratin 14 (K14)-Cre or inducible Cre-lox systems, would permit tissue-restricted deletion and allow direct assessment of fungal colonization, immune cell recruitment, and barrier integrity in physiologically relevant settings [181]. Complementarily, lentiviral-mediated siRNA delivery represents a tractable approach for long-term ITG $\beta 4$ suppression in skin. Use of keratinocyte-targeted viral vectors applied topically or intradermally could suppress ITG $\beta 4$ expression at

colonization sites, enabling dynamic evaluation of fungal burden and persistence over time.

Therapeutic characterization of ITG β 4 is equally important. Monoclonal antibodies directed against the extracellular domain of ITG β 4 could be applied in murine or porcine skin colonization models to evaluate whether blocking receptor–fungal interactions decreases fungal adhesion and limits transmission. Because antibodies act transiently, small-molecule–based strategies should also be explored. Proteolysis-targeting chimeras (PROTACs) that recruit ITG β 4 to the ubiquitin–proteasome pathway represent an innovative approach for durable receptor depletion [182]. Such strategies would need to be optimized for epithelial delivery but could offer long-term suppression of receptor availability and thereby reduce fungal colonization. These studies would not only validate ITG β 4 as a mediator of *C. auris* colonization but also establish the receptor as a tractable target for decolonization therapies in high-risk patient populations.

EGFR and c-MET in *L. prolificans* pathogenesis

In contrast to *C. auris*, the data presented here establish a role for EGFR and c-MET in mediating airway epithelial interactions with *L. prolificans*. Both receptors were consistently activated following fungal contact *in vitro*, and functional blockade attenuated epithelial responses. However, historically the fungal ligands responsible for triggering these pathways remain unidentified. Discovery of these ligands should be a major priority. Candidate-based approaches could include biochemical pulldown of *L. prolificans* surface proteins followed by mass spectrometry, while unbiased forward genetic or CRISPR-based fungal mutagenesis screens could reveal adhesins or secreted

proteins required for receptor activation [183, 184]. Once candidate ligands are identified, their role can be confirmed through targeted deletion in fungal strains and functional validation in epithelial binding assays. Such work would provide a mechanistic link between fungal molecules and host receptor engagement.

From a therapeutic perspective, EGFR and c-MET are particularly attractive because they are already well-studied in oncology, with multiple inhibitors available. First-generation inhibitors such as gefitinib (EGFR) and crizotinib (c-MET) were ineffective in preliminary *in vivo* fungal infection models, likely due to limited selectivity, suboptimal pharmacokinetics, or inadequate dosing. However, second- and third-generation kinase inhibitors—such as osimertinib (EGFR) or capmatinib/tepotinib (c-MET)—may yield greater activity owing to their improved specificity and ability to penetrate lung tissue [185, 186]. These agents should be systematically tested in murine models of pulmonary lomentosporiosis to evaluate their capacity to reduce fungal adhesion, mitigate epithelial injury, or restore protective immune responses. Additionally, antibody-based blockade of EGFR and c-MET could be explored in infection models as a strategy to interrupt receptor signaling without systemic kinase inhibition.

***In Vivo* validation through conditional knockout systems**

Ultimately, receptor function must be validated in physiologic animal models. Because global knockouts of EGFR and c-MET are embryonically lethal, conditional, tissue-specific deletion strategies are essential. Lung epithelium-specific knockout models (e.g., using surfactant protein C (SPC)-Cre or inducible Cre drivers) could enable selective ablation of EGFR, c-MET, or ITG β 4 within airway epithelia [187]. These

models would permit direct testing of receptor function during fungal conidial adhesion, germination, epithelial injury, and dissemination. Comparative infection studies in receptor knockout versus wild-type mice would clarify whether receptor engagement is an essential determinant of fungal pathogenesis and would provide a robust framework for evaluating therapeutic interventions.

Appendix

Supplementary tables

Table S1. The proteomic LC-MS analysis identified and prioritized list of host proteins that are able to bind two isolates of *Candida auris*.

Gene	Identified protein	Peptides	<i>Candida auris</i>	
			AR-0382	AR-0387
PLCD3	1-phosphatidylinositol 4,5-bisphosphate phosphodiesterase delta-3	19	820470	1212600
HSD17B10	3-hydroxyacyl-CoA dehydrogenase type-2	17	6411430	1004980
SCD	Acyl-CoA desaturase	5	2289370	2700670
SLC35B2	Adenosine 3'-phospho 5'-phosphosulfate transporter 1	4	403956	459404
ADGRG1	Adhesion G-protein coupled receptor G1	2	147629	245523
APMAP	Adipocyte plasma membrane-associated protein	17	2579060	4080210
MACROD1	ADP-ribose glycohydrolase MACROD1	10	1369840	2027370
LRPAP1	Alpha-2-macroglobulin receptor-associated protein	10	526303	980070
TAP1	Antigen peptide transporter 1	10	732389	1061450
TAP2	Antigen peptide transporter 2	14	540569	1117350
ATP5MD	ATP synthase membrane subunit DAPIT, mitochondrial	4	3607430	4557260
ABCD3	ATP-binding cassette sub-family D member 3	14	624955	1008080
BCAP31	B-cell receptor-associated protein 31	14	7776760	1477710
BCCIP	BRCA2 and CDKN1A-interacting protein	4	368100	527222
KCTD10	BTB/POZ domain-containing adapter for CUL3-mediated RhoA degradation protein 3	4	901776	858760
KCTD12	BTB/POZ domain-containing protein KCTD12	5	348977	732140
CDH1	Cadherin-1	15	6006750	8413760
CDH13	Cadherin-13	4	923973	1607180
CDH3	Cadherin-3	11	1454040	2933330
IGF2R	Cation-independent mannose-6-phosphate receptor	4	333599	498604
CD109	CD109 antigen	19	1148450	1809480
CD151	CD151 antigen	4	406215	803031
ALCAM	CD166 antigen	11	446011	878911
CD44	CD44 antigen	8	3411160	7663840
CD9	CD9 antigen	3	658534	1200070

CDC42EP1	Cdc42 effector protein 1	2	525524	732779
CISD1	CDGSH iron-sulfur domain-containing protein 1	4	1046050	1270170
CISD2	CDGSH iron-sulfur domain-containing protein 2	5	1001390	1797930
CDK5RAP3	CDK5 regulatory subunit-associated protein 3	19	958978	1399470
MNAT1	CDK-activating kinase assembly factor MAT1	5	728173	1045620
CDKN2AIP	CDKN2A-interacting protein	5	291920	500003
CDIPT	CDP-diacylglycerol--inositol 3-phosphatidyltransferase	5	568926	822754
CDC42	Cell division control protein 42 homolog	9	1043250	1650740
CDC5L	Cell division cycle 5-like protein	20	2370090	3340890
CDC27	Cell division cycle protein 27 homolog	2	654299	1012590
SLC44A2	Choline transporter-like protein 2	9	121290	443442
CLDN1	Claudin-1	2	690806	1230810
CLDN4	Claudin-4	3	869488	1455510
CLPTM1	Cleft lip and palate transmembrane protein 1	14	1498950	2254800
CCDC115	Coiled-coil domain-containing protein 115	2	696128	1143560
CCDC124	Coiled-coil domain-containing protein 124	7	945332	2112310
CCDC137	Coiled-coil domain-containing protein 137	4	829302	1051250
CCDC47	Coiled-coil domain-containing protein 47	17	3069260	4762820
CCDC50	Coiled-coil domain-containing protein 50	8	2040640	3624790
CCDC51	Coiled-coil domain-containing protein 51	4	803377	1162770
CCDC84	Coiled-coil domain-containing protein 84	2	482208	561383
CCDC86	Coiled-coil domain-containing protein 86	11	3252650	2817030
CCDC9	Coiled-coil domain-containing protein 9	3	735535	948876
CCDC9B	Coiled-coil domain-containing protein 9B	7	576441	816100
CDCP1	CUB domain-containing protein 1	8	213877	895808
CDK1	Cyclin-dependent kinase 1	2	858281	1108290
CDK11A;CDK11B	Cyclin-dependent kinase 11B	12	1746970	2350040
CDK12	Cyclin-dependent kinase 12	3	377432	555269
CDK13	Cyclin-dependent kinase 13	3	446868	707104
CDK2	Cyclin-dependent kinase 2	4	1072440	1537580
CDK2AP1	Cyclin-dependent kinase 2-associated protein 1	2	336286	375147
CDK7	Cyclin-dependent kinase 7	4	365327	573780
CDK9	Cyclin-dependent kinase 9	6	626843	1012910
DCD	Dermcidin	2	916722	856374
ADAM10	Disintegrin and metalloproteinase domain-containing protein 10	7	1270380	1995330
ADAM15	Disintegrin and metalloproteinase domain-containing protein 15	3	533109	804427

ADAM9	Disintegrin and metalloproteinase domain-containing protein 9	3	426722	965008
CD3EAP	DNA-directed RNA polymerase I subunit RPA34	5	1536340	2359530
EPHA1	Ephrin type-A receptor 1	10	297632	606073
EPHB3	Ephrin type-B receptor 3	6	183533	523946
EGFR	Epidermal growth factor receptor	33	3581480	6155790
EPS8	Epidermal growth factor receptor kinase substrate 8	8	1253960	1954910
EPS8L1	Epidermal growth factor receptor kinase substrate 8-like protein 1	14	830772	1338250
EPS8L2	Epidermal growth factor receptor kinase substrate 8-like protein 2	25	3071190	4921570
SLC29A1	Equilibrative nucleoside transporter 1	2	897760	1744940
KDELR1	ER lumen protein-retaining receptor 1	3	739165	1282330
KDELR2	ER lumen protein-retaining receptor 2	7	1226020	2109580
EMC1	ER membrane protein complex subunit 1	27	3135550	4384080
EMC2	ER membrane protein complex subunit 2	12	4996520	6654450
EMC3	ER membrane protein complex subunit 3	4	1040390	1263790
EMC4	ER membrane protein complex subunit 4	3	1125070	1454560
EMC6	ER membrane protein complex subunit 6	2	3776290	4981730
EMC7	ER membrane protein complex subunit 7	6	2350320	3867790
EMC8	ER membrane protein complex subunit 8	5	3466160	5118440
GPAA1	Glycosylphosphatidylinositol anchor attachment 1 protein	5	619187	905210
GOLIM4	Golgi integral membrane protein 4	10	1781710	3375720
GOSR1	Golgi SNAP receptor complex member 1	6	1644870	2637350
GOSR2	Golgi SNAP receptor complex member 2	2	417485	790196
GPRC5C	G-protein coupled receptor family C group 5 member C	6	492251	1043760
GRB2	Growth factor receptor-bound protein 2	6	558302	772690
GHITM	Growth hormone-inducible transmembrane protein	9	4520350	6358290
SLC7A1	High affinity cationic amino acid transporter 1	4	1083550	2418810
LEMD3	Inner nuclear membrane protein Man1	13	874082	1311620
ITPRIP	Inositol 1,4,5-trisphosphate receptor-interacting protein	7	60821	122325
ITM2B	Integral membrane protein 2B	2	232210	428141
ITGA2	Integrin alpha-2	18	1258200	2474300
ITGA3	Integrin alpha-3	23	2263330	3428030
ITGAV	Integrin alpha-V	19	335123	685304
ITGB1	Integrin beta-1	21	1925450	3490300
ITGB6	Integrin beta-6	2	2429160	5117100
ITGB4	Isoform of P16144, Isoform Beta-4A of Integrin beta-4	65	4979700	8107270

ITGA6	Isoform of P23229, Isoform Alpha-6X1A of Integrin alpha-6	37	7513350	12017200
PCDH1	Isoform of Q08174, Isoform 2 of Protocadherin-1	15	1841560	2959330
SLC7A5	Large neutral amino acids transporter small subunit 1	9	6858220	10637500
LENG1	Leukocyte receptor cluster member 1	3	290034	627878
LSR	Lipolysis-stimulated lipoprotein receptor	15	1407770	2106300
LAMP1	Lysosome-associated membrane glycoprotein 1	5	305192	735905
MST1R	Macrophage-stimulating protein receptor	6	368309	578347
MMGT1	Membrane magnesium transporter 1	2	886511	1573560
PGRMC1	Membrane-associated progesterone receptor component 1	9	1611360	3248220
PGRMC2	Membrane-associated progesterone receptor component 2	6	523072	1063880
DNAJC19	Mitochondrial import inner membrane translocase subunit TIM14	7	2500030	2455930
TIMM17A	Mitochondrial import inner membrane translocase subunit Tim17-A	2	370571	671340
TIMM21	Mitochondrial import inner membrane translocase subunit Tim21	4	1233860	1635390
TIMM44	Mitochondrial import inner membrane translocase subunit TIM44	22	2660790	3627390
TIMM50	Mitochondrial import inner membrane translocase subunit TIM50	10	2286980	2853290
OXA1L	Mitochondrial inner membrane protein OXA1L	6	1430950	2057550
B9J08_005138	Mitochondrial outer membrane protein porin	15	7449710	1555790
SLC16A1	Monocarboxylate transporter 1	6	2595810	3266410
UNC5B	Netrin receptor UNC5B	8	318368	604320
SLC1A5	Neutral amino acid transporter B(0)	9	3635870	7134630
NPC1	NPC intracellular cholesterol transporter 1	8	427968	863162
NUP210	Nuclear pore membrane glycoprotein 210	20	299474	557049
NUDCD1	NudC domain-containing protein 1	9	375090	591344
OCLN	Occludin	13	2266850	4398410
CDC73	Parafibromin	15	1362190	2006910
CASK	Peripheral plasma membrane protein CASK	36	592370	1106200
PEX14	Peroxisomal membrane protein PEX14	2	707574	1207030
PEX16	Peroxisomal membrane protein PEX16	4	231135	349822
ATP2B1	Plasma membrane calcium-transporting ATPase 1	9	126691	262738
ATP2B4	Plasma membrane calcium-transporting ATPase 4	39	1742950	2785950
PLGRKT	Plasminogen receptor (KT)	3	1134230	1656580
PLXNA1	Plexin-A1	19	652998	1223410

PLXNB2	Plexin-B2	39	1325480	2053340
CDC40	Pre-mRNA-processing factor 17	4	1014800	1059790
PDCD4	Programmed cell death protein 4	23	1595010	2331710
PDCD6	Programmed cell death protein 6	5	196183	283326
PTGFRN	Prostaglandin F2 receptor negative regulator	5	519320	897091
ADRM1	Proteasomal ubiquitin receptor ADRM1	3	1134060	1933180
PDCD11	Protein RRP5 homolog	3	500188	630506
FAT2	Protocadherin Fat 2	16	668018	790325
REEP3	Receptor expression-enhancing protein 3	6	1240760	1081950
REEP4	Receptor expression-enhancing protein 4	4	562866	698047
RACK1	Receptor of activated protein C kinase 1	19	1333910	1746690
			0	0
PTPRK	Receptor-type tyrosine-protein phosphatase kappa	9	352234	696345
ATP6AP2	Renin receptor	8	1462440	2827060
RXRA	Retinoic acid receptor RXR-alpha	14	709058	1389980
SCAMP2	Secretory carrier-associated membrane protein 2	2	618730	1121450
SCAMP3	Secretory carrier-associated membrane protein 3	5	2441040	4018840
STRAP	Serine-threonine kinase receptor-associated protein	11	1394220	1875820
TMEM97	Sigma intracellular receptor 2	2	1209730	1494000
SRPRA	Signal recognition particle receptor subunit alpha	15	1304930	1966370
SRPRB	Signal recognition particle receptor subunit beta	11	2153640	3499000
SIGIRR	Single Ig IL-1-related receptor	4	209031	440415
SLC2A1	Solute carrier family 2, facilitated glucose transporter member 1	6	1687940	2962790
SLCO3A1	Solute carrier organic anion transporter family member 3A1	4	123878	223335
ESRRA	Steroid hormone receptor ERR1	2	226601	300268
SMARCD1	SWI/SNF-related matrix-associated actin-dependent regulator of chromatin subfamily D member 1	3	604443	851174
SMARCD2	SWI/SNF-related matrix-associated actin-dependent regulator of chromatin subfamily D member 2	12	1826970	2428620
VAT1	Synaptic vesicle membrane protein VAT-1 homolog	11	1210180	2445510
TSPAN14	Tetraspanin-14	3	4071650	3911540
TMX1	Thioredoxin-related transmembrane protein 1	9	1753440	2525780
TMX2	Thioredoxin-related transmembrane protein 2	8	1350460	2234080

TMX4	Thioredoxin-related transmembrane protein 4	3	559374	1223370
THRAP3	Thyroid hormone receptor-associated protein 3	21	1413460	1777180
TFRC	Transferrin receptor protein 1	18	4135050	7661590
TRAM1	Translocating chain-associated membrane protein 1	5	1852620	2703940
TM9SF1	Transmembrane 9 superfamily member 1	4	781235	1340310
TM9SF2	Transmembrane 9 superfamily member 2	11	1318470	1311720
TM9SF3	Transmembrane 9 superfamily member 3	9	1596060	2578610
TM9SF4	Transmembrane 9 superfamily member 4	9	1287130	2264840
TMED10	Transmembrane emp24 domain-containing protein 10	7	9728370	1289760
TMED2	Transmembrane emp24 domain-containing protein 2	3	4364330	3301460
TMED3	Transmembrane emp24 domain-containing protein 3	3	523697	647897
TMED4	Transmembrane emp24 domain-containing protein 4	4	2148250	3037210
TMED5	Transmembrane emp24 domain-containing protein 5	6	1750870	2415650
TMED9	Transmembrane emp24 domain-containing protein 9	6	3546600	5262860
GPNMB	Transmembrane glycoprotein NMB	4	4799620	7235630
TMEM106B	Transmembrane protein 106B	8	467116	805160
TMEM109	Transmembrane protein 109	4	4510400	7236920
TMEM11	Transmembrane protein 11, mitochondrial	5	676326	1146900
TMEM126A	Transmembrane protein 126A	5	808219	1288850
TMEM14C	Transmembrane protein 14C	3	1061240	1312200
TMEM160	Transmembrane protein 160	2	206616	282467
TMEM205	Transmembrane protein 205	2	347394	560633
TMEM214	Transmembrane protein 214	3	229789	547772
TMEM238	Transmembrane protein 238	4	794878	822513
TMEM245	Transmembrane protein 245	4	306301	460596
TMEM41A	Transmembrane protein 41A	2	909557	1676470
TMEM41B	Transmembrane protein 41B	4	328826	424563
TMEM43	Transmembrane protein 43	15	1782230	3379110
TMEM51	Transmembrane protein 51	2	189926	443601
TACSTD2	Tumor-associated calcium signal transducer 2	12	4864810	8474080
PTPN1	Tyrosine-protein phosphatase non-receptor type 1	15	3148700	4536600
HACD2	Very-long-chain (3R)-3-hydroxyacyl-CoA dehydratase 2	3	1291820	1766660
HACD3	Very-long-chain (3R)-3-hydroxyacyl-CoA dehydratase 3	11	3054660	4707450
VAMP3	Vesicle-associated membrane protein 3	2	679206	1132340

VAMP8	Vesicle-associated membrane protein 8	4	606931	1050470
VAPA	Vesicle-associated membrane protein-associated protein A	10	2506290	5630140
VAPB	Vesicle-associated membrane protein-associated protein B/C	7	863329	1505960
LMAN2	Vesicular integral-membrane protein VIP36	9	1915840	3474060
LRRC8A	Volume-regulated anion channel subunit LRRC8A	11	626732	1081760
SLC30A1	Zinc transporter 1	4	1215880	1958960
SLC30A7	Zinc transporter 7	4	1083220	1525460

Table S2. The proteomic LC-MS analysis identified INTGB4 and other surface proteins that are able to bind *L. proliferans*.

Protein group	Protein name	Genes	Protein description	Peptides	HSAE C1-KT	CSPA matches
O15031	PLXB2_HUMAN	PLXN B2	Plexin-B2	23	406153	O1503 1
P02786	TFR1_HUMAN	TFRC	Transferrin receptor protein 1	22	775282	P0278 6
P08195;P08195-2;P08195-3;P08195-4	4F2-2_HUMAN;4F2-3_HUMAN;4F2-4_HUMAN;4F2_HUMAN	SLC3 A2	4F2 cell-surface antigen heavy chain	17	304087 0	P0819 5
P10586;P10586-2	PTPRF-2_HUMAN;PTPRF_HUMAN	PTPRF	Receptor-type tyrosine-protein phosphatase F	16	183845	P1058 6
P16144;P16144-2;P16144-4	ITB4-2_HUMAN;ITB4-4_HUMAN;ITB4_HUMAN	ITGB4	Integrin beta-4	14	659255	P1614 4

References:

1. Bongomin, F., et al., *Global and Multi-National Prevalence of Fungal Diseases-Estimate Precision*. J Fungi (Basel), 2017. **3**(4).
2. Henao-Martinez, A.F., et al., *Invasive pulmonary aspergillosis real-world outcomes: Clinical features and risk factors associated with increased mortality*. Med Mycol, 2023. **61**(8).
3. Jeffery-Smith, A., et al., *Candida auris: a Review of the Literature*. Clin Microbiol Rev, 2018. **31**(1).
4. Denning, D.W., *Global incidence and mortality of severe fungal disease*. Lancet Infect Dis, 2024. **24**(7): p. e428-e438.
5. Hoenigl, M., et al., *Global guideline for the diagnosis and management of rare mould infections: an initiative of the European Confederation of Medical Mycology in cooperation with the International Society for Human and Animal Mycology and the American Society for Microbiology*. Lancet Infect Dis, 2021. **21**(8): p. e246-e257.
6. Briano, F., et al., *Candida auris Candidemia in Critically Ill, Colonized Patients: Cumulative Incidence and Risk Factors*. Infect Dis Ther, 2022. **11**(3): p. 1149-1160.
7. Brown, G.D., et al., *Hidden killers: human fungal infections*. Sci Transl Med, 2012. **4**(165): p. 165rv13.
8. Morrissey, C.O., et al., *Mucorales: A systematic review to inform the World Health Organization priority list of fungal pathogens*. Med Mycol, 2024. **62**(6).
9. Petrikos, G., et al., *Epidemiology and clinical manifestations of mucormycosis*. Clin Infect Dis, 2012. **54 Suppl 1**: p. S23-34.
10. Yasinskaya, Y., et al., *Food and Drug Administration Public Workshop Summary-Development Considerations of Antifungal Drugs to Address Unmet Medical Need*. Clin Infect Dis, 2023. **77**(3): p. 380-387.
11. Cortez, K.J., et al., *Infections caused by Scedosporium spp.* Clin Microbiol Rev, 2008. **21**(1): p. 157-97.
12. Jenks, J.D., et al., *Rare mould infections caused by Mucorales, Lomentospora prolificans and Fusarium, in San Diego, CA: the role of antifungal combination therapy*. Int J Antimicrob Agents, 2018. **52**(5): p. 706-712.
13. Ramirez-Garcia, A., et al., *Scedosporium and Lomentospora: an updated overview of underrated opportunists*. Med Mycol, 2018. **56**(suppl_1): p. 102-125.
14. Konsoula, A., et al., *Lomentospora prolificans Disseminated Infections: A Systematic Review of Reported Cases*. Pathogens, 2022. **12**(1).
15. Kim, J.Y., et al., *Clinical Features and Outcomes of Invasive Fusariosis: A Case Series in a Single Center with Literature Review*. Infect Chemother, 2023. **55**(2): p. 290-294.
16. Nucci, M., et al., *Invasive Fusariosis in Patients with Hematologic Diseases*. J Fungi (Basel), 2021. **7**(10).
17. Rossow, J., et al., *Factors Associated With Candida auris Colonization and Transmission in Skilled Nursing Facilities With Ventilator Units, New York, 2016-2018*. Clin Infect Dis, 2021. **72**(11): p. e753-e760.
18. Sokou, R., et al., *Candida auris Infection, a Rapidly Emerging Threat in the Neonatal Intensive Care Units: A Systematic Review*. J Clin Med, 2024. **13**(6).

19. Reitzel, R.A., et al., *Minocycline-EDTA-Ethanol Antimicrobial Catheter Lock Solution Is Highly Effective In Vitro for Eradication of Candida auris Biofilms*. *Antimicrob Agents Chemother*, 2020. **64**(4).
20. Koleri, J., et al., *Candida auris Blood stream infection- a descriptive study from Qatar*. *BMC Infect Dis*, 2023. **23**(1): p. 513.
21. Benedict, K., et al., *Candida auris–Associated Hospitalizations, United States, 2017-2022*. *Emerg Infect Dis*, 2023. **29**(7): p. 1485-1487.
22. Griffith, N. and L. Danziger, *Candida auris Urinary Tract Infections and Possible Treatment*. *Antibiotics (Basel)*, 2020. **9**(12).
23. Ortiz-Roa, C., et al., *Mortality Caused by Candida auris Bloodstream Infections in Comparison with Other Candida Species, a Multicentre Retrospective Cohort*. *J Fungi (Basel)*, 2023. **9**(7).
24. Choudhury, S., et al., *Candida auris infections in ICU patients: risk factors, outcomes, and antifungal resistance patterns*. *Crit Care*, 2025. **29**(1): p. 332.
25. Kim, H.Y.P., et al., *Candida auris-a systematic review to inform the world health organization fungal priority pathogens list*. *Med Mycol*, 2024. **62**(6).
26. Neoh, C.F., et al., *Invasive Scedosporium and Lomentospora prolificans Infections in Australia: A Multicenter Retrospective Cohort Study*. *Open Forum Infect Dis*, 2023. **10**(2): p. ofad059.
27. Chen, S.C., et al., *Scedosporium and Lomentospora Infections: Contemporary Microbiological Tools for the Diagnosis of Invasive Disease*. *J Fungi (Basel)*, 2021. **7**(1).
28. Seidel, D., et al., *Prognostic factors in 264 adults with invasive Scedosporium spp. and Lomentospora prolificans infection reported in the literature and FungiScope((R))*. *Crit Rev Microbiol*, 2019. **45**(1): p. 1-21.
29. Neoh, C.F., et al., *Scedosporiosis and lomentosporiosis: modern perspectives on these difficult-to-treat rare mold infections*. *Clin Microbiol Rev*, 2024. **37**(2): p. e0000423.
30. Ghasemian, R., et al., *Fatal pulmonary Scedosporium aurantiacum infection in a patient after near-drowning: A case report*. *Curr Med Mycol*, 2021. **7**(4): p. 38-42.
31. Wu, Y., et al., *Antifungal Susceptibility Profiles and Drug Resistance Mechanisms of Clinical Lomentospora prolificans Isolates*. *Antimicrob Agents Chemother*, 2020. **64**(11).
32. Jenks, J.D., et al., *Clinical characteristics and outcomes of invasive Lomentospora prolificans infections: Analysis of patients in the FungiScope((R)) registry*. *Mycoses*, 2020. **63**(5): p. 437-442.
33. Sato, K., et al., *Disseminated Lomentospora prolificans infection that could have been predicted: A case report*. *IDCases*, 2024. **37**: p. e02046.
34. Johnston, N., et al., *Successful management of Lomentospora prolificans septic arthritis and osteomyelitis in an immunocompetent child: A case report*. *Med Mycol Case Rep*, 2025. **48**: p. 100704.
35. Lee, J., M. Wilson, and N. Casey, *Eradication of Lomentospora prolificans Osteomyelitis of the Wrist with Combination Antifungal Therapy, Voriconazole Bone Cement, and Surgical Debridement*. *Case Rep Orthop*, 2020. **2020**: p. 8271471.

36. Dong, M., et al., *A case of Lomentospora prolificans endophthalmitis treated with the novel antifungal agent Olorofim*. J Ophthalmic Inflamm Infect, 2024. **14**(1): p. 13.
37. Chowdhary, A., C. Sharma, and J.F. Meis, *Candida auris: A rapidly emerging cause of hospital-acquired multidrug-resistant fungal infections globally*. PLoS Pathog, 2017. **13**(5): p. e1006290.
38. Tsay, S., et al., *Approach to the Investigation and Management of Patients With Candida auris, an Emerging Multidrug-Resistant Yeast*. Clin Infect Dis, 2018. **66**(2): p. 306-311.
39. Perlin, D.S., *Echinocandin Resistance in Candida*. Clin Infect Dis, 2015. **61 Suppl 6**(Suppl 6): p. S612-7.
40. Biagi, M.J., et al., *Development of High-Level Echinocandin Resistance in a Patient With Recurrent Candida auris Candidemia Secondary to Chronic Candiduria*. Open Forum Infect Dis, 2019. **6**(7): p. ofz262.
41. Sharma, D., et al., *Impact of FKS1 Genotype on Echinocandin In Vitro Susceptibility in Candida auris and In Vivo Response in a Murine Model of Infection*. Antimicrob Agents Chemother, 2022. **66**(1): p. e0165221.
42. Spruijtenburg, B., et al., *Whole genome sequencing analysis demonstrates therapy-induced echinocandin resistance in Candida auris isolates*. Mycoses, 2023. **66**(12): p. 1079-1086.
43. Lockhart, S.R., et al., *Simultaneous Emergence of Multidrug-Resistant Candida auris on 3 Continents Confirmed by Whole-Genome Sequencing and Epidemiological Analyses*. Clin Infect Dis, 2017. **64**(2): p. 134-140.
44. Healey, K.R., et al., *Limited ERG11 Mutations Identified in Isolates of Candida auris Directly Contribute to Reduced Azole Susceptibility*. Antimicrob Agents Chemother, 2018. **62**(10).
45. Munoz, J.F., et al., *Genomic insights into multidrug-resistance, mating and virulence in Candida auris and related emerging species*. Nat Commun, 2018. **9**(1): p. 5346.
46. Chowdhary, A., et al., *A multicentre study of antifungal susceptibility patterns among 350 Candida auris isolates (2009-17) in India: role of the ERG11 and FKS1 genes in azole and echinocandin resistance*. J Antimicrob Chemother, 2018. **73**(4): p. 891-899.
47. Prasad, R., et al., *The ABCs of Candida albicans Multidrug Transporter Cdr1*. Eukaryot Cell, 2015. **14**(12): p. 1154-64.
48. Pristov, K.E. and M.A. Ghannoum, *Resistance of Candida to azoles and echinocandins worldwide*. Clin Microbiol Infect, 2019. **25**(7): p. 792-798.
49. Morschhauser, J., et al., *The transcription factor Mrr1p controls expression of the MDR1 efflux pump and mediates multidrug resistance in Candida albicans*. PLoS Pathog, 2007. **3**(11): p. e164.
50. Rybak, J.M., et al., *Mutations in TAC1B: a Novel Genetic Determinant of Clinical Fluconazole Resistance in Candida auris*. mBio, 2020. **11**(3).
51. Grant, V.C., et al., *Characterizing Safety and Clinical Outcomes Associated with High-Dose Micafungin Utilization in Patients with Proven Invasive Candidiasis*. Trop Med Infect Dis, 2022. **7**(2).

52. Vitale, R.G., *Role of Antifungal Combinations in Difficult to Treat Candida Infections*. J Fungi (Basel), 2021. **7**(9).
53. Ghannoum, M., et al., *Ibrexafungerp: A Novel Oral Triterpenoid Antifungal in Development for the Treatment of Candida auris Infections*. Antibiotics (Basel), 2020. **9**(9).
54. Wiederhold, N.P., et al., *Ibrexafungerp Demonstrates In Vitro Activity against Fluconazole-Resistant Candida auris and In Vivo Efficacy with Delayed Initiation of Therapy in an Experimental Model of Invasive Candidiasis*. Antimicrob Agents Chemother, 2021. **65**(6).
55. Ghannoum, M., et al., *Efficacy of Ibrexafungerp (SCY-078) against Candida auris in an In Vivo Guinea Pig Cutaneous Infection Model*. Antimicrob Agents Chemother, 2020. **64**(10).
56. Espinel-Ingroff, A. and N.P. Wiederhold, *A Mini-Review of In Vitro Data for Candida Species, Including C. auris, Isolated during Clinical Trials of Three New Antifungals: Fosmanogepix, Ibrexafungerp, and Rezafungin*. J Fungi (Basel), 2024. **10**(5).
57. Wiederhold, N.P., et al., *Efficacy of Delayed Therapy with Fosmanogepix (APX001) in a Murine Model of Candida auris Invasive Candidiasis*. Antimicrob Agents Chemother, 2019. **63**(11).
58. Locke, J.B., et al., *Activity of rezafungin against Candida auris*. J Antimicrob Chemother, 2025. **80**(6): p. 1482-1493.
59. Blez, D., et al., *Invasive bone and joint infections from the French Scedosporiosis/lomentosporiosis Observational Study (SOS) cohort: no mortality with long-term antifungal treatment and surgery*. Med Mycol, 2023. **61**(3).
60. Troke, P., et al., *Treatment of scedosporiosis with voriconazole: clinical experience with 107 patients*. Antimicrob Agents Chemother, 2008. **52**(5): p. 1743-50.
61. Czech, M.M., et al., *Clinical significance and antifungal susceptibility profile of 103 clinical isolates of Scedosporium species complex and Lomentospora prolificans obtained from NIH patients*. J Clin Microbiol, 2025. **63**(4): p. e0155024.
62. Georgacopoulos, O., et al., *In Vitro Activity of the Novel Antifungal Olorofim against Scedosporium and Lomentospora prolificans*. Microbiol Spectr, 2023. **11**(1): p. e0278922.
63. Alkhazraji, S., et al., *Fosmanogepix (APX001) Is Effective in the Treatment of Immunocompromised Mice Infected with Invasive Pulmonary Scedosporiosis or Disseminated Fusariosis*. Antimicrob Agents Chemother, 2020. **64**(3).
64. Romani, L., *Immunity to fungal infections*. Nat Rev Immunol, 2011. **11**(4): p. 275-88.
65. Kean, R., et al., *Transcriptome Assembly and Profiling of Candida auris Reveals Novel Insights into Biofilm-Mediated Resistance*. mSphere, 2018. **3**(4).
66. Horton, M.V., et al., *Candida auris Forms High-Burden Biofilms in Skin Niche Conditions and on Porcine Skin*. mSphere, 2020. **5**(1).
67. Castro, L.A., et al., *Candida auris infection in the central catheter of a patient without sepsis symptoms*. Colomb Med (Cali), 2019. **50**(4): p. 293-298.

68. Santana, D.J., et al., *A Candida auris-specific adhesin, Scf1, governs surface association, colonization, and virulence*. Science, 2023. **381**(6665): p. 1461-1467.
69. Zhao, G., et al., *Adhesin Als4112 promotes Candida auris skin colonization through interactions with keratinocytes and extracellular matrix proteins*. Nat Commun, 2025. **16**(1): p. 5673.
70. Konwar, A., et al., *Insights into the evolution of Candidalysin and recent developments*. Arch Microbiol, 2025. **207**(9): p. 206.
71. Phan, Q.T., et al., *Candida albicans stimulates formation of a multi-receptor complex that mediates epithelial cell invasion during oropharyngeal infection*. PLoS Pathog, 2023. **19**(8): p. e1011579.
72. Yang, J., et al., *Interference of Malassezia restricta in the invasion of Staphylococcus aureus into human keratinocytes*. Med Mycol, 2025. **63**(9).
73. Liu, H., et al., *Epidermal growth factor receptor signaling governs the host inflammatory response to invasive aspergillosis*. mBio, 2024. **15**(12): p. e0267124.
74. Alqarihi, A., et al., *GRP78 and Integrins Play Different Roles in Host Cell Invasion during Mucormycosis*. mBio, 2020. **11**(3).
75. Holt, A.M. and J.E. Nett, *Innate immune response to Candida auris*. Curr Opin Microbiol, 2024. **80**: p. 102510.
76. Das, D., H. HogenEsch, and S. Thangamani, *Intestinal colonization with Candida auris and mucosal immune response in mice treated with cefoperazone oral antibiotic*. Front Immunol, 2023. **14**: p. 1123200.
77. Eix, E.F. and J.E. Nett, *Modeling Candida auris skin colonization: Mice, swine, and humans*. PLoS Pathog, 2022. **18**(9): p. e1010730.
78. Horton, M.V., et al., *Candida auris Cell Wall Mannosylation Contributes to Neutrophil Evasion through Pathways Divergent from Candida albicans and Candida glabrata*. mSphere, 2021. **6**(3): p. e0040621.
79. Huang, X., et al., *Murine model of colonization with fungal pathogen Candida auris to explore skin tropism, host risk factors and therapeutic strategies*. Cell Host Microbe, 2021. **29**(2): p. 210-221 e6.
80. Johnson, C.J., et al., *Emerging Fungal Pathogen Candida auris Evades Neutrophil Attack*. mBio, 2018. **9**(4).
81. Weerasinghe, H., et al., *Candida auris uses metabolic strategies to escape and kill macrophages while avoiding robust activation of the NLRP3 inflammasome response*. Cell Rep, 2023. **42**(5): p. 112522.
82. Miramon, P., A.W. Pountain, and M.C. Lorenz, *Candida auris-macrophage cellular interactions and transcriptional response*. Infect Immun, 2023. **91**(11): p. e0027423.
83. Willems, H.M.E., et al., *Comparative Analysis of the Capacity of the Candida Species To Elicit Vaginal Immunopathology*. Infect Immun, 2018. **86**(12).
84. Das, D., et al., *The Emerging Fungal Pathogen Candida auris Induces IFN γ to Colonize the Skin*. PLoS Pathog, 2025. **21**(4): p. e1013114.
85. Bryak, G., et al., *Yeast and filamentous Candida auris stimulate distinct immune responses in the skin*. mSphere, 2024. **9**(7): p. e0005524.

86. Salgado, R.C., et al., *The network interplay of interferon and Toll-like receptor signaling pathways in the anti-Candida immune response*. Sci Rep, 2021. **11**(1): p. 20281.
87. Singh, S., et al., *The NDV-3A vaccine protects mice from multidrug resistant Candida auris infection*. PLoS Pathog, 2019. **15**(8): p. e1007460.
88. Liporagi-Lopes, L.C., et al., *Lomentospora prolificans synthesizes several types of melanin*. mSphere, 2025. **10**(4): p. e0096324.
89. Aor, A.C., et al., *Ultrastructural viewpoints on the interaction events of Scedosporium apiospermum conidia with lung and macrophage cells*. Mem Inst Oswaldo Cruz, 2018. **113**(10): p. e180311.
90. de Mello, T.P., et al., *Insights into the interaction of Scedosporium apiospermum, Scedosporium aurantiacum, Scedosporium minutisporum, and Lomentospora prolificans with lung epithelial cells*. Braz J Microbiol, 2020. **51**(2): p. 427-436.
91. Pinto, M.R., et al., *Involvement of peptidorhamnomannan in the interaction of Pseudallescheria boydii and HEp2 cells*. Microbes Infect, 2004. **6**(14): p. 1259-67.
92. Santos, A.L.S., et al., *Fibronectin-binding molecules of Scedosporium apiospermum: focus on adhesive events*. Braz J Microbiol, 2023. **54**(4): p. 2577-2585.
93. Martinez-Alarcon, D., et al., *Biochemical and structural studies of target lectin SapL1 from the emerging opportunistic microfungus Scedosporium apiospermum*. Sci Rep, 2021. **11**(1): p. 16109.
94. Gil, M.L., et al., *Binding of extracellular matrix proteins to Aspergillus fumigatus conidia*. Infect Immun, 1996. **64**(12): p. 5239-47.
95. Namvar, S., et al., *Aspergillus fumigatus-Host Interactions Mediating Airway Wall Remodelling in Asthma*. J Fungi (Basel), 2022. **8**(2).
96. Liu, H., et al., *Use of a human small airway epithelial cell line to study the interactions of Aspergillus fumigatus with pulmonary epithelial cells*. mSphere, 2023. **8**(5): p. e0031423.
97. Figueiredo, R.T., et al., *TLR4 recognizes Pseudallescheria boydii conidia and purified rhamnomannans*. J Biol Chem, 2010. **285**(52): p. 40714-23.
98. Xisto, M., et al., *Glucosylceramides From Lomentospora prolificans Induce a Differential Production of Cytokines and Increases the Microbicidal Activity of Macrophages*. Front Microbiol, 2019. **10**: p. 554.
99. Guegan, H., et al., *Deciphering the Role of PIG1 and DHN-Melanin in Scedosporium apiospermum Conidia*. J Fungi (Basel), 2023. **9**(2).
100. Konsoula, A., et al., *Lomentospora prolificans: An Emerging Opportunistic Fungal Pathogen*. Microorganisms, 2022. **10**(7).
101. Xisto, M.I., et al., *Peptidorhamnomannan negatively modulates the immune response in a scedosporiosis murine model*. Med Mycol, 2016. **54**(8): p. 846-55.
102. Buldain, I., et al., *The Host Immune Response to Scedosporium/Lomentospora*. J Fungi (Basel), 2021. **7**(2).
103. Bidaud, A.L., A. Chowdhary, and E. Dannaoui, *Candida auris: An emerging drug resistant yeast - A mini-review*. J Mycol Med, 2018. **28**(3): p. 568-573.
104. Forsberg, K., et al., *Candida auris: The recent emergence of a multidrug-resistant fungal pathogen*. Med Mycol, 2019. **57**(1): p. 1-12.

105. Du, H., et al., *Candida auris: Epidemiology, biology, antifungal resistance, and virulence*. PLoS Pathog, 2020. **16**(10): p. e1008921.
106. Jacobs, S.E., et al., *Candida auris Pan-Drug-Resistant to Four Classes of Antifungal Agents*. Antimicrob Agents Chemother, 2022. **66**(7): p. e0005322.
107. Garcia-Bustos, V., et al., *Characterization of the Differential Pathogenicity of Candida auris in a Galleria mellonella Infection Model*. Microbiol Spectr, 2021. **9**(1): p. e0001321.
108. Forgacs, L., et al., *Comparison of in vivo pathogenicity of four Candida auris clades in a neutropenic bloodstream infection murine model*. Emerg Microbes Infect, 2020. **9**(1): p. 1160-1169.
109. Horton, M.V., A.M. Holt, and J.E. Nett, *Mechanisms of pathogenicity for the emerging fungus Candida auris*. PLoS Pathog, 2023. **19**(12): p. e1011843.
110. Balakumar, A., et al., *Single-cell transcriptomics unveils skin cell specific antifungal immune responses and IL-1Ra- IL-1R immune evasion strategies of emerging fungal pathogen Candida auris*. PLoS Pathog, 2024. **20**(11): p. e1012699.
111. Saito, S. and T. Tsuchiya, *Characteristics of n-octyl beta-D-thioglucoopyranoside, a new non-ionic detergent useful for membrane biochemistry*. Biochem J, 1984. **222**(3): p. 829-32.
112. Aslam, B., et al., *Proteomics: Technologies and Their Applications*. J Chromatogr Sci, 2017. **55**(2): p. 182-196.
113. Yang, H., et al., *Integrin beta4 as a Potential Diagnostic and Therapeutic Tumor Marker*. Biomolecules, 2021. **11**(8).
114. Wang, L., et al., *The roles of integrin beta4 in vascular endothelial cells*. J Cell Physiol, 2012. **227**(2): p. 474-8.
115. Qi, L., et al., *Integrin alpha6beta4 requires plectin and vimentin for adhesion complex distribution and invasive growth*. J Cell Sci, 2022. **135**(2).
116. Ruan, S., et al., *Integrin beta4-Targeted Cancer Immunotherapies Inhibit Tumor Growth and Decrease Metastasis*. Cancer Res, 2020. **80**(4): p. 771-783.
117. Hao, N., et al., *Laminin-integrin a6b4 interaction activates notch signaling to facilitate bladder cancer development*. BMC Cancer, 2022. **22**(1): p. 558.
118. Son, T.W., et al., *Netrin-1 protects hypoxia-induced mitochondrial apoptosis through HSP27 expression via DCC- and integrin alpha6beta4-dependent Akt, GSK-3beta, and HSF-1 in mesenchymal stem cells*. Cell Death Dis, 2013. **4**(3): p. e563.
119. van de Veerdonk, F.L., et al., *Host-microbe interactions: innate pattern recognition of fungal pathogens*. Curr Opin Microbiol, 2008. **11**(4): p. 305-12.
120. Tai, Y.L., et al., *An EGFR/Src-dependent beta4 integrin/FAK complex contributes to malignancy of breast cancer*. Sci Rep, 2015. **5**: p. 16408.
121. Koivusalo, S., et al., *Regulation of Kinase Signaling Pathways by alpha6beta4-Integrins and Plectin in Prostate Cancer*. Cancers (Basel), 2022. **15**(1).
122. Lim, J.U., et al., *Targeting the Tumor Microenvironment in EGFR-Mutant Lung Cancer: Opportunities and Challenges*. Biomedicines, 2025. **13**(2).
123. Chadebech, P., et al., *Use of human reconstructed epidermis to analyze the regulation of beta-defensin hBD-1, hBD-2, and hBD-3 expression in response to LPS*. Cell Biol Toxicol, 2003. **19**(5): p. 313-24.

124. Tohyama, M., et al., *dsRNA-mediated innate immunity of epidermal keratinocytes*. *Biochem Biophys Res Commun*, 2005. **335**(2): p. 505-11.
125. Zhao, X., et al., *Laminin-bound integrin alpha6beta4 promotes non-small cell lung cancer progression via the activation of YAP/TAZ signaling pathway*. *Front Oncol*, 2022. **12**: p. 1015709.
126. Poester, V.R., et al., *Nikkomycin Z for the treatment of experimental sporotrichosis caused by Sporothrix brasiliensis*. *Mycoses*, 2023. **66**(10): p. 898-905.
127. Wiederhold, N.P., et al., *Evaluation of nikkomycin Z with frequent oral administration in an experimental model of central nervous system coccidioidomycosis*. *Microbiol Spectr*, 2024. **12**(10): p. e0135624.
128. Zhang, X., et al., *Synthesis, Antifungal Activity, and 3D-QASR of Novel 1,2,3,4-Tetrahydroquinoline Derivatives Containing a Pyrimidine Ether Scaffold as Chitin Synthase Inhibitors*. *J Agric Food Chem*, 2022. **70**(30): p. 9262-9275.
129. Munro, C.A., et al., *Regulation of chitin synthesis during dimorphic growth of Candida albicans*. *Microbiology (Reading)*, 1998. **144 (Pt 2)**: p. 391-401.
130. Lee, K.K., et al., *Elevated cell wall chitin in Candida albicans confers echinocandin resistance in vivo*. *Antimicrob Agents Chemother*, 2012. **56**(1): p. 208-17.
131. Czajka, K.M., et al., *Molecular Mechanisms Associated with Antifungal Resistance in Pathogenic Candida Species*. *Cells*, 2023. **12**(22).
132. van der Neut, R., et al., *Epithelial detachment due to absence of hemidesmosomes in integrin beta 4 null mice*. *Nat Genet*, 1996. **13**(3): p. 366-9.
133. van der Neut, R., et al., *Partial rescue of epithelial phenotype in integrin beta4 null mice by a keratin-5 promoter driven human integrin beta4 transgene*. *J Cell Sci*, 1999. **112 (Pt 22)**: p. 3911-22.
134. Thurber, G.M., S.C. Zajic, and K.D. Wittrup, *Theoretic criteria for antibody penetration into solid tumors and micrometastases*. *J Nucl Med*, 2007. **48**(6): p. 995-9.
135. Baek, S.C., et al., *Sustainable systemic delivery via a single injection of lentivirus into human skin tissue*. *Hum Gene Ther*, 2001. **12**(12): p. 1551-8.
136. Jakobsen, M., et al., *Robust Lentiviral Gene Delivery But Limited Transduction Capacity of Commonly Used Adeno-Associated Viral Serotypes in Xenotransplanted Human Skin*. *Hum Gene Ther Methods*, 2015. **26**(4): p. 123-33.
137. Renner, S., et al., *Update on Respiratory Fungal Infections in Cystic Fibrosis Lung Disease and after Lung Transplantation*. *J Fungi (Basel)*, 2020. **6**(4).
138. Culibrk, L., C.A. Croft, and S.J. Tebbutt, *Systems Biology Approaches for Host-Fungal Interactions: An Expanding Multi-Omics Frontier*. *OMICS*, 2016. **20**(3): p. 127-38.
139. Watkins, T.N., et al., *Inhibition of EGFR Signaling Protects from Mucormycosis*. *mBio*, 2018. **9**(4).
140. Shen, Y., et al., *InIB-dependent internalization of Listeria is mediated by the Met receptor tyrosine kinase*. *Cell*, 2000. **103**(3): p. 501-10.
141. Kavaliauskas, P., et al., *Multiple roles for hypoxia inducible factor 1-alpha in airway epithelial cells during mucormycosis*. *Nat Commun*, 2024. **15**(1): p. 5282.
142. Mylonakis, E., et al., *Galleria mellonella as a model system to study Cryptococcus neoformans pathogenesis*. *Infect Immun*, 2005. **73**(7): p. 3842-50.

143. Bergin, D., et al., *Superoxide production in Galleria mellonella hemocytes: identification of proteins homologous to the NADPH oxidase complex of human neutrophils*. Infect Immun, 2005. **73**(7): p. 4161-70.
144. Tsai, C.J., J.M. Loh, and T. Proft, *Galleria mellonella infection models for the study of bacterial diseases and for antimicrobial drug testing*. Virulence, 2016. **7**(3): p. 214-29.
145. Gebremariam, T., et al., *Anti-CotH3 antibodies protect mice from mucormycosis by prevention of invasion and augmenting opsonophagocytosis*. Sci Adv, 2019. **5**(6): p. eaaw1327.
146. Piao, C.Q., et al., *Immortalization of human small airway epithelial cells by ectopic expression of telomerase*. Carcinogenesis, 2005. **26**(4): p. 725-31.
147. Liu, H., et al., *Novel Host Pathways Govern Epithelial Cell Invasion of Aspergillus fumigatus*. Microbiol Spectr, 2023. **11**(4): p. e0008423.
148. Neves-da-Rocha, J., et al., *Insights and Perspectives on the Role of Proteostasis and Heat Shock Proteins in Fungal Infections*. Microorganisms, 2023. **11**(8).
149. Swiatnicki, M.R., et al., *Elevated phosphorylation of EGFR in NSCLC due to mutations in PTPRH*. PLoS Genet, 2022. **18**(9): p. e1010362.
150. Dickenson, R.E., et al., *EGFR1 regulates oral epithelial cell responses to Candida albicans via the EGFR- ERK1/2 pathway*. Virulence, 2024. **15**(1): p. 2435374.
151. Lowenstein, E.J., et al., *The SH2 and SH3 domain-containing protein GRB2 links receptor tyrosine kinases to ras signaling*. Cell, 1992. **70**(3): p. 431-42.
152. Yarden, Y. and M.X. Sliwkowski, *Untangling the ErbB signalling network*. Nat Rev Mol Cell Biol, 2001. **2**(2): p. 127-37.
153. Mitsudomi, T. and Y. Yatabe, *Epidermal growth factor receptor in relation to tumor development: EGFR gene and cancer*. FEBS J, 2010. **277**(2): p. 301-8.
154. Peschard, P., et al., *A conserved DpYR motif in the juxtamembrane domain of the Met receptor family forms an atypical c-Cbl/Cbl-b tyrosine kinase binding domain binding site required for suppression of oncogenic activation*. J Biol Chem, 2004. **279**(28): p. 29565-71.
155. Jeffers, M., et al., *Degradation of the Met tyrosine kinase receptor by the ubiquitin-proteasome pathway*. Mol Cell Biol, 1997. **17**(2): p. 799-808.
156. Abella, J.V., et al., *Met/Hepatocyte growth factor receptor ubiquitination suppresses transformation and is required for Hrs phosphorylation*. Mol Cell Biol, 2005. **25**(21): p. 9632-45.
157. Qi, J., et al., *Multiple mutations and bypass mechanisms can contribute to development of acquired resistance to MET inhibitors*. Cancer Res, 2011. **71**(3): p. 1081-91.
158. Yang, Y.H., et al., *Successful Treatment of Lomentospora Prolificans Infection Following Allogeneic Hematopoietic Stem Cell Transplantation: A Case Report and Literature Review*. Infect Drug Resist, 2025. **18**: p. 3617-3628.
159. Yamamura, A., *Growth factors involved in vascular remodeling in pulmonary arterial hypertension*. J Smooth Muscle Res, 2025. **61**: p. 82-92.
160. Rodriguez-Tudela, J.L., et al., *Epidemiology and outcome of Scedosporium prolificans infection, a review of 162 cases*. Med Mycol, 2009. **47**(4): p. 359-70.

161. Johnson, L.S., R.K. Shields, and C.J. Clancy, *Epidemiology, clinical manifestations, and outcomes of Scedosporium infections among solid organ transplant recipients*. *Transpl Infect Dis*, 2014. **16**(4): p. 578-87.
162. Lackner, M., et al., *Infection and colonisation due to Scedosporium in Northern Spain. An in vitro antifungal susceptibility and molecular epidemiology study of 60 isolates*. *Mycoses*, 2011. **54 Suppl 3**: p. 12-21.
163. Gamaletsou, M.N., et al., *Osteoarticular Mycoses*. *Clin Microbiol Rev*, 2022. **35**(4): p. e0008619.
164. Seidel, D., et al., *Invasive Scedosporium spp. and Lomentospora prolificans infections in pediatric patients: Analysis of 55 cases from FungiScope(R) and the literature*. *Int J Infect Dis*, 2020. **92**: p. 114-122.
165. Whitsett, J.A. and T. Alenghat, *Respiratory epithelial cells orchestrate pulmonary innate immunity*. *Nat Immunol*, 2015. **16**(1): p. 27-35.
166. Roilides, E., et al., *Host immune response against Scedosporium species*. *Med Mycol*, 2009. **47**(4): p. 433-40.
167. de Groot, P.W., et al., *Adhesins in human fungal pathogens: glue with plenty of stick*. *Eukaryot Cell*, 2013. **12**(4): p. 470-81.
168. Bausch-Fluck, D., et al., *A mass spectrometric-derived cell surface protein atlas*. *PLoS One*, 2015. **10**(3): p. e0121314.
169. Jiang, W., et al., *Airway epithelial integrin beta4-deficiency exacerbates lipopolysaccharide-induced acute lung injury*. *J Cell Physiol*, 2021. **236**(11): p. 7711-7724.
170. Liu, C., et al., *Wound repair and anti-oxidative capacity is regulated by ITGB4 in airway epithelial cells*. *Mol Cell Biochem*, 2010. **341**(1-2): p. 259-69.
171. Wu, C., et al., *BioGPS: an extensible and customizable portal for querying and organizing gene annotation resources*. *Genome Biol*, 2009. **10**(11): p. R130.
172. Lackner, M.d.H., G.S; Yang, L.; et al *Proposed nomenclature for Pseudallescheria, Scedosporium and related genera*. *Fungal Diversity*, 2014. **67**: p. 1-10.
173. Salkin, I.F., et al., *Scedosporium inflatum, an emerging pathogen*. *J Clin Microbiol*, 1988. **26**(3): p. 498-503.
174. Lee, E.C., et al., *The integrin alpha 6 beta 4 is a laminin receptor*. *J Cell Biol*, 1992. **117**(3): p. 671-8.
175. Parimon, T. and P. Chen, *alpha(6)beta(4) Integrin Directs Alveolar Epithelial Migration*. *Am J Respir Cell Mol Biol*, 2017. **56**(4): p. 413-414.
176. Stewart, R.L. and K.L. O'Connor, *Clinical significance of the integrin alpha6beta4 in human malignancies*. *Lab Invest*, 2015. **95**(9): p. 976-86.
177. Cong, H., et al., *ITGB4/CD104 mediates zika virus attachment and infection*. *Nat Commun*, 2024. **15**(1): p. 10729.
178. Liu, H., et al., *Aspergillus fumigatus CalA binds to integrin alpha5beta1 and mediates host cell invasion*. *Nat Microbiol*, 2016. **2**: p. 16211.
179. Jawhara, S., et al., *Integrin alphaXbeta(2) is a leukocyte receptor for Candida albicans and is essential for protection against fungal infections*. *J Immunol*, 2012. **189**(5): p. 2468-77.

180. Dowling, J., Q.C. Yu, and E. Fuchs, *Beta4 integrin is required for hemidesmosome formation, cell adhesion and cell survival*. J Cell Biol, 1996. **134**(2): p. 559-72.
181. Hafner, M., et al., *Keratin 14 Cre transgenic mice authenticate keratin 14 as an oocyte-expressed protein*. Genesis, 2004. **38**(4): p. 176-81.
182. Ruffilli, C., et al., *Proteolysis Targeting Chimeras (PROTACs): A Perspective on Integral Membrane Protein Degradation*. ACS Pharmacol Transl Sci, 2022. **5**(10): p. 849-858.
183. Brymora, A., V.A. Valova, and P.J. Robinson, *Protein-protein interactions identified by pull-down experiments and mass spectrometry*. Curr Protoc Cell Biol, 2004. **Chapter 17**: p. Unit 17 5.
184. Uthayakumar, D., et al., *CRISPR-Based Genetic Manipulation of Candida Species: Historical Perspectives and Current Approaches*. Front Genome Ed, 2020. **2**: p. 606281.
185. Katsuya, Y., et al., *Comparison of the Efficacy of EGFR Tyrosine Kinase Inhibitors Erlotinib and Low-dose Osimertinib on a PC-9-GFP EGFR Mutant Non-small-cell Lung Cancer Growing in the Brain of Nude Mice*. In Vivo, 2020. **34**(3): p. 1027-1030.
186. Dong, Y., et al., *MET-Targeted Therapies and Clinical Outcomes: A Systematic Literature Review*. Mol Diagn Ther, 2022. **26**(2): p. 203-227.
187. Gui, Y.S., et al., *SPC-Cre-ERT2 transgenic mouse for temporal gene deletion in alveolar epithelial cells*. PLoS One, 2012. **7**(9): p. e46076.